UAB

PhD Thesis in Physics Science

_____

ELECTRODYNAMICS AND PHASE TRANSITIONS IN MATERIALS WITH MAGNETIC MONOPOLES

Fernando Ignacio López Bara

_____

Director: Fernando M López Aguilar

Electromagnetism Group

Physics Department

Autonomous University of Barcelona

September 2018

UAB

Fernando María López Aguilar, Professor Emerit at Physics Department of the Universitat Autònoma de

Barcelona and *Fernando Ignacio López Bara,* PhD student of Physics of the same University

MANIFEST THAT:

This memory for obtaining the PhD in Physical Sciences contains the research that *Fernando Ignacio López Bara*

has carried out collaborating in the general overview of the issue, in the delimitation of the objectives of the work

of the thesis, in the corresponding computational programming, on the achievement and discussion of the results

and the derivation and publication of the research articles, all these elements of the investigation under the direction

of *Fernando María López Aguilar*

Bellaterra, September 7th, 2018.

Signature of the director: Signature of PhD student

Acknowledgements

The history of knowledge has had and has two parallel versions although sometimes they seem divergent, one is based on how Nature behaves and the other how to use the phenomena that arise in it for the benefit of society and, why not, the economy. Until 2012, only the second one made sense to me. Since then I am combining and complementing the second with the dedication to the understanding of the first. The motivation, direction and in the last stage the stimulus in adding the understanding and search of the operation of the phenomena to the utility which can be obtained from them, I owe it to my director, so I cannot think of saying anything better than thanks

On the other hand, any project only with motivation, direction and my own effort may not be enough, it is necessary a favorable environment, calm and emotional spirit to overcome the doubts that arise when the road is difficult, as well as to find the tenacity and perseverance necessary when the results are not as expected. For the construction of that environment and encouragement to follow the path outlined, I have to thank Sergio López Bara, Eva López Bara and Iolanda Rodríguez Flores. Besides, I am grateful to Mary Bardon O'Connor for her help in writing the articles that we have published, and we hope to continue publishing.

And in general, thanks to all those who have contributed to the completion of this research work and that have not been cited here.

Objectives and Summary

The work is addressed to analyze two parts that are intimately related. The first one refers to studying the global states and characteristics of their magnetic structures of the compounds called spin-ices and in the second part the behaviors under the electromagnetic interaction in infinite media and in confined systems (waveguides) are analyzed.

The main novelty in these compounds is the existence of excited global states at low-temperatures in which structural entities that mimic the behavior of magnetic monopoles arise. In the first part, the low temperature excited states or quasiparticles are studied in compounds of the type $(REE)_2 Ti_2 O_7$, where REE refers to one of the 15 lanthanides, fundamentally $Dy_2 Ti_2 O_7$ and $Ho_2 Ti_2 O_7$. At these temperatures (between 0.05 K and 0.17 K) there is a phase transition with characteristics similar to a Bose Einstein condensate whose individual components are in the form of magnetic dipoles (two monopoles, one with positive magnetic charge and the other negative connected by the "Coulomb interaction" and separated by a distance equivalent to the high of each tetrahedron of the crystalline structure which we described in the text). By increasing the temperature, said dipoles are broken forming a magnetic plasma of free and quasi-free positive and negative magnetic charges whose statistic is of the Fermi-Dirac type. The thermodynamic transition processes are described by analytical models for low energy excitation states and we describe the successive phase transitions. We determine the thermodynamic potentials, specific heat and entropy in which we can show the two possible phase transitions that occur in these compounds.

In the second part, we make an analysis of the modified Maxwell equations as well as the generalized Lorentz force in the presence of these magnetic charges. The solution of these equations allows us to obtain data that may have empirical interest in order to detect magnetic monopoles in other natural compounds. We study the transverse electromagnetic propagation in these materials by adding a strong external electric field with which we deduce the density of monopoles per unit volume and the effective mass of the same.

We deduce the solutions of these dual Maxwell equations in confined media with rectangular and circular symmetries. In these media in the magnetic plasma phase we obtain the non-linear equation of the system order

parameter. The characteristics and properties of the solutions of the modified Maxwell equations are determined in the form of TM modes, obtaining magnetic conductivity as a function of frequency (called magnetricity), magnetic susceptibility, as well as peaks in electromagnetic absorption and other data such as the frequencies of precession and the characteristic frequency of plasma or frequency of plasmon. The achieving of these two frequencies allows us to determine the specific mass assigned to these quasiparticles, being physical magnitude is basic for determining and justifying the conduction properties.

The fundamental objective of this part is to perform a systematic analysis to detect in other materials the presence of these possible effective magnetic charges that may appear and have appeared in other artificial compounds even at room temperature, with the practical interest that this novelty may have. The last objective of this second part of the thesis is to make a prospective to study the possibilities of new materials with which to build "magnetronic" devices that allow to transmit energy and information. The reasons why we do the study of two apparently disconnected parts with which we jointly formulate a unitary thesis is because although the first global state is similar, not totally equal, to a Bose-Einstein condensate with very clear interest within condensed matter and the second is clearly a state with characteristics of magnetic plasma, only the second has characteristics that can be used directly in circuit applications, which is one of the fundamental objectives of the second part. Therefore, the possible distinguishing between these two states requires a clear experimental mechanism which the electromagnetic propagation allows us to obtain. Another exclusively theoretical objective from a classical Physics point of view is the deduction of the solutions of the dual Maxwell equations in waveguides whose knowledge is scarce.

Index

Introduction

One of the "dogmas" of physics that is most trusted in that it will never be properianly false is that the divergence of the magnetic-induction vector of the averaged electromagnetic field which is evaluated in an elementary volume and propagating in either vacuum or in any material medium must always be null. However, Paul Andrew Mauricius Dirac at 1931 [1] formalized both quantitatively and qualitatively the idea of the existence of magnetic monopole.

This concept is explained by means of an object resembling an extremely long solenoid in the form of a rope that has been called Dirac's string. When the separation between the poles of this solenoid is extremely large, the inter-pole interaction is weakened until it can reach a point in which the mentioned interaction can be considered zero. At that limit, each of the poles under the magnetic field behave as magnetic charges suffering a Lorentz force that would be opposite in direction for the south pole and of the same direction for the north one. When there is not rigidity in the material of this solenoid in such a way that the splitting in the extremes can be increased, then, the magnetic field would produce an increase in the separation of the poles with the possibility of increasing its length. Therefore, in these circumstances, in the limit, each of the poles would behave as independent poles or monopoles. Besides, according to Dirac's idea, the monopoles would have an effective magnetic charge which the external magnetic field should produce a generalized Lorentz force similar to that which the electric field produces to the electric charge. On the other hand, in the Dirac model, the effective magnetic charge should be quantized according to the expression $g = h / (e \mu_0)$, h is the Planck constant, e the electric charge, and μ_0 is the vacuum magnetic permeability. The quantization of the magnetic charge, according this author, was a condition for explaining the electric charge quantization.

Five decades after, Cabrera [2] presented an empirical event in which this author justified the features of the superconducting current generated in a squid device by means of the magnetic monopole crossing through it. Unfortunately, this event has been never repeated. In any case, since Dirac argued the quantization electric charge is only possible explained via the existence of an also quantized magnetic charge, the theoretical research of the magnetic charge in the electrodynamics is a recurrent issue [3-8]. These circumstances have provoked, at the

present time, a systematic experimental pursuit of the magnetic charge existence in both the high energy physics [6] and within the material media [7-22].

Despite numerous attempts for obtaining evidences of elemental particles with magnetic charges, in both high energy physics and the cosmological radiation detection [6], the pristine Dirac idea of quantized magnetic charges has not been confirmed with any empirical evidence; only Cabrera's experiment results have been presented as a possible indication of monopoles existence. However, the recurrent issue of the existence of magnetic charges has recently received an important bang in a different sense to that which the pioneers of this theme attempted to design. Actually, recent experiments in solid materials, concretely in the so-called "spin-ices" [7-9,11-26] and the topological insulators [10] and also as a synthetized model of an actual one pole magnet [27] have been carried out detecting structural entities whose behaviour is mimetic to that of the magnetic charges.

These magnetic entities are not elemental particles with quantized magnetic charge but several low energy excitations whose half time life is large enough as to be detected. These entities are constituted of determined modifications in the magnetic structure which the nature designs creating an effective behaviour as that of the magnetic charges. The properties that present these effective magnetic monopoles within the spin-ices and described in these cited experiments make these compounds possible candidates for constructing devices able to propagate both information and energy.

The most extended studies about these magnetic entities are those arising from rare earth compounds of Holmium or Dysprosium and whose chemical formula are $Ho_2Ti_2O_7$ and $Dy_2Ti_2O_7$, and crystalizing in a pyrochlore type [28]. The main feature of this crystal consists of regular tetrahedra linked in each vertex to contiguous identical ones in which each vertex there is a rare earth whose magnetic moment is in the direction (1,1,1). Besides, in the ground state of the many-particle system, two magnetic moments of each tetrahedron are directed toward inside and other two toward outside the tetrahedra. Therefore, the magnetization of the system, in this ground state tends to zero. The crucial point in the spin-ice phenomenology raises when a magnetic moment $\vec{\mu}$ of a vertex suffer a spin flip and then the two contiguous tetrahedra losses their magnetic moment neutrality since one of them has three $\vec{\mu}$ coming on and one coming out, and the another tetrahedron vice versa. The magnetic structure of the spin-

ices is one in which the spin-flips can be produced with a minimal energy increase and the transmission of these spin flips can progress in the successive contiguous tetrahedra with small energy increases.
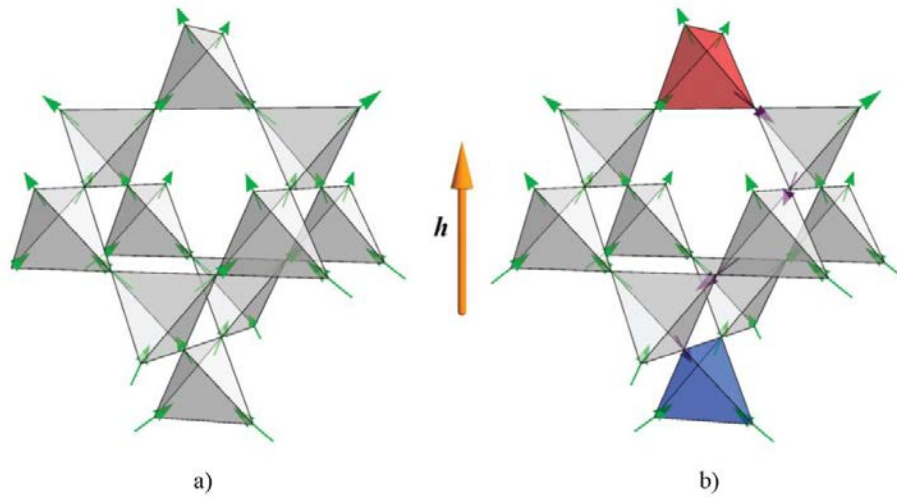
Figure 1.-Schematic generation of two magnetic charges [29].

In Fig. 1a, there is a schematic ground state of the linked tetrahedron without spin-flips. In Fig. 1b, the spin-flips has travelled in the crystal and two magnetic charges have been formed in the extremes of a virtual Dirac's string.

Castelnovo et al. designs at 2008 [7,8] the so-called dumbbell model in order to analyze the phenomenology of these spin-flips which progressively appear according to the system is located in low-energy excitation states due to the thermal energy. Bramwell et al. [12] initiates their studies about the mobility of these entities with the presence of external magnetic fields.

The main ingredient of this model is the substitution of the magnetic moments $\vec{\mu}_i$ of each vertex by a dipole of magnetic charges $\pm q_m$ in such a way that $\pm q_m = \pm |\vec{\mu}|/l$ being $\vec{\mu}$ a vector which starts in the negative q_m charge and ends in the positive one. Therefore, inside each tetrahedron without any spin-flip there are two positive and two negative charges in this model. When a spin-flip occurs, one of the two connected tetrahedra of the corresponding pair has $(+3\,q_m$ and $-1\,q_m$) and another one $(-3\,q_m$ and $+1\,q_m$). Consequently, the pair of tetrahedra

with a spin-flip is similar to a magnetic charge dipole whose magnetic charge is $g=+2|\bar{\mu}|/L$ in a tetrahedron and

$g=-2|\bar{\mu}|/L$ in its contiguous one, and L being the separation of two centers of the two contiguous tetrahedron.

When the spin-flip progresses through the crystal, the separation of the positive and negative charges increases and them the interaction energy between the two charges is $W_{ij}=\mu_0 g_i g_j /8\pi\, r_{ij}$, with $r_{ij}=\left|\vec{r_i}-\vec{r_j}\right|$, where $\vec{r_i}$

and $\vec{r_j}$ are the position of the two charges of the dipole, and g_i and g_j are equal to $\pm 2|\bar{\mu}|/a$, where a is the splitting length between the two centers of the contiguous tetrahedra participating on the spin flip (i.e. the height o each tetrahedron). When the spin flip runs the crystal, the resulting magnetic charges progressively interacts more weakly forming crystal structures that present similitudes to the Dirac's strings. The crystal dynamic allows the increase of the length of these strings which, in the limit, the resulting monopoles can be considered quasi-free magnetic charges. In this scenario, on a hand the constant volume specific heat [30] and the magnetic susceptibility [31] have been recently measured.
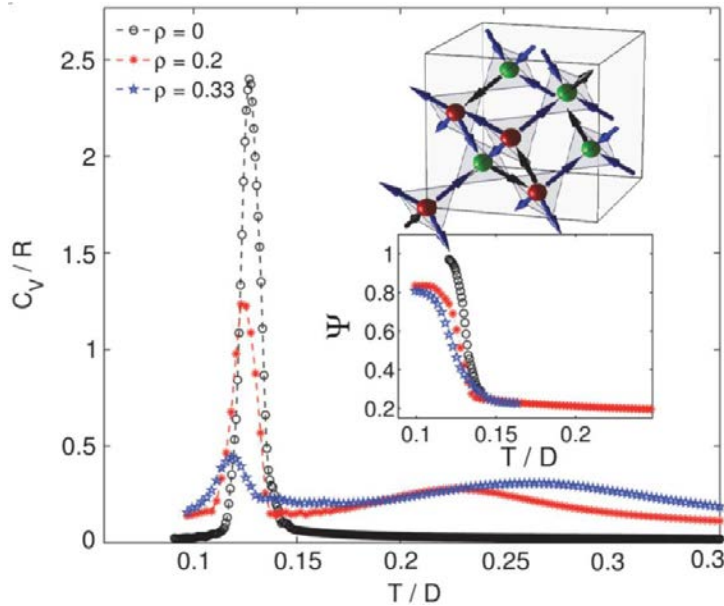
Figure 2.-Experimental specific heat [30].

In this figure, the specific heat for constant volume is carried out and, in this analysis, can be observed a sharp peak which can be attributed to the boson condensate formed by pole-antipole pairs which are coupled via the Coulomb interaction among the monopoles.
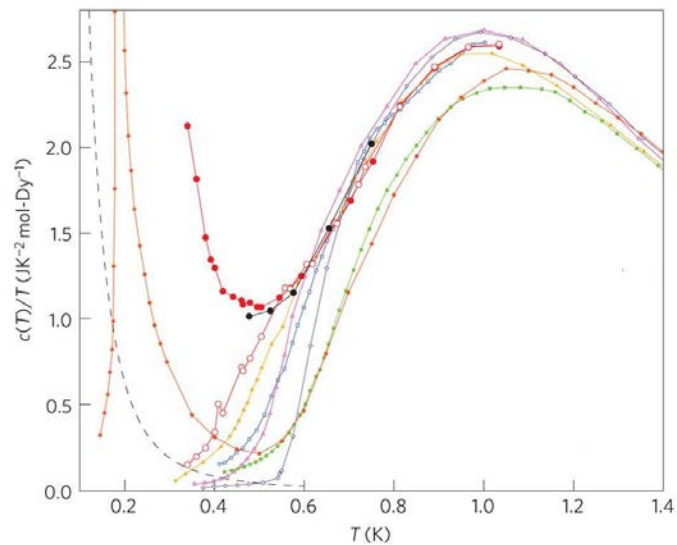
Figure 3. Several results of specific heat in work by Pomaransky et al [32].
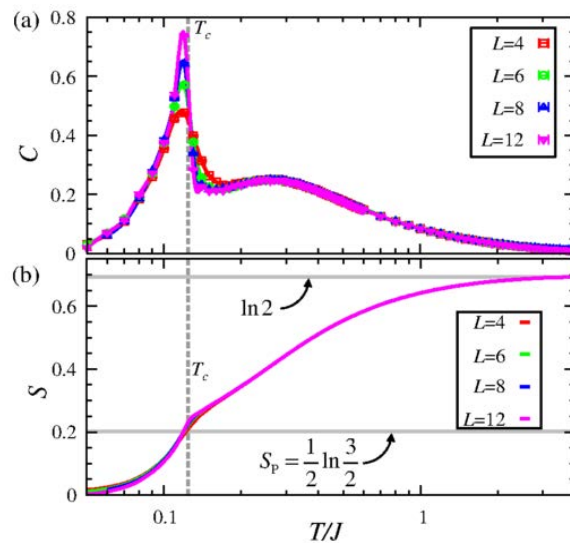
Figure 4. Especific heat and entropy coming from Kato and Shigeki [33].

In both independent experiments, two significative peaks appear in their experimental results, one of them appears to very low temperature, which is much sharper when the density of free magnetic charges is small and the another peak is wider and its cusp is less than that of the former peaks. These peaks in both different experiments coincide in the same temperature and may be interpreted by existence of different phase transitions.

15

The low temperature transition seems to occur when the pole-antipole pair configuration can be dominant. This many-particle state is formed when all possible spin flips are simultaneously produced given the fact that in a crystal all the vertexes are equal and therefore present the same probability for the occurrence of the spin-flips due to the crystalline coherence. Later we will discuss in what vertexes there may be and in which no spin flips, as well as what are the restrictions for these changes of direction in the magnetic moments. When the temperature increases the pole-antipole pairs are progressively broken with the correspondent generation of unconfined monopoles of different magnetic charge sign.

The explanation of these many-particle states in both their structure and dynamics are main goals of this thesis, as well as the prospective of possible applications. The finding of possible applications is carried out from the electromagnetic propagation phenomena in a quasi-particle system with magnetic charges submerged in a gas of magnetic dipoles and Dirac' strings of different lengths, these issues being the other main objective of this thesis.

Therefore, in this scenario we consider that there are two extremal states: the condensed magnetic pole-antipole pair configuration which is logic that can exist to low temperature and a state of quasi-free magnetic charges constituting true magnetic plasma. The experimental results of adiabatic response give evidence of monopole plasma oscillations in weak applied field, and unconventional critical behaviour in strong applied field. Really, the actual situation can be any possible intermediate state between the two extremal states where the confined dipoles, Dirac-like strings of different lengths and free magnetic charges coexist. For this diversity of different one body components which constitute the many-particle system, we introduce a two-quantum fluid model in order to explain the previous experimental data. Then, the electromagnetic propagation both in unlimited and confined substrates can put in evidence the different possibilities where the effective masses of the free charges and the density of carrier magnetic charges can be important parameters in the distinction of the different states. Consequently, in this thesis, we carry out a double study of the electromagnetic propagation.

On a hand, we analyze the linear response functions of an unconfined plasma state of the spin-ices by means of a transversal electromagnetic wave assisted with a constant and intense electric field whose direction is normal to the phase plane of the wave. On the other hand, we analyze the different modes within a wave microguide

which we suppose fulfilled of this spin-ice material. In the first process, we determine the plasmon frequency and the linear response function in the plasma phase. This linear response allows us to determine the effective mass of the magnetic charges connecting it with the main absorption frequency. This frequency is provoked by the precession oscillation of the magnetic charges under the action of the external electric field.

In the second analysis, we obtain a methodology for describing the electromagnetic propagation in confined waves both rectangular and cylindrical symmetry. This propagation is strongly dependent on the density of the magnetic charges. In addition, in this second study, we determine the mobility of the magnetization. This analysis allows to clearly discriminate the proportion of each corporative state for a determined temperature according to the behaviour under the electromagnetic wave propagation. On the other hand, as it is recently measured, the relaxation time of the excitation states which defines the magnetic charges is depending on the density of free monopoles and its mobility, physical variables which, at the present time, there is not a clear experimental procedure for obtaining them. With these two complementary analyses, we propose simple methodologies for determining these magnitudes which can clarify the classical mechanism of the movement the charges within both the magnetic plasma and the pole-antipole condensation state. These results are, in our opinion, interesting since although the concept of magnetic monopoles in spin-ice is clearly, conceptually and progressively consolidated, the mechanism of monopole mobility should start to be explained in order to obtain technological advantages of possible future devices.

CHAPTER 1: Master Formulae of Dumbbell Model

1. Dumbbell model

The magnetic interaction energy between the magnetic moments of the rare earth atoms of the antiferromagnetic network located at the vertices of the tetrahedrons can be expressed as a dipole-dipole interaction, which is commonly accepted considering both the short and long range and his expression is [7]:

$$E = J\sum_{i,j}\left[\vec{\mu}_i \cdot \vec{\mu}_j + \frac{\mu_0}{4\pi}D\left(\frac{\vec{\mu}_i \cdot \vec{\mu}_j}{r_{ij}^3} - \frac{3(\vec{\mu}_j \cdot \vec{r}_i)(\vec{\mu}_j \cdot \vec{r}_j)}{r_{ij}^5}\right)\right] \tag{1.1}$$

where J and D are empirically deductible coupling constants and the distance between the magnetic moments $\vec{\mu}_i$ and $\vec{\mu}_j$ is In this equation (1.1) The energy values are equal, except for quantitatively negligible errors, to those which come from considering the coulombian type interaction of magnetic charges that can be expressed in the following way:

$$E = \frac{1}{2}\sum_{i,j(r_{ij}\neq 0)}\frac{\mu_o}{4\pi}\frac{g_i g_j}{r_{ij}} + \sum_{i,j}\delta_{ij}\upsilon g_i g_j \tag{1.2}$$

where g_i and g_j are the magnetic charges whose values are given by $g=2|\vec{\mu}|/l$, where $|\vec{\mu}|$ is the module of the vector which has its origin in the negative magnetic charge and its end is in the positive magnetic charge (the atomic magnetic moments is given in Bohr magnetons), l is the separation between the barycenter of two contiguous tetrahedra. Besides, the term $\Sigma_0 = \upsilon g^2$ is the energy by generating a pair coupling (self-energy or rest energy). The interaction energy of two magnetic charges $\mu_0 g_i g_j / 4\pi r_{ij}$ implies each of them generates a magnetic field whose expression is:

$$\vec{B}(r) = \frac{\mu_0 g_i}{4\pi}\frac{\vec{r}-\vec{r}_i}{|\vec{r}-\vec{r}_i|^3} \tag{1.3}$$

The dumbbell model outlined above theoretically justifies the idea of magnetic monopoles in the spin-ices [7]. Besides, the conductance of equivalent magnetic charges in these materials [12,13] experimentally ratifies the effective existence of entities whose behaviour is mimetic to the magnetic monopoles. These experiments have been coined as "magnetricity", dual property of the electricity based on the conductance of hydrolyzed water ions

under strong electric field. Therefore, the magnetricity is the qualitative determination of the magnetic charge mobility inside of the spin-ices under the external magnetic field [12,13]. In the coulomb phase of the magnetic plasma into the spin-ices [25], the deconfined monopoles coexist with Dirac's string and confined magnetic dipoles, although the presence of effective magnetic charges can even be majority. Due to the dual symmetry, the external constant magnetic field interaction with the magnetic charge sea in this plasma phase modifies the density of magnetic charge distribution in such a way that when the magnetostatic equilibrium is attained, the effective magnetic charges stop moviment such as it occurs in the electronic conductors. $\sum \vec{F} = 0$. Therefore, inside this magnetic sea, the resulting magnetic field is vanishing, and then, we have that the force over any charge inside of the material is:

$$\vec{F}_{(\vec{r}_i)} = g^i \left(\vec{B}_{(\vec{r}_i)} \right) = g^i \left(\vec{B}_{ex(\vec{r}_i)} + \sum_{j \neq i} \vec{B}_{j(\vec{r}_i)} \right) = g^i \left(\vec{B}_{ex(\vec{r}_i)} + \sum_{j \neq i} \frac{\mu_0 g^j \left(\vec{r}_i - \vec{r}_j \right)}{\left| \vec{r}_i - \vec{r}_j \right|^3} \right) = 0 \tag{1.4}$$

where $\vec{B}_{(\vec{r}_i)}$ is the magnetic field generated by the g_j -charge and interacting with the g_i one. On the other hand, the magnetic field created by the g_j magnetic charges can be expressed as $\vec{B}_{(\vec{r})} = -\nabla \phi_m \left(\vec{r} \right)$. Consequently, the magnetic potential should be constant inside the magnetic sea of the plasma inside the spin-ices in the Coulomb phase. All these arguments lead to consider that the spin-ice materials can imply the total magnetic field screening. Actually, the dual magnetic charge Poisson equation, $\nabla^2 \phi_m \left(\vec{r} \right) = -\mu_0 \rho_m \left(\vec{r} \right)$, accomplishes the unicity theorem. Therefore, any solution of this equation in a determined volume V, which satisfies the condition $\phi_m \left(\vec{r} \right) = 0$ in all points of the closed surface containing V is the only solution of $\phi_m \left(\vec{r} \right)$ in all points of volume V. Hence, in any hollow surrounded of a material with mobile magnetic charges within it, the magnetic potential is constant and therefore the magnetic field is zero independently of the external magnetic field acting over this hollow. The only reservation for this magnetic field screening in the spin-ice-like materials is that the number of free magnetic charges within the spin-ice plasma state should be enough for compensating the external field within the material. This suggest an analysis consisting of the determination of evolution of the density $\rho_m \left(\vec{r} \right)$ in function of the external magnetic field, spatial localization and temperature, since these physical variables modify the formation of new magnetic monopoles via the creation of new spin flip within the magnetic structure.

2. Classical T-evolution of the systems with magnetic charges

The magnetic charge conduction properties imply that a good approximation of treating the dynamic of these monopoles is by considering to them as macroscopic classical objects, using the quantum local spins as classical magnetic moments whose movement produces effects such as precession and plasmon frequencies. Therefore, a main aspect of the phenomena of the spin-ice systems come from the density of effective monopoles when temperature increases. The increase of this density can induce properties such the magnetricity, magnetic field shielding, optical conduction features, etc, that can be effective in the charge sea inside the spin-ice structure.

Although, we consider that the origin and generation of the entities which emulate the behaviour of magnetic charges have quantum nature and origin, the importance can arise from the possible applications for transmitting, in a better way than that of electronic charges, the electromagnetic signals in such a way that can be constituted true magnetronic devices in a dual symmetric procedure to the electronic devices. In next section the quantum nature of the magnetic sea inside these materials is analyzed, however, we think that to know the space-temporal evolution of the macroscopic fields are basic for determining these possible future applications. Hence, we can need to analyze from Classical Physics the relation between the magnetic potential and the other electromagnetic Maxwell macroscopic fields within the magnetic charge sea and its relationship with the magnetic charge density which is appearing with the increasing temperature.

The starting point of this analysis is the determination of the temperature evolution of the appearance of the magnetic charges: The T-evolution implies the appearance of the presence of a number of magnetic monopoles whose production is due to the successive generation of Dirac's strings and posterior creation of two free magnetic charges of different sign for each string. Then, we can establish the following statistical formulation:

$$N(T) = \int_V \rho(\vec{r}, T) dV \tag{1.5}$$

where $N(T)$ is the total number of magnetic charges to T-temperature and $\rho(\vec{r}, T)$ the volumic density function of these charges. This function can be given by the Maxwell-Boltzmann statistics (25) by means of the expression:

$$\rho(\vec{r}, T) = \sum_j \delta(\vec{r} - \vec{r}_j) \exp\left(-\beta\left[g_j \phi(\vec{r}_j) + \Sigma_0\right]\right) \tag{1.6}$$

where $\phi\left(\vec{r}\right)$ is the potential of the magnetic field which interacts with these charges, and Σ_0 is the self-energy

[7], i.e. the necessary energy for generating a magnetic monopole; $\beta = \left(K_B T\right)^{-1}$ (with K_B being the Boltzmann

constant and T absolute temperature); g_i is the magnetic charge of the new quasi-particles arising with growth

temperature. Then, $N\left(T\right)$ can be given by:

$$N\left(T\right) = \sum_{i}^{M} \left\langle \rho\left(\vec{r},T\right)\right\rangle_{\Delta V_i} \Delta V_i \tag{1.7}$$

$$\left\langle \rho\left(\vec{r},T\right)\right\rangle_{\Delta V_i} = \frac{1}{\Delta V_i}\int_{\Delta V_i} \rho\left(\vec{r},T\right)dV = \frac{1}{\Delta V_i}\sum_{j}\exp\left(-\beta\left[g_i\phi\left(\vec{r}\right)+\Sigma_0\right]\right) = n\left(\vec{r}_i\right) \tag{1.8}$$

and this allows us to define the density of new particles as:

$$n\left(\vec{r}\right) = n_0 \exp\left(-\beta\left[\phi\left(\vec{r}\right)+\Sigma_0\right]\right), \tag{1.9}$$

where $n\left(\vec{r}\right)$ is the density of magnetic charges depending on the spatial localization; this is the density of the total

confined magnetic charges in any element of volume ΔV_i in the dumbbell model in a homogeneous system. If now

we consider the gradient of this scalar potential, this becomes:

$$\nabla n\left(\vec{r}\right) = -n\left(\vec{r}\right)\beta g \nabla \phi\left(\vec{r}\right) \tag{1.10}$$

and therefore:

$$\nabla\left(\ln\left[n\left(\vec{r}\right)\right]+\beta g\phi\left(\vec{r}\right)\right) = 0 \tag{1.11}$$

and consequently:

$$\ln\left[n\left(\vec{r}\right)\right]+\beta g\phi\left(\vec{r}\right) = C \tag{1.12}$$

from this later expression, we can determine the magnetic (dual of electric) scalar potential in function of

temperature and the spatial localization, whose expression is:

$$\phi\left(\vec{r},T\right) = -\frac{K_\beta T}{g}\ln\left[n\left(\vec{r}\right)\right]+\frac{K_\beta T}{g}C \tag{1.13}$$

with C being a constant, which should be determined via the physical conditions for the critical temperatures. For

$T = T_C$, the corporative system is in a low energy excitation state whose energy $g\phi_0$ can be experimentally

determined. This state can be, for instance, closer to a perfect coulombian and plasma state, and then $n\left(\vec{r}\right) = n_0$

where n_0 is the maximum possible value of positive magnetic charges in a critical plasma state. Hence, in this

case $\phi\left(\vec{r}\right) = \phi_0$, with ϕ_0 being a constant potential similar to those existing in the dual conducting electric plasma

state. In a consequence, we have the following value for the C-constant:

$$C = \frac{g}{K_\beta T_c}\phi_0 + \ln\left[n_0\right] \tag{1.14}$$

from this expression we obtain that the solution of the magnetic potential for a g-charge is:

$$\boxed{\phi\left(\vec{r},T\right) = \frac{K_\beta T}{g}\ln\left[\frac{n_0}{n\left(\vec{r}\right)}\right] + \frac{T}{T_c}\phi_0} \tag{1.15}$$

where T_c is a critical temperature for which there is the maximum number of free magnetic charges and then the

$\phi\left(\vec{r}\right) -$ potential is ϕ_0. To obtain equation (1.15), it is necessary to know the values of the magnetic potential, ϕ_0,

and the density of magnetic charge carriers, n_0, at some critical point, which may well be that coming from any

of the phase transitions that arise in these materials. The above equation is important (this is a master formula

which is used in several points of this work of the chapters 2 and 3) since relates the scalar magnetic potential with

temperature and density of monopoles. In order to obtain information about this density, $n\left(\vec{r}\right)$, we can use two

ways, one of them is to take experimental results if they are available (in chapters 4 and 5, we give possible

experiments of electromagnetic propagation which allow to obtain these $n\left(\vec{r}\right)$ and n_0.

Another theoretical process is to find a systematic analysis for determining the spatial diffusion of magnetic

monopoles which may produce a $\vec{r}$ distribution in function of temperature. From this latter option, we can consider

the following mathematical procedure for obtaining $n\left(\vec{r}\right)$. We start from Eq. (10) $\nabla n\left(\vec{r}\right)\big/n\left(\vec{r}\right) = -\beta g\nabla\phi\left(\vec{r}\right)$ and

taking into account divergence in both side of this equality, we obtain:

$$\nabla\left(\frac{\nabla n\left(\vec{r}\right)}{n\left(\vec{r}\right)}\right) = -\beta g\nabla^2\phi\left(\vec{r}\right) \tag{1.16}$$

and taking into account the Poisson equation for the magnetic charges:

$$\nabla^2\phi\left(\vec{r}\right) = -\mu_0\left|g\right|\left(n^+\left(\vec{r}\right) - n^-\left(\vec{r}\right)\right) = -\mu_0 gn\left(\vec{r}\right)$$

(1.17)

where the sign $\pm$ indicates the corresponding density of positive and negative magnetic charges. From Eq. (1.16) and the above Poisson magnetic equation of potential, it is straightforward to obtain the following equation for the spatial evolution of $n^\pm\left(\vec{r}\right)$:

$$\frac{1}{n^\pm\left(\vec{r}\right)}\nabla^2 n^\pm\left(\vec{r}\right) - \frac{1}{\left(n^\pm\right)^2\left(\vec{r}\right)}\left(\nabla n^\pm\left(\vec{r}\right)\right)^2 = \pm\mu_0\beta\left|g\right|^2\left(n^+\left(\vec{r}\right) - n^-\left(\vec{r}\right)\right)$$

(1.18)

where $n^+\left(\vec{r}\right)$ and $n^-\left(\vec{r}\right)$ are the number/volume of positive and negative magnetic charges. These two equations are general for cases in which the dynamic of the charged particles can be treated by means of a classical potential. The solutions depend on both the symmetry and the dimension of the magnetic system and their achievements can be very complex. Complexity which can be softened considering physical conditions. Another expression deduced for the density of particles can directly be deduced from (1.16) and (1.17) and then the two equations (1.18) are converted in an identical equation whose expression is:

$$\boxed{n\left(\vec{r}\right)\nabla^2\left(\vec{r}\right) - \left(\nabla n\left(\vec{r}\right)\right)^2 = \mu_0\beta\left|g\right|^2 n^3\left(\vec{r}\right)}$$

(1.19)

where $n\left(\vec{r}\right)$ is the total density of magnetic charges. This Eq. (1.19) is very complex problem in obtaining the general solution of the differential equation and can be converted in another more simplified:

$$\nabla^2 u\left(\vec{r}\right) = \alpha\exp\left[u(\vec{r})\right]$$

(1.20)

where $\alpha = \mu_0\beta\left|g\right|^2$ and the transformation of Eq. (1.19) to Eq. (1.20) is obtained by means the change $n\left(\vec{r}\right) = \exp\left[u\left(\vec{r}\right)\right]$, and then the non-linear and inhomogeneous differential Eq. (1.19) is converted in the linear and inhomogeneous Eq. (1.20) and both equations being second order differential equations in partial derivatives. Obviously, Eqs. (1.19) and (1.20) depend on the dimensions and symmetries of the physical systems and should be deduced via the procedures of differential equations in partial derivatives.

The easiest particular solution for Eq. (1.19) which can serve of guide is the consideration of one-dimension system, this equation has the following expression:

$$n(x)\frac{d^2n(x)}{dx^2}-\left(\frac{dn(x)}{dx}\right)^2=\mu_0\beta|g|^2\,n^3(x) \tag{1.21}$$

and this equation has the following particular solution:

$$n(x,T)=\frac{2K_\beta T}{\mu_0\,|g|^2\,x^2} \tag{1.22}$$

This expression is important because determines as the number of magnetic charges decreases with the distance from the center of formation of magnetic charges and increases lineally with temperature.
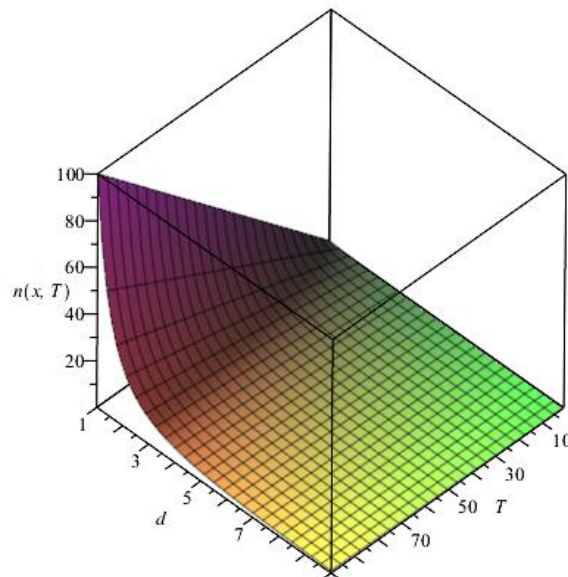
Figure 5.-T-evolution of the density of free magnetic charges.
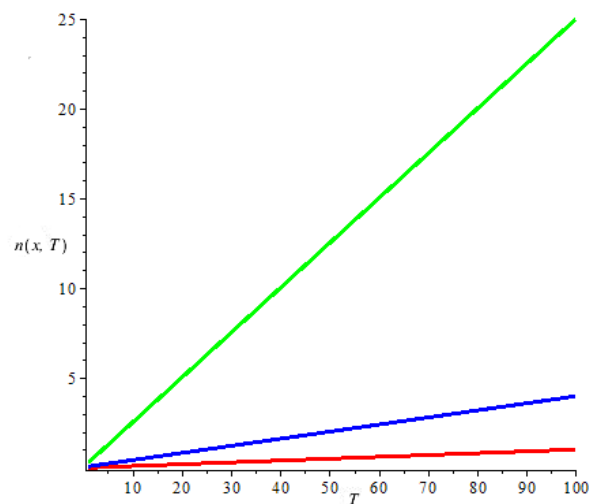
Figure 6.-Variation of the density of magnetic charges vs. temperature.

This figure represents the number of free magnetic charges per volume unit in function of temperature for three distances of the initial center of magnetic charges formation.
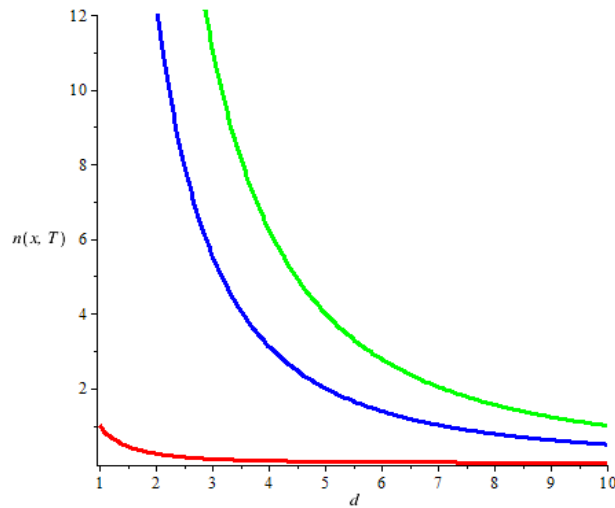
Figure 7.-Variation of the density of magnetic charges vs. distance.

In this figure, we give the density of free magnetic charges in function the distance of the initial center of the formation of the charges. For slightly larger than plasma physics temperature, the spatial evolution of this density (red line) is almost constant. These results are compatible with the theoretical idea of the constant existence of the magnetic charge density in the plasma state spin-ice phase. The blue line corresponds to $10\,T_C$ and for this temperature the increasing density is faster than the red line but much less fast than that for $100\,T_C$ (green line).

The density of magnetic charge carriers is one of the most important magnitudes in order to configurate the different phases of the spin-ices. In addition, in next sections in which we analyze different electromagnetic propagation, we prove the decisive dependence on this density of all properties of EM transmission in possible devices constituted by material containing magnetic charges. The reasons for this importance are of two types: in a first place the electromagnetic transmission of information improve when the density of free magnetic charges tends to a maximum and in a second place, this microwave conductivity is blocked in the Bose condensate phase is closed. This tendency is limited for large temperature since from a determined increasing limit the magnetic structure can be affected even destroyed and then the magnetic entities tend to disappear.

Other magnitude which can have an important role in the phase transition is the magnetic interaction among magnetic charges for temperatures larger than T_C . For these temperatures, this energy interaction per unity of magnetic charge in a system in one spatial dimension becomes:

$$\phi\left(x,T\right)=\frac{K_{\beta}T}{g}\ln\left[\frac{\mu_0 n_0 g^2 x^2}{2K_{\beta}T}\right]+\frac{T}{T_c}\phi_0 \tag{1.23}$$

This interaction, according to Eq. (1.23), whose physical units are volts per seconds/meters tends to ϕ_0 when $T \rightarrow T_c$ (critical temperature for which the system evolution towards a magnetic plasma), and its variation with temperature is given in the following figures.
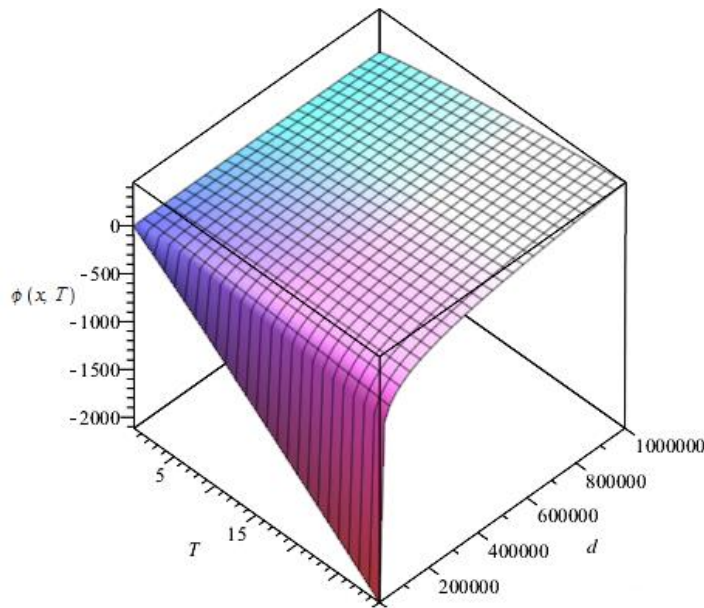
Figure 8.-Interaction potential energy for each free magnetic charge.

In this figure, we represent the energy interaction for each magnetic charge in function of the temperature and distance from the initial site where is provoked the presence of the magnetic charges.
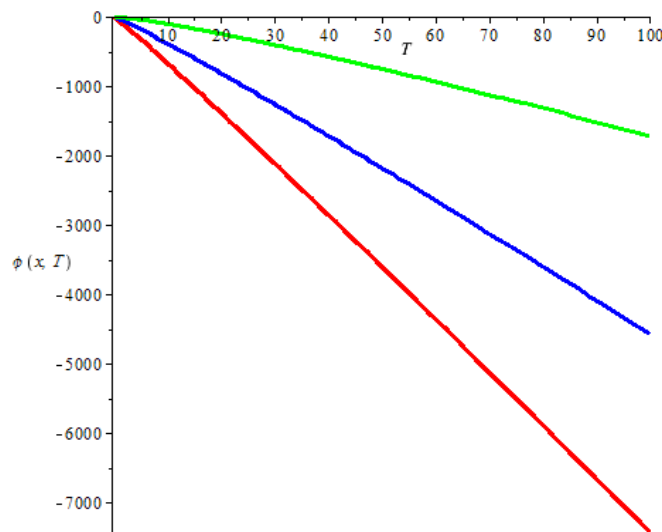
Figure 9.-Variation of energy interaction vs. temperature.

The dependence on temperature is almost lineal and for increasing distance the variation with temperature, the energy interaction is decreasing.
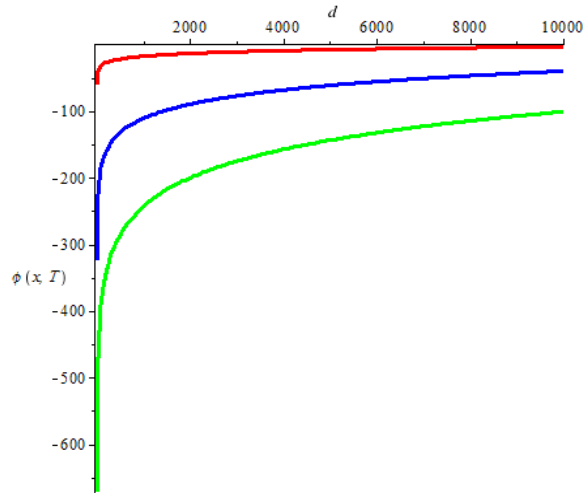
Figure 10.-Variation of the energy interaction vs. distance.

This figure represents the variation of the energy interaction for each magnetic monopole in function of distance for three temperatures. The red curve corresponds to temperature slightly greater than the critical temperature and therefore, the value is almost constant with the distance since the plasma state transition phase is closed (this constant value of the potential is coherent with the behaviour in an electric plasma dual of the spin-ice magnetic plasma). According to temperature increases, the absolute value of variation of this energy increases because the density of magnetic charges also increases.

In the case of zero magnetic field inside the spin-ice material (i.e. for the case of perfect magnetic field screening within the material), from Eq. (1.4) it is obvious that $n\left(\vec{r}\right)$ has to be constant due to the characteristic of the dual "metallic" phase of the magnetic plasma state. In addition, if the divergence of $\vec{B}$-field is zero, $\nabla \cdot \vec{B} = 0$, this implies that $\nabla^2 \phi\left(\vec{r}\right) = 0$ and then Eq. (1.19) is:

$$n\left(\vec{r}\right)\nabla^2 n\left(\vec{r}\right) - \left(\nabla n\left(\vec{r}\right)\right)^2 = 0 \tag{1.24}$$

There are two types of solutions for this equation. The first of them is an exponential analytical form whose kind can be $n\left(\vec{r}\right) = A\exp\left(\alpha \vec{k}\vec{r}\right)$, where the parameter A and α are two scalar parameters where α can be either

28

real or complex number and $\vec{k}$ is a wave vector which indicate the propagation of the wave of generation of magnetic monopoles. These parameters become determined via the symmetry properties of the systems. The possible results of the distribution of the density of magnetic charges coming from this latter solution contains those "crystal" periodic structures which have been detected and described recently [34] in the phases in which the coulombian potential can produce.

The second kind of particular solution of the above differential equation of $n\left(\vec{r}\right),$ is the $n\left(\vec{r}\right)=n_0$, with n_0 being a real constant. This solution which seems obvious is the particular solution which has a clear and robust physical meaning. This constant can be zero, i.e. $n_0=0$, then, this implies that the sum of positive and negative magnetic charges that, due to the assumed premises of the dumbbell model, implies a jellium-like system. In this system which the density of negative charges in compensated with an equal density of magnetic positive charges ie identical to that of the classical plasma state of the perfect electric metallic state.

3. Thermodynamic rigorous treatment of the classical monopole system

The probability that a magnetic charge to be formed in a place of crystalline network that in the case of the spin-ices compounds will be in a vertex of one of its tetrahedra will be given by means of the following expression:

$$n\left(\vec{r_i}\right)=\frac{\exp\left(-\beta\left[\,|\,g_i\,|\,\phi\left(\vec{r_i}\right)+\Sigma_0\,\right]\right)}{\sum_j\exp\left(-\beta\left[\,|\,g_i\,|\,\phi\left(\vec{r_i}\right)+\Sigma_0\,\right]\right)} \tag{1.25}$$

where all the variables have been previously defined. And if we consider a step to the continuum we will have the following equality:

$$n\left(\vec{r_i}\right)\xrightarrow{\text{continuum}}n\left(\vec{r}\right)=\frac{\exp\left(-\beta\left[\,|\,g\,|\,\phi\left(\vec{r}\right)+\Sigma_0\,\right]\right)}{\frac{1}{V}\int_v\exp\left(-\beta\left[\,|\,g\,|\,\phi\left(\vec{r}\right)+\Sigma_0\,\right]\right)dV} \tag{1.26}$$

and calculating the gradient of the continuous expression of the mentioned probability we have the following (see Appendix A):

$$\nabla n\left(\vec{r}\right)=n\left(\vec{r}\right)(-\beta|g|)\left(\nabla\phi\left(\vec{r}\right)-\left\langle\nabla\phi\left(\vec{r}\right)\right\rangle\right) \tag{1.27}$$

and this equation can be simplified as follows:

$$\nabla\left\{\ln\left[n\left(\vec{r}\right)\right]+\beta\,|\,g\,|\,\phi\left(\vec{r}\right)\right\}=\vec{C} \qquad (1.28)$$

where the constant vector of the right-hand side of the above equality is:

$$\vec{C}=\beta\,|\,g\,|\,\left\langle\nabla\phi\left(\vec{r}\right)\right\rangle \qquad (1.29)$$

and in a crystal of great symmetry this constant vector becomes null, and then, we have

$$\ln\left[n\left(\vec{r}\right)\right]+\beta\,|\,g\,|\,\phi\left(\vec{r}\right)=C \qquad (1.30)$$

whose solution is equal to that of the heuristic treatment of former section. If on the contrary, we consider that the constant vector $\vec{C}$ is different from zero, then:

$$f(\vec{r})=\ln\left[n\left(\vec{r}\right)\right]+\beta\,|\,g\,|\,\phi\left(\vec{r}\right) \qquad (1.31)$$

and it is a function defined in all space in which the surfaces $f(\vec{r})=C$ whose gradients of these functions are plane whose normal characteristic vector is $\vec{C}$. Then, the system in equilibrium is formed by maintaining constant the function $f(\vec{r})$ in parallel planes whose characteristic vector is the aforementioned vector $\vec{C}=\beta\,|\,g\,|\,\left\langle\nabla\phi\left(\vec{r}\right)\right\rangle$.

This distribution being confirmed by some experimental data obtained by Sazonov et al. [50]. Otherwise, the solution of the differential equation (1.27) is the Eq. (1.15):

$$\phi\left(\vec{r},T\right)=\frac{K_{\beta}T}{g}\ln\left[\frac{n_0}{n\left(\vec{r}\right)}\right]+\frac{T}{T_c}\phi_0$$

where n_0 is the probability of having a magnetic charge at temperature T_c in each tetrahedron in which the spin-flips is possible, and ϕ_0 is its magnetronic potential. This magnetronic potential $\phi\left(\vec{r},T\right)$ is zero for 0 K and ϕ_0 at T= T_c, and at any temperature T, this potential is related with the probability of obtaining in all crystal sites a magnetic charge given by Eq, (1.26). This expression being essential in the quantum mechanics analysis which it is considered as follows.

4.   Classical Electrodynamics of Dumbbell model. Different magnetic fields within spin-ices

It is necessary to define with precision the different concepts of magnetic field within a solid in general and in spin-ices in particular, given that although we are talking about magnetic monopoles and magnetic charges, we are going to demonstrate, because it is crucial in the contents that follow then, that the divergence of the "Maxwell field" within the spin-ices remains zero. Therefore, it is necessary to explain this apparent contradiction. On the one hand, there is the field that corresponds to Maxwell's equations. This field is a macroscopic field that is defined as a middle field on a volume element, which although being the differential element of mathematical integrations, is of a dimension of several orders of magnitude greater than the atomic or molecular dimensions [36,37]. This field has the particularity that it is of zero divergence even in the "spin-ices" [25], this fact, as I said, could put in question the concept of monopoles whose genuine definition seems to be that which is field source whose divergence is different of zero.

However, the micromagnets that give rise to the Dirac strings in these materials and that their presence grows with that of the outer magnetic field initially have atomic dimensions. Therefore, the analysis of this field in these dimensions is important because it is one that has the responsibility for the electrodynamics of the system in these materials. Therefore, it is necessary to review the concepts of the different microscopic, molecular and local fields, as well as their relationship with the macroscopic field or Maxwell field.

We are going to prove that there are entities defined as magnetic monopoles in "spin-ices" [7-9, 11-14, 19, 25] which are of such a nature that the equation $\nabla \cdot \left\langle \vec{B} \right\rangle = 0$ is valid, where the field $\left\langle \vec{B} \right\rangle$ is the field named of Maxwell and that refers to the middle field in a volume element where many molecules exist, for that reason an analysis of the different scales in which the different electromagnetic fields are defined must be done.

The macroscopic scale, whose definition is simple as the word itself indicates, is that of macroscopic objects ranging from the dimension of the Universe to the dimensions of the laboratory samples to which we wish to make measurements to determine their electromagnetic properties, such as function dielectric, magnetic susceptibility, conductivity, etc. These samples come to be in the order of centimeters in each linear dimension.

Secondly, it should be considered that the properties of materials are defined or determined by physical variables that are deduced from mathematical integrations in an enclosure normally of one, two or three Euclidean dimensions, where the integrand has a certain variability. For example, the magnetic field depends on the current density function, and the electric field of charge density. So, it will be that the integration of the physical variable whether scalar or vector will come defined by $C = \int_R I(x,y,z,t)d^n r$, where n is the dimension of the enclosure. This integration is calculated in such a way that the value of the variable is given by $C(t) = \sum_{i,j,k} I(x_i, y_j, z_k, t) \Delta x_i \Delta y_j \Delta z_k$ where $\Delta x_i \Delta y_j \Delta z_k = \Delta \upsilon$, being a volume element called differential in which it is assumed that the variable $I(x_i, y_j, z_k, t)$ remains constant in a moment of time, t. That is, if that variable had variability in the volume element $\Delta \upsilon$, that element would have to be reduced and the number in the summation increased, or alternatively, if the dimensions of this volume element are less than the empirical measurement capacity, it is necessary to conform with determining the average value of that variable in the volume element. This second situation is what Maxwell thought and is that when the dimensions of $\Delta \upsilon$ are less than 10^{-9} and 10^{-12} υ , with υ being the size of the macroscopic object, it is difficult for any probe that can directly or indirectly evaluate the variable $I(x_i, y_j, z_k, t)$. Therefore, Maxwell's field is always taken as mean values in the differential enclosures [36,37].

However, the dimensions of the entities that are capable of being called magnetic charges, which come from so-called micromagnets, have atomic dimensions that are in the range between 10^{-21} and 10^{-24} the minimum macroscopic dimensions, υ , that I have set in 10^{-6} m^3 . Which implies that in each differential element of volume, $\Delta \upsilon$,can contain between $\approx 10^9$ and 10^{12} molecules or micromagnets. Consequently, the fields that affect these micromagnets cannot be defined as Maxwell fields, that is, middle fields in the volume element.

Hence, in this section we perform an analysis of the different electromagnetic fields within the two models that Castelnovo et al. [7, 8] demonstrated to be equivalent: the magnetic structure configuration of magnetic moments and the "dumbbells". In classical electromagnetism, a potential magnetic vector is associated with each unit entity that has a magnetic moment $\vec{m_i}$. This magnetic potential defines a magnetic field at a point that is usually

called the microscopic field [36-42], $\vec{B}'(\vec{r}) = \nabla \times \dfrac{\mu_0}{4\pi} \sum_i \int_{V'} \dfrac{\vec{J}_i(\vec{r}')}{|\vec{r}-\vec{r}'|} d^3r'$, where $J_i(r')$ is the electric current of the particle,

or structural entity that generates magnetic field and the magnetic moment is defined by $\vec{m}_i = \dfrac{1}{2} \int \vec{r} \times \vec{J}_i(\vec{r}) d^3r$.

The field called macroscopic or magnetic medium in matter, which appears in Maxwell's standard equations [36,37], can be obtained by means of the following processes [40,42]. In the first step, the contribution of all the magnetic moments in matter is determined by excluding a small volume, $\Delta\upsilon$, which can be chosen spherical without loss of generality and in order to simplify. This small volume is defined in the infinitesimal scale and is the one that contains the point where the electric and magnetic fields must be calculated. The dimensions of this volume are small enough to consider the fields, charge and current densities of the Maxwell equations constant throughout this volume element. But the dimensions of $\Delta\upsilon$ are large enough to contain a large number of tetrahedral molecules of "spin-ices". A second contribution is the magnetic field of mean value created by the magnetic dipole moments of the molecules within this differential volume element. These two terms constitute the so-called macroscopic fields or middle fields of the magnetic (or dielectric) material, which are those of the standard Maxwell equations.

When considering the model of "Dumbbell" with magnetic charges, the average value of the field generated by all these charges located in a small spherical volume can be written as:

$$\left\langle \vec{b} \right\rangle_{\nabla\upsilon} = \frac{1}{\Delta V} \int_{\Delta V} \vec{B} dV = -\frac{3}{4\pi R^3} \frac{\mu_0}{4\pi} \sum_i \int_{\Delta V} \nabla \left(\frac{g_i}{|\vec{r}-\vec{r}_i|} \right) d^3r =$$

$$= -\frac{3}{4\pi R^3} \frac{\mu_0}{4\pi} \sum_i g_i \int_{\Delta V} \left(\frac{\vec{n}}{|\vec{r}-\vec{r}_i|} \right) dS = -\frac{\mu_0}{4\pi R^3} \sum_i g_i \vec{r}_i = -\frac{\mu_0}{3} \vec{P}_m$$

where $\vec{P}_m$ is the polarization of the magnetic dipole charge formed by a split of the monopole and antimonopole pair confined, in a similar way to what occurs in the electric field with electric dipoles. The integral of above equation $\oint_{\Delta S} \dfrac{\vec{n}}{|\vec{r}-\vec{r}_i|} dS$ obviously depends on the geometry of $\Delta\upsilon$ and it is a determining factor in the final result of the formulation of the equation, but another geometry different from the spherical shape preserves the functional dependence of the mean value field $\left\langle \vec{b} \right\rangle_{\Delta V}$. An indication to obtain the value of the integral is the following

$\oint_{\Delta S} \dfrac{\vec{n}}{\left|\vec{r}-\vec{r_i}\right|} dS = \vec{e}_z \int_0^\pi \dfrac{R^2 \cos\theta \sin\theta}{\left(R^2 + r_i^2 - 2Rr_i\cos\theta\right)^{1/2}} d\theta = \dfrac{4\pi \vec{r_i}}{3}$. The calculation of the average magnetic field generated by

all the charges located in a small spherical volume $\left(\Delta V = \dfrac{4}{3}\pi R^3\right)$ is $<\vec{b}>_{\Delta V} = -\dfrac{\mu_0}{4\pi R^3}\sum_i g_i \vec{r_i} = -\dfrac{\mu_0}{3}\vec{P}_m$, and in

an analogous way we can obtain the average value of the electric field in the volume element if we consider that

there are electric charges and therefore its value [36,37,41,42] is $\left\langle \vec{e}' \right\rangle_{\Delta V} = -\dfrac{1}{4\pi\varepsilon_0 R^3}\sum_i q\vec{r_i} = -\dfrac{1}{3\varepsilon_0}\vec{P}_e$.

The average value of the magnetic field in the volume created by the magnetic moments from the electric

charge currents corresponding to the molecules inside the element can be obtained by means of:

$$\left\langle \vec{b}' \right\rangle_{\Delta V} = \frac{1}{\Delta V}\int_{\Delta V} \nabla \wedge \vec{A}(\vec{r}) d^3r = \frac{3}{4\pi R^3}\frac{\mu_0}{4\pi}\int_{\Delta V}\int_{\Delta V} \nabla \times \frac{\vec{J}_e(\vec{r}')}{\left|\vec{r}-\vec{r}'\right|} d^3r' d^3r = \frac{3}{4\pi R^3}\frac{\mu_0}{4\pi}\int_{\Delta V}\oint_{\Delta S}\vec{n} \times \frac{\vec{J}_e(\vec{r}')}{\left|\vec{r}-\vec{r}'\right|} dS d^3r' =$$

$$= \frac{3}{4\pi R^3}\frac{\mu_0}{4\pi}\int_{\Delta V}\left(\oint_{\Delta S}\frac{\vec{n}}{\left|\vec{r}-\vec{r}'\right|} dS\right) \times \vec{J}_e(\vec{r}') d^3r' = \frac{\mu_0}{4\pi R^3}\int_{\Delta V}\vec{r}' \times \vec{J}_e(\vec{r}') d^3r' = \frac{2\mu_0}{4\pi R^3}\vec{m}_e = \frac{2\mu_0}{3}\vec{M}_e$$

where $\vec{M}_e$ is the macroscopic magnetization due to electric currents which are the magnetic moment of the

lanthanide atoms which are in the vertexes of the tetrahedra, such as it is commented throughout the text. For the

validity of the "dumbbells" model, equation it is necessary that $K\vec{P}_m = \mu_0 \vec{M}_e$. So if the contribution of the magnetic

field of the molecules out volume $\Delta\upsilon$ is $\vec{B}_0$, the averaged field $\left\langle \vec{B}' \right\rangle$ coming from the spin configuration is

$\left\langle \vec{B}' \right\rangle = \vec{B}_0 + \left\langle \vec{b}' \right\rangle_{\Delta V} = \vec{B}_0 + \dfrac{2}{3}\mu_0 \vec{M}_e$ and the magnetic fields due to the magnetic charges according to the dumbbells

is $<\vec{B}>_{\Delta V} = \vec{B}_o + <\vec{b}>_{\Delta V} = \vec{B}_o - \dfrac{K}{3}\vec{P}_m = \vec{B}_o - \dfrac{\mu_0}{3}\vec{M}_e$.

Therefore, the difference between the average magnetic fields $\left\langle \vec{B}' \right\rangle$ and $\left\langle \vec{B} \right\rangle$ is: $\left\langle \vec{B}' \right\rangle = \left\langle \vec{B} \right\rangle + \mu_0 \vec{M}_e$,

consequently, one should differentiate two magnetic fields, the averaged magnetic field $\left\langle \vec{B} \right\rangle$ coming from the

dumbbell model and that coming from spin configuration $\left\langle \vec{B}' \right\rangle$, which is the only field whose divergence is zero,

defined by the standard Maxwell equations, in such a way that, $\nabla \cdot \left\langle \vec{B} \right\rangle = \mu_0 \rho_m$, where, we have $\rho_m = -\nabla \cdot P_m$

which is the density of magnetic charges . In the "spin-ices" it is a three-dimensional system in which there is no long-range ordering, therefore they are disordered magnetic systems [38,39,41], and, as a consequence, the macroscopic magnetization $\vec{M}_e = 0$ and $\left\langle \vec{B} \right\rangle = \left\langle \vec{B}' \right\rangle$.

The fact of annulment of the macroscopic magnetization defined via either the classical way or the existence of entities which mimic the magnetic charges is coherent with the jellium solution for the Eq. (1.19). This solution implies a "metallic" null density of magnetic charges as a valid solution for this differential equation, (1.19), when one considers the 3-dimensional problem. The mathematical derivation of the general solution of this very complex non-linear and second order differential equation in partial derivatives is a very difficult to find. This implies that the particular solution of this metallic null density in which the density of positive magnetic charges is equal to that of the negative ones is a valid image in which there is concordance with the recent interpretations [11-13, 25] of the magnetic field in "spin-ices" that emphasizes the fact that in these structures, the magnetic monopoles are such that Maxwell's magnetic field continues satisfying the following equation

$$\nabla \cdot \left\langle \vec{B} \right\rangle = 0 \tag{1.32}$$

Such as we have proven. Therefore Eq. (1.19) and its apparent trivial particular solution in which $gn(\vec{r}) = g^+ n^+(\vec{r}) + g^- n^-(\vec{r}) = |g|\left(n^+(\vec{r}) - n^-(\vec{r}) \right) = 0$, is the only solution of Eq. (1.19) which allows us to consider the condition (1.32), in which there is a certain consensus in the theory of the spin-ice phenomena. This equation is very relevant in the spin-ices because it is paradoxical and apparently contradictory with the fact of talking about magnetic monopoles and magnetic charges. But as we have demonstrated in this section there is no contradiction because the field whose divergence is zero even existing these entities that partially mimic the magnetic charges, is the average field of Maxwell, while the microscopic or molecular fields can have divergence not null in these dual electrodynamics. On the other hand, it forces us to reinterpret the concept of magnetic charge when it is only possible to introduce it in the case of density of these quasi-particles being zero. This being so strange, that is why we use space in this document in the demonstration from the definitions of the different fields that the divergence of the field is zero when this fact already published in 2011 [41], but it is the conciliation with the solution of equation (1.19) that legitimizes the strange condition (1.32) when one can continue talking about magnetic monopoles.

CHAPTER 2: Many-Body States as Independent Magnetic Fluids

1.   Low energy excitation states and phase transitions in spin-ice systems

There is a certain confusion that could be described as bibliographic chaos, full of contradictions in experimental results about the nature of the global excited states of the system at low, very low, temperatures (between 0.05K and 0.5K) in the case of spin-ices. Therefore, between this chapter 2 and the next 3, we discuss three possible natures of the excited state of lowest temperature in which there are the discrepancies that we show at the end of chapter 3. On the contrary, in the states of quasi- free magnetic charges, perhaps with less theoretical interest because there is a certain consensus based on a state of magnetic plasma, a concept that is recognized with clarity, appears as the ideal situation to find experimental applications for electromagnetic propagation that allows the construction of "electronics devices"which in this case should be named "magnetronic devices".

Consequenly, in the present chapter we study the global excitation states of the system at low temperatures. We determine the properties of many-particle states from their individual components. The objective of this study is to delimit the possibilities that these states have for obtaining devices in which the electromagnetic propagation allows to design applications of circuital order that transmit energy and information. In turn, we analyze phase transitions between different many-particle states. We consider that the low temperature transition occurs when the pole-antipole pair configuration is suddenly constituted via the generation of the spin flips in all the possible vertexes. The formation magnetic dipoles according to the dumbbell model implies that the nature of one-body components of the many-body state can be bosonic since the simplest components are constituted of two magnetic charges in a confined and composed particle. When the temperature increase the pole-antipole pairs are progressively broken with the correspondent generation of unconfined monopoles of different charge sign which gives to the system a magnetic plasma configuration composed by fermionic quasiparticles. This requires the fermionic proposal for magnetic monopoles whose nature arises from previous theoretical and experimental analysis and we think that it requires explanation. One of the first and most interesting analysis in this sense emerged in 1997 with the comparison made by Witten [43] between the quark-antiquark coupling inside hadrons with that formed by the magnetic poles of a dipole and its consequent definition of pole-antipole coupling.

A new comparison [24] in this regard appears talking about spin-ice restricting this comparison. In this new analysis, the comparision is established between the Dirac strings and monopoles, considering these monopoles on the spin-ices as monopoles-antimonopoles pairs with an implicit boson character. More recently, the magnetic monopoles in spin-ices had assigned directly a character of fermionic entities which are empirically detected [44]. In this direction other authors of other experimental results consider the similarity of coupled pole-antipole with a generally analogy to excitons in a semiconductor [45]. From our own experience we think that the phase transitions which in some experimental results have been defined as a first order phase transition [55] without modifying the crystalline structure, it is plausible to consider that can come from a change of symmetry respect to the spin statistic of its components with increasing temperature. In this chapter, we analyze from classical and quantum statistical physics the temperature evolution of the generation of the magnetic structures which mimic magnetic charges. We deduce some equations and magnitudes which govern the presence of the several many-body states which are experimentally detected. On one hand, the dumbbell model justifies the idea of the existence of magnetic monopoles in the spin-ices [7]. Moreover, the conductance of equivalent magnetic charges in these materials [12] experimentally ratifies the effective existence of entities whose behavior is mimetic to the magnetic monopoles.

These experiments have been coined as magnetricity, dual property of the electricity based on the conductance of hydrolized water ions under strong electric field. Therefore, the magnetricity is the quantitative determination of the magnetic charge mobility inside of the spin-ices under the external magnetic field [12]. All these experiments determined that in the coulomb phase of the magnetic plasma into the spin-ices [25], the deconfined monopoles coexist with Dirac's string and confined magnetic dipoles, although the presence of effective magnetic charges can even be majority. The new and more recent experiments on thermodynamic functions have detected phases that allow us to specify the possible states at low temperature and their phase transitions. The objective of this chapter is to try to find a coherent analytic theory for the temperature evolution of these many-body states from the nature of their one-body components. In these conditions we find analytic expressions of internal energy, free energy, specific heat and entropy which allows us to determine the temperature evolution of the corresponding phases, being these the main achievement of this chapter, where the master formula which allow us to carry out these state thermodinamic functions is the equation (1.15).

2.   Quantum T-evolution of the magnetic charge density

As previously mentioned, the first possible global state of the spin-ice system , can be explained by the sudden generation of pole-antipole pairs whose many-body state is similar to a BEC condensation [46-49]. This pair condensation is manifested via the highest peak of specific heat [30] which appears at lowest temperature. The corresponding many-body state is configured in either a double layer [50] or in quasi free pair structure when the attractive interaction among the charges of different sign is larger than the repulsive among the magnetic charges of the same sign. In these cases, the system may be considered as installed in a coherent Bose-Einstein condensate whose bosonic components are constituted of particle-antiparticle pairs. This state implies that all bosonic particles are in the wave function whose linear momentum is null. While the evolution with the temperature of the individual and free magnetic charges should be treated via the Fermi-Dirac statistics, the dipole-antidipole pairs in both the case of random positions and doble layer structure should be analyzed by the Bose-Einstein statistics. All these points should be valid under the assumption of the fact that the quasiparticles which constitute the magnetic charge are fermionic.

Bramwell in 2009 experienced about the mobility of the magnetic charges in the presence of external magnetic field. Therefore, these findings of 2009 stimulated the research of the nature of corporate or many-body states that are formed in the gas. Since 2013, the nature of a quasiparticle gas in the spin-ice system is interpreted in the light of the experimental data of specific heat [30], magnetic susceptibility [51, 52] and entropy [32,53,54]. These results were determinants for considering that this gas of magnetic entities experimentally detected by Bramwell and whose theoretical analysis had been formulated by Castelnovo and others in 2008, present successive phase transitions. These phase transitions whose nature, either first or second order is not completely determined lead to think in the nature of different quantum many-body states which given the disposition of its components could be called macroscopic quantum states. The interpretations of the many-body states and their complex evolution with temperature is a goal of this chapter. The first of these quantum states is formed with a large number of confined dipoles, with possibility of some mobility. Therefore, this many-body state is formed by individual components with integer spin (usually zero, but possibly one). What would be caused when the attractive force pole-antipole was enough to generate a real Bose-Einstein condensate. This first quantum state is constituted

at very low temperature and the phenomenology of its transition is made evident by the narrow peak that occurs in both the specific heat and magnetic susceptibility. The phase transition to a possibly more interesting state in order to obtain technological applications, occurs approximately at 0.36K and recently was announced that can be a phase transition of first kind [55] detected in the evolution of the speed of sound at that temperature. This second abrupt change of states could be interpreted over the change of a BEC condensate with bosonic components to a magnetic plasma state constituted of individual and free magnetic charges which are fermions. Another third transition is cited also reflected in measures of specific heat [30]. This has been, for the moment less studied and seems to be involved in the creation of a crystal structure of magnetic charges [56].

3.   Bosonic components for lowest energy many body state

As said in above paragraph, the first global state of the spin-ice system corresponding to the highest peak of specific heat is explained by the presence of a pole-antipole pair condensation [50]. This state presents similarities with those situations in which particle- antiparticles are coupled forming composite entities which travel within the many-body system. One of them is a determined mesonic soup [43] in which each particle is constituted with a quark and the corresponding antiquark, other different quark-antiquark meson combinations present sensible differences with pole-antipole pair state. However, the most parallel many-body system with this state which is object of our study is the electron-hole condensate, i.e. the so called electron-hole condensation (exciton condensation) which can appear in the semimetals [45,57-59]. In these cases the systems may be installed in either a BCS-like quantum macroscopic state or a Bose-Einstein coherent many-body state [60, 61] whose boson components are constituted of particle- antiparticle pairs of magnetic charges.

3.1. BCS-like quantum macroscopic state

An coherent and quantum macroscopic state is one which can be analized to the ligth of the BCS-like theory. This new ground state implies that all pseudo-bosonic particles can be defined by means of the following many-body wave-function $|\Phi_0> = \prod_k \left(u_k + v_k \alpha_{k\sigma}^\dagger \beta_{-k-\sigma}^\dagger \right)|0>$, where u_k and v_k are real parameters (sometimes named coherent parameters) which become fixed via the minimization of energy [60, 61] with respect them; $\alpha_{k\sigma}^\dagger (\beta_{-k-\sigma}^\dagger)$ is a creation operator of a magnetic positive (negative) charge whose linear moment and spin is

$k\sigma(-k-\sigma)$ and $|0>$ is a true vacuum state in where there is no pole-antipole pair formed. Then, the corresponding Hamiltonian is:

$$H = \sum_{k\sigma}\varepsilon_k\alpha^\dagger_{k\sigma}\alpha_{k\sigma} + \sum_{k\sigma}\varepsilon_k\beta^\dagger_{k\sigma}\beta_{k\sigma} + \sum_{kk'\sigma}V_{kk'}\alpha^\dagger_{k\sigma}\beta^\dagger_{-k-\sigma}\beta_{-k'-\sigma}\alpha_{k'\sigma} \tag{2.1}$$

where $V_{kk'}$ is the effective attractive interaction which induces the pole-antipole pairs based on a positive charge and a negative charge coupled to null linear total moment. The qualitative treatment of this attractive interaction is intuitive enough since when the pairs are formed and they constitute a many body coherent system, each of these pairs can be mobile structural entities whose magnetic charge is zero and therefore these pairs do interact weakly among themselves. However, the quantitative study of this attractive interaction can present multiple possibilities and this important point is out of the initial aim of this chapter and it is an objective for a possible future new paper. A simplified analysis can be carried out by considering some assumptions such as the isotropy in the $V_{kk'} = -|V_0|$ -interaction. The main field approximation energy evolution of temperature of the system can be easily deduced from the similarities with the BCS analysis [60, 61].

The main result is $E(T) = -\dfrac{2g_0^2(T)}{|V_0|} + \int_{n\delta}^{(1-n)\delta}N_0(\varepsilon)\left\{\varepsilon - \dfrac{\varepsilon^2}{[\varepsilon^2 + g_0^2(T)]^{1/2}}\right\}d\varepsilon$, where $E(T)$ is the energy of the system for a T-temperature; $N_0(\varepsilon)$ is the density of states in function of energy ε which corresponds to the spectrum without considering attractive interaction, $2g_0^2(T)$ is the BCS-like gap in function of temperature determined by the following equation: $1 = \dfrac{|V_0|}{2}\int_{n\delta}^{(1-n)\delta}\dfrac{[1-2n_F(T)]N_0(\varepsilon)d\varepsilon}{[\varepsilon^2 + g_0^2(T)]^{1/2}}$, where $n_F(T)$ is the number of particles in the Fermi-Dirac statistics; the n-parameter of the integration limits (whose interval is $0 \le n \le 1$) indicates the proportion of the band of the magnetic charge states which is occupied, i.e. it is the proportion of magnetic charges that form pole-antipole pairs; δ is the bandwidth and N is the number of positive magnetic charges which is equal to that of negative ones. The latter expression allows us to relate the different variables of the many-body state: δ, g_0 , $|V_0|$, N_0 and T_V (this would be the temperature of phase transition). For the asymptotic value of temperature when $T \to 0$, the fermi function $n_F(T) \to 0$ tends to zero and then, we have the relationship $\tanh\left[\dfrac{\delta}{|V_0|N_0}\right] = \dfrac{\delta}{(4g_0^2 + \delta^2)^{1/2}}$ when $T \to T_V$, the

gap $g_0(T_V) \to 0$ tends to zero and then, for instance, for the semi-occupation of the δ-band, we have the second relationship:

$$\frac{(1.14\delta)^2 - 4(K_\beta T_V)^2}{(1.14\delta)^2 + 4(K_\beta T_V)^2} = \frac{\delta}{(4g_0^2 + \delta^2)^{1/2}}$$

in this relation between the different parameters which determine the many body state, T_V and g_0 can be obtained from available literature and therefore with the two latter expressions can be fixed δ and $|V_0|$. On the other hand, the quantitative results of the energy depends on the density of states of system without considering the attractive interaction. If for the sake of simplicity, we consider a rectangular constant density of states, $N_0(\varepsilon) = N/\delta$, we have the following expression for the energy of the pole-antipole condensation ground state:

$$E_0 = -\frac{2g_0^2}{|V_0|} + 4N\delta(1-2n) - 2N(1-n)[(1-n)^2\delta^2 + g_0^2]^{1/2} - 2Nn(n^2\delta^2 + g_0^2)^{1/2} + \frac{2Ng_0^2}{\delta}\ln\left\{\frac{(1-n)\delta + \left[(1-n)^2\delta^2 + g_0^2\right]^{1/2}}{-n\delta + [n^2\delta^2 + g_0^2]^{1/2}}\right\}$$

On the other hand, we can obtain more information of this many-body state from the denominator of the above expression of $E(T)$, $E = \text{sign}(\varepsilon)(\varepsilon^2 + g_0^2(T))^{1/2}$. This energy corresponds to the spectrum of quasi-particle states considering the attractive interaction [63, 64] and the zero energy being located in E_F. This spectrum implies the existence of the typical BCS-gap and the following density of quasiparticle states and the specific heat for constant volume becomes:

$$C_V(T) = \Re\left\{\int_{-\delta/2}^{\delta/2} \frac{N_0(W)W}{\left[1 - (g_0/W)^2 + i\theta\right]^{1/2}} \frac{dn_F(T)}{dT} dW\right\} \tag{2.2}$$

this latter expression yields a specific heat with a large peak at the basis of the BCS gap where the density of states of quasiparticles presents a maximum. This peak in the lower edge of the BCS gap may correspond with the highest peak to lowest temperature of the specific heat which appears in the experimental data.

This many-body state is interesting from a theoretical point of view, because it is a source of phenomenology that emerges from the physical coherence in this BCS state. In addition, following a BCS-like methodology, we can deduce that this system has no magnetic conductivity to a zero frequency, i.e. in this state, the spin-ice does not have magnetricity, and therefore, it is an magnetic insulator, such as this happens in the exciton condensate.

Therefore, the magnetic conductivity and electromagnetic energy propagation and their potential circuital applications are more limited than that which exists in the state of magnetic plasma. The study of electromagnetic propagation in frequency of this state of antipole pole pairs can be based on the determination of the linear response of the frequency dependent conductivity and magnetic permeability obtained by means of the corresponding Kubo formulas, which are our ongoing research. Another perspective on this dimerization of pole-antipole pairs is to take into account the 1-spin coupling between positive and negative monopoles. This possibility may be interesting from a theoretical point of view and deserves electromagnetic propagation analysis with exclusiveness.

The existence of a BCS-like state can not be excluded "a priori" given the simultaneous existence with the same probability of a positive and another negative charge, and the attractive effective interaction that can arise at the time of their presence. However, the condition of existence of a gap between the quasi-particles that are generated by such interaction should have consequences in the specific heat that are not clarified in the experimental results. Therefore, although this possibility, in principle, should not be neglected, it appears that the existence of boson condensate association pole-antipole seems more likely than the BCS state. Consequently, we will test the bosonic condensate and the comparison of the our results of specific heat and entropy considering the expression (2.2) with the experimental results will determine the plausibility of our assumptions.

3.2. Bose-Einstein state

Another alternative to BCS coupling of pole-antipoles is the consideration of strict dipoles whose components have integer spin which can be in both s and p spin wave-functions. In this study, we do not consider any many-particle wave function coherent with the Bose-Einstain state, but we consider this state from its bosonic components. Consequently, the derivation of all expressions of this subsection should be deduced within the Bose-Einstein Statistical Mechanics. The consideration of a p-coupling for the spin wavefunctions should be manifested in the vector character of the order parameter. However in order to prospect this possibility, we would require some more experimental results which, at our knowledge, are not still available in the literature corresponding to the spin-ice materials. Therefore, we analyze the second option explained in the introduction of this subsection, which is the possibility of a Bose-Einstein state for the phase corresponding to the first peak of the specific heat, and then, we have used the above mentioned statistics for the components of the many-body system and we obtain the internal

energy, the specific heat, the free energy and entropy. The diference with the BCS-like wavefunctions is that the pairs are static in this phase.The essential characteristic of this model and its possible difference with the statistical models formulated in other previous references is that we analyze the dependence of the generated results obtained from analytical expressions in functions of the parameters which reflect the properties of the quantum macroscopic state.

3.2.1. Internal energy, specific heat and entropy with bosonic components of system

In this subsection, we give the development of mathematical determination of the thermodynamic functions of former sections. The U- internal energy is given by:

$$U = \sum_i \frac{K_B T \ln(n_0) - K_B T \ln(n_i) + \frac{|g_i| \phi_0}{T_v} T - b}{\exp\left(\ln(n_0 / n_i) + \frac{|g_i| \phi_0}{K_B T_v} - \frac{b + \mu}{K_B T} \right) - 1} \qquad (2.3)$$

where the numerator of this expression is given by the energy of forming each i-pole-antipole pair which is

$\varepsilon_i = g\phi_0(r,T) - b$, with $\phi_0(r,T)$ given in master formula Eq. (1.15) of the chapter 1 and $b = \frac{\mu_0 \mu_r g^2}{8\pi d} - \Sigma_0$; and the

summatory runs over all possible states corresponding to the continuous probability of each pair to be formed for a given temperature and extended to all pairs of tetrahedra of the system. Extending this expression to the continuum, we easily can obtain the following integral expression for the U-energy:

$$U_{BEC} = \frac{N}{n_0} \int_0^{n_0} \frac{A_1(T)n}{z_1 n_0 - n} dn - \frac{K_\beta T}{N n_0} \int_0^{n_0} \frac{n\ln(n)}{z_1 n_0 - n} dn = \frac{N A_1(T)}{n_0} I_1 - \frac{N K_\beta T}{n_0} I_2 \qquad (2.4)$$

where $I_1 = \int_0^{n_0} \frac{n \, dn}{n_0 z_1 - n} = n_0 \left[-1 - z_1 \ln\left(1 - z_1^{-1}\right) \right]$ and $I_2 = \int_0^{n_0} \frac{n\ln(n) dn}{n_0 z_1 - n} = \sum_{p=0}^{\infty} \frac{n_0}{z_1^{p+1}} \left(\frac{\ln n_0}{p+2} - \frac{1}{(p+2)^2} \right)$ and in

addition, we have:

$$A_1(T) = K_\beta T \ln(n_0) + \frac{|g| \phi_0}{T_v} T - b \qquad (2.5)$$

$$z_1 = \exp\left(\frac{|g| \phi_0}{K_\beta T_v} - \frac{b + \mu}{K_\beta T} \right) \qquad (2.6)$$

Therefore, we obtain for the internal U-energy per pole-antipole pair, the following formula:

$$u_{BEC} = \frac{U}{Nn_0} = \frac{1}{n_0}\left\{ A_1(T)\left[-1-z_1\ln\left(1-z_1^{-1}\right)\right] - K_\beta T \sum_{p=0}^{\infty} z_1^{-p-1}\left(\frac{\ln n_0}{p+2} - \frac{1}{(p+2)^2}\right)\right\} \tag{2.7}$$

where Nn_0 is the total number of pairs of tetrahedroms multiplied by the probability of the existence for each of these particle-antiparticle pairs. This energy depends on two physical variables, n_0 which can be deduced from the experimental data measured in the transition temperature T_v [12, 62] and ϕ_0 which can be indirectly deduced from the asymptotic entropy measurements, such as we will discuss in the section of results [see Eq. (2.25)]

The specific heat can complement the idea about the possible different phases and phase transitions which a system suffers with the increasing (or decreasing) temperature. c_v, volume constant specific heat per particle, for the situation of a system whose U-energy per particle, in this case for each pole-antipole pair given in the former equation is given by derivative of the U-energy respect to temperature:

$$c_v = \frac{K_\beta}{n_0}\left\{\left(\ln(n_0) + \frac{|g|\phi_0}{K_\beta T_v}\right)\left[-1-z_1\ln\left(1-z_1^{-1}\right)\right]\right\} +$$

$$\frac{K_\beta}{n_0}\left\{\frac{-A_1(T)(b+\mu)}{(K_\beta T)^2}\left(z_1\ln(1-z_1^{-1}) + \frac{z_1}{(z_1-1)}\right) - \sum_{p=0}^{\infty} z_1^{-p-1}\left(1 - \frac{(p+1)(b+\mu)}{K_\beta T}\right)\left(\frac{\ln(n_0)}{p+2} - \frac{1}{(p+2)^2}\right)\right\} \tag{2.8}$$

The increase of c_v given in Eq. (2.8) is very abrupt at low temperatures getting up a narrow peak which announces the existence of a mentioned possible phase transition whose final state is the condensation of bosonic quasiparticles at very low temperatures. Therefore, now we study other thermodynamic state functions which allow us to complete the knowledge of different phases. From a standpoint of statistical physics, free energy can be obtained by the following expression:

$$F_{BEC} = \frac{1}{\beta}\sum_i \ln\left\{1 - \exp\left[-\beta(\varepsilon_i - \mu)\right]\right\} \tag{2.9}$$

where all variables have been previously defined in previous sections of this chapter. Making an extension, considering a continuous set of states, similar to what was done with the internal energy, we obtain the following free energy if we consider the value of , ε_i of expression of master formula of Eq. (1.15):

$$F_{BEC} = K_B T \sum_i \ln\left\{1 - \exp\left[-\ln\left(\frac{n_0}{n_i}\right) - \frac{|g_i\phi_0|}{K_B T_v} + \frac{b+\mu}{K_B T}\right]\right\} = \frac{NK_B T}{n_0}\int_0^{n_0} \ln\left(1 - \frac{n}{n_0}z_2\right)dn \tag{2.10}$$

then, we have:

$$f_{BEC} = \frac{F_{BEC}}{Nn_0} = -\frac{K_\beta T}{n_0}\left[\left(-1+z_2^{-1}\right)\ln|1-z_2|+1\right] \tag{2.11}$$

where:

$$z_2 = \exp\left(-\frac{|g_i\phi_0|}{K_\beta T_v}+\frac{b+\mu}{K_\beta T}\right) \tag{2.12}$$

and from these latter equation, we can obtain entropy by means of the following:

$$s_{BEC} = -\frac{\partial f_{BEC}}{\partial T} = \frac{K_\beta}{n_0}\left\{\left[-1+z_2^{-1}\left(1+\frac{b+\mu}{K_B T}\right)\right]\ln|1-z_2|+1+\frac{b+\mu}{K_\beta T}\right\} \tag{2.13}$$

when we determined the internal energy, specific heat, free energy and entropy (u, c_v , f and s) for higher

temperatures than that of the transition temperature, T_V , above we have the fermionic gas and below the bosonic

condensate.

4. Fermionic gas in a magnetic plasma state

For higher temperatures the pole-antipole pairs are broken appearing in an increasing way and then, free

magnetic charges can travel in the crystal progressively forming a neutral magnetic plasma when temperature

increases. Then, the determination of internal energy, U, in this case is carried out by means of a similar

mathematical procedure which also can also be seen in the latter section of this chapter, and, obviously, we will

use the Fermi-Dirac statistics due to the single magnetic charges are fermions i.e., we have the following expression

for the internal energy, free energy, specific heat and entropy.

4.1. Internal energy, specific heat and entropy in a magnetic plasma state

In this section in a similar way to the 3.2.1 section, we give idea of the mathematical derivation of the U

energy, specific heat, free energy and entropy for higher temperatures than T_V the particle.antiparticle (pole-

antipole) pairs are broken appearing in an increasing way free magnetic charges which can can travel in the crystal

progressively forming when temperature increases an neutral magnetic plasma. Then, the U-energy, can be

determined from Fermi-Dirac statistics, i.e., we have it that:

$$U_{Plasma} = N\sum_i \frac{K_B T \ln(n_0) - K_B T \ln(n_i) + \frac{|g_i|\phi_0}{T_C} T + a}{\exp\left[\ln\frac{n_0}{n_i} + \frac{|g|\phi_0}{K_B T_C} + \frac{a-\mu}{K_B T}\right] + 1}$$

(2.14)

where $a = \Sigma_0$ is the self-energy of the magnetic charge, concept which is introduced by dumbbell model by Castelnovo et al in 2008. Extending this expression to the continuum, we easily can obtain the following integral expression for the U-energy:

$$u_{Plasma} = \frac{U}{Nn'_0}\left(\int_0^{n_0} \frac{A_2(T)n\,dn}{z_3 n'_0 + n} - K_B T \int_0^{n_0} \frac{n\ln(n)\,dn}{z_3 n'_0 + n}\right)$$

(2.15)

$$A_2(T) = K_B T \ln(n'_0) + \frac{|g|\phi'_0}{T_C} T + a$$

(2.16)

$$z_3 = \exp\left(\frac{|g|\phi'_0}{K_B T_C} + \frac{a-\mu}{K_B T}\right)$$

(2.17)

and consequently, we have u energy per magnetic charge the following expression:

$$u_{Plasma} = \frac{U}{Nn'_0} = \frac{1}{n'_0}\left[A_2(T)g(z_3) - K_\beta T \sum_{p=0}^{\infty} (-)^p C z_3^{-p-1}\right]$$

(2.18)

$$g(z_3) = 1 - z_3 \ln\left(1 + \frac{1}{z_3}\right)$$

(2.19)

$$C = \frac{\ln(n'_0)}{p+2} - \frac{p+1}{(p+2)^2}$$

(2.20)

The specific heat can be obtained via the derivative of the former function (2.18) with temperature. The way for obtaining the entropy is similar to that of he case of the BEC state but considering the corresponding free energy which in the fermionic case of the components of the many-body state is:

$$F_{Plasma} = -\frac{1}{\beta}\sum_i \ln\left\{1 + \exp\left[-\beta(\varepsilon_i - \mu)\right]\right\} = -\frac{1}{\beta}\sum_i \ln\left\{1 + \exp\left[-\ln\left(\frac{n_0}{n_i}\right) - \frac{|g_i|\phi'_0}{K_B T_C} - \frac{a-\mu}{K_B T}\right]\right\} = -\frac{NK_B T}{n_0}\int_0^{n_0} \ln\left(1 + \frac{n}{n_0}z_4\right)dn$$

(2.21)

With similar mathematical derivation to those of bosonic case, we obtain the free energy for each particle in the plasma state

$$f_{Plasma} = \frac{F_{Plasma}}{Nn_0} - \frac{K_\beta T}{2n_0}\left[-1 + \left(1 + \frac{1}{z_4}\right)\ln(1 + z_4)\right]$$

(2.22)

where

$$z_4 = \exp\left(-\frac{|g|\phi_0'}{K_\beta T_C} - \frac{a-\mu}{K_\beta T} \right)$$

(2.23)

and finnaly, entropy is obtained by means of the derivative of f -function with respect temperature changing the sign:

$$s_{Plasma} = -\frac{\partial f_{Plasma}}{\partial T} = \frac{K_\beta}{n_0} \left\{ \left[1 + z_4^{-1}\left(1 - \frac{a-\mu}{K_B T} \right) \right] \ln|1+z_4| - 1 + \frac{a-\mu}{K_\beta T} \right\}$$

(2.24)

5. Results

The T-evolution of the U-energy is sensitive respect to all variables of the functions z_1 and z_2, since for determined values of a and b above defined, there is a large increase of this energy due to the generation of spin flips among contiguous tetrahedrons. These spin-flips produce, according to the dumbbell model, a pair of magnetic monopoles of different sign inserted in each pair of tetrahedrons. The existence, then, of attractive interaction among the components of these pairs implies a re-organization of the localization of these pairs due to a minimization energy principle and a posterior increase of energy under the progressive increase of temperature.

This T-evolution can provide thermodynamic behavior of the first phase transitions whose study and determination is one of the objectives of this research. The minimization of the u-function could be the cause of the existence of the many-body state whose individual pair components constitute a Bose-Einstein condensed generated by the attractive pole-antipole interaction. What should be determined is if the spin symmetry of the individual pairs and consecuently the order parameter, is a scalar or a vector. This dichotomy could be solved by the fact that the coupling between the spins of pole and antipole should be either type s or p. Continuing the increase of temperature we show, in Fig. 11, the u-energy when considering the components of the many-body system are free charges. In this case, there is the same number of positive charges and negative ones and therefore, this system is a neutral magnetic system. The evolution with temperature of this internal energy is the continuation of that coming from the pole-antipole pairs of the systems and then, this energy implies the breaking of the pairs and its constitution of free charges.
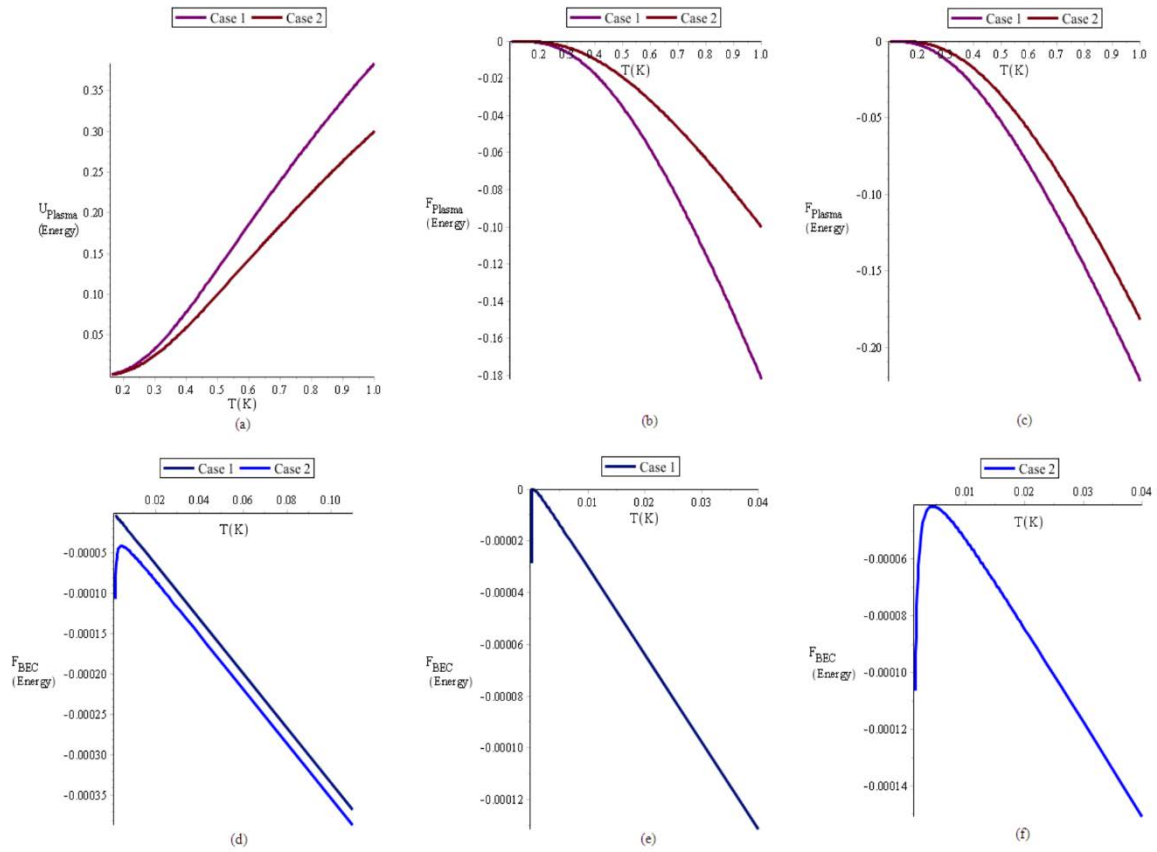
Figure 11: Evolution of the internal and free energy of the system.

In this Fig. 11, we show two cases, as examples of the evolution of the internal energy, U, and the thermodynamic potential, f of the system in the plasma state and in a state composed of pole–antipole pairs. All results are per individual component of the many-body state of the system. In (a) we show the u-energy of equation (2.18) for the case 1, $\left| g \right| \phi_0' / K_B T_C = 2$, and 2.3 in the case 2. (b) It represents f of equation (2.22) for $\left| g \right| \phi_0' / K_B T_C = 2.4$, the case 1 and 3 for the case 2. (c) The same as (b) but in both cases $\left| g \right| \phi_0' / K_B T_C = 2.4$ and $\Sigma_0 = 0.75$ and 0.95 for cases 1 and 2, respectively. (d) We give results for the f functions in the BEC state of Eq. (2.11), in case 1 with the unidimensional set $b\beta = 0.001\beta$, and $b\beta = -0.045\beta$ in case 2. (e) and (f) are more detailed drawings of the cases 1 and 2 of (d).

The different behaviour in its thermal evolution of the free energies coming from (2.11) and (2.22), corresponding to the BEC phase and plasma phase, respectively is consistent with the existence of different

phases. The specific heat as derived from Eqs. (2.8) and (2.15) should give more support to this idea of different phases of the system. In Fig. 12a, we give a result using parameter values that define the internal energy and with it we evolve expressions from the boson system and fermionic one. Both curves intersect at one point. In the case of Fig. 12, the cutting point is into $0.11K$, however, obviously, this cut depends on the parameter values of the two expressions of internal energy. The parameters which have greater influence in the results of the specific heat are the a energy in the fermionic case and b energy in the bosonic one i.e., the self-energy minus the chemical potential in the fermionic system and the interaction energy in the Bose-Einstein system.
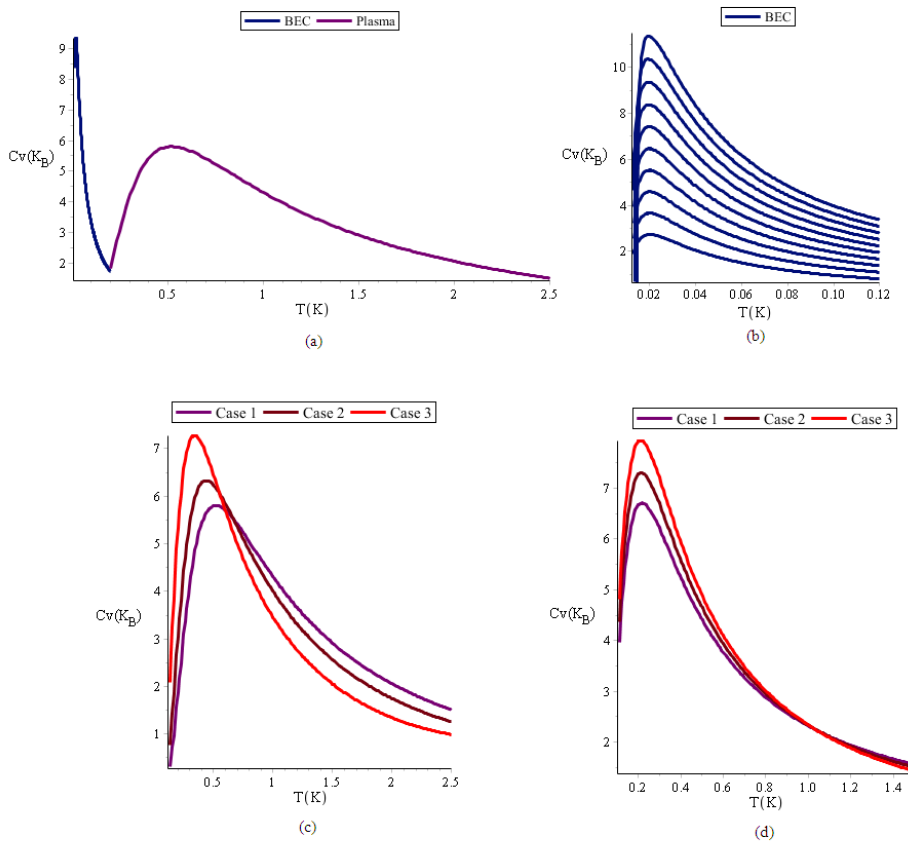
Figure 12: The specific heat vs. temperature.

In figure 12a, we give examples of the evolution with temperature of the specific heat per magnetic charge. In the first part of this figure, the system evolves according to Eq. (2.8) to about 0.11 K. From this temperature, the system is composed of free magnetic charges. In Fig. 12b, we give the different variations of temperature of c_v corresponding to the bosonic system whose expression of c_v is Eq. (2.8), for values of dimensionless parameter set: $b\beta = \dfrac{0.060, 0.055.....0.020, 0.015}{K_B T}$, respectively. The smaller the value of b, the smaller the maximum of the

curve. The temperature of this maximum remains practically constant when the value of the corresponding maximum increases and the temperature of the larger maximum is close to 20mK. In Fig. 12c corresponds the specific heat when the system is in the plasma state in which the monopoles can quasi-freely move inside of the material. In this figure, we show, c_v for different values of the self-energy of each magnetic charge. The different curves correspond to the following values of a-parameter, $a\beta = \dfrac{0.93,0.85,0.80,0.72......,0.32,0.24}{K_B T}$, the maximum of c_v decreases according to the a-value increases. In addition, when the maximum decreases its corresponding temperature increases.

On the other hand, the specific heat of the c_v is increasing with increasing values of the relationships between $g\phi_0$ and $K_\beta T_v$ in the case of boson components, and on the contrary when the individual components are free magnetic charges. In Fig. 12d show the evolution of specific heat in the case where the magnetic charges are free and therefore are fermions. The different curves correspond to different values of the relationship $|g|\phi_0 / K_\beta T_C$ and correspond to different values of entropy; these values of entropy being between $k_B \ln 2$ and $k_B(\ln 2 - 0.5\ln 1.5).$ All these results of Fig. 12 are compatible with the experiments recently made [30,33,54]. One can carry out a description of the state of the many-body system from the specific heat. For 0 K, the system is in the ground state and each tetrahedron has null magnetic moments since no spin-flip occurs. When T increases the spin-flips are produced in a stochastic process at any side of the crystal, one can suppose that if the material is homogeneous by symmetry reasons, then the probability for appearance of the spin-flips is similar in all pairs of tetrahedra. We want to note that there can be negative b-values, since the atractive interaction among magnetic charges of different sign is contained in them. These $b < 0$ values can generate decreasing values of the u-internal energy with increasing temperatures in a small T-interval and always at very low temperatures. This latter T-evolution would be a narrow T-zone with negative c_v ; however, this possibility is necessary to analyze whether it corresponds to a true physical situation or it is a spurious result of the mathematical model. In any case, the increasing of c_v to these low temperatures can be extremely fast such as seen in Fig. 12b. When the value of specific heat reaches the maximum, it should be interpreted that the maximum value of pole-antipole confined pairs has been achieved. However, the value of this maximum theoretically depends on the other parameters of the

model, essentially of $|g|\phi_o / K_\beta T_v$. The thermal re-organization of the pole-antipole pairs within the crystal is due to the principle of energy minimization aided by the atractive interaction energy among the positive and negative charges. Then, the specific heat has negative derivative with respect T up to c_v reaches its minimum when the BEC phase transition tends to disappear. This T in the results of Fig. 12a is approximately at 0.11K. Temperature lower than that experimentally detected for the possible first order phase transition. However, with the model which we are describing, by modifying the other parameters, the theoretical and the experimental transition temperatures can be approached. Moreover, we think that may not have unanimity for neither nature nor the quantitative temperature value for this phase transition. From T corresponding to the c_v minimum, the confined pole-antipole pairs begin to be broken and then, the Dirac strings and the remaining pairs still confined coexist with free charges. Therefore, since this temperature may exist magnetricity by movement of these magnetic free charges. From the temperature at which the second relative maximum is found, the specific heat begins to decrease, probably by increasing the magnetic charge annihilations by recombinations or pole-antipole. The analysis can be completed by means of the study of entropy within this model in both possible states whose one body components are bosons and fermions.
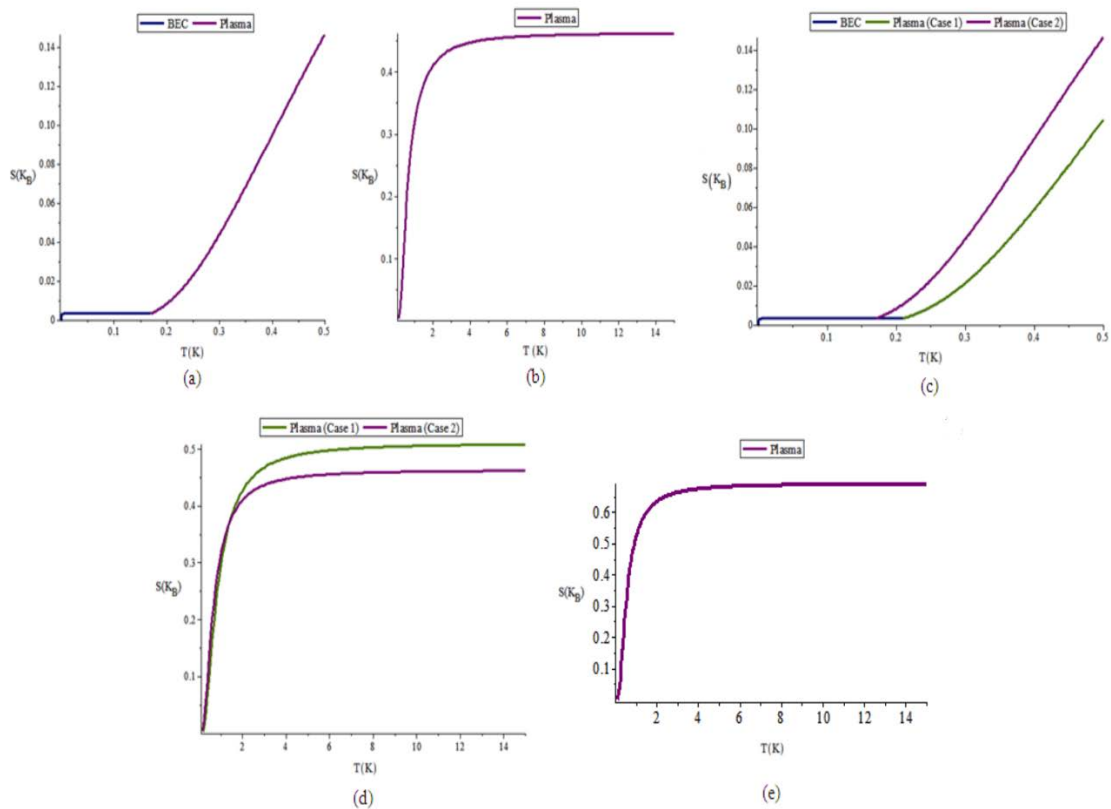

Figure 13: Evolution of entropy with temperature.

The Fig.13a is determined with Eq. (2.13) using the following values $|g|\phi_0 = 5K_\beta T_V$, $b\beta = -10^{-3}/K_B T$ and

Eq. (2.24) with $|g|\phi_0 = 2.3K_\beta T_C$, and $n_0 = 0.095$; the Fig.13b is determined also with Eq. (2.24) and the same

values as Fig. 13a. In the Fig.13c, we compare the results of two calculations with Eq. (2.24), maintaining the same

parameters in Eq. (2.13), in this figure, the curve in green is determine with $|g|\phi_0 = 2.3K_\beta T_C$, and $a\beta = 1.2/K_B T$

front the case of Fig.13a with $a\beta = 1.5/K_B T$. The Fig.13d is the same of Fig.13b but drawing the two cases of

Fig.13c. The Fig.13e corresponds to entropy considering the following light variations in the governing parameters

$|g|\phi_0 = 2.3K_\beta T_C$, and $a\beta = 1/K_B T$ and $n_0 = 0.070$.

Therefore, in Fig.13, we determine entropy from Eq. (2.13) for the bosonic many-body phase and Eq. (2.24)

for the fermionic phase. We study the nature of the thermodynamic transition and analyze in these examples its

corresponding critical temperature according to the relative situation between the two curves in the proximity of the

point in which this transition can occur. Certainly, these results show that the phase transition can be adjusted by

the parameters that determine the value of entropy in both phases.

However, when we adjust the transition temperature varying the parameters in both expressions of entropy,

then the asymptotic value of entropy when T tends to sufficiently high temperature values is fixed. The final value

of this asymptote depends on the adjustable parameters used for obtaining the temperature of transition. In the

Fig. 3a, we present the results of the two expressions of entropy coinciding at 0.17K, and then, the asymptotic

value of entropy is $\sim 0.47K_B$. These results as well as the results of specific heat given in Fig.12 are coherent with

those of Ref.[54].

The asymptotic value of this entropy is close to the full entropy minus the value of so-called Pauling's entropy

$[K_B(\ln2 - 0.5\ln1.5)]$. In Fig. 13c we present two different adjusted values of the entropy which imply two different

transition temperatures, 0.17K and 0.22K and the corresponding asymptotic values of entropy are represented in

the Fig. 13d. In these Figs.13c and 13d, one can see that the higher transition temperature the greater is the

asymptotic value of the entropy. In addition, the asymptotic value the entropy for the transition temperature close

to 0.22 Kelvin is approximately 0.49 K_B.

In any case, from inspection of the expression of plasma state entropy, for an asymptotic value s_0, the following expression is satisfied:

$$\left[1+\exp\left(\frac{|g|\phi_0}{K_B T_C}\right)\right]\ln\left[1+\exp\left(-\frac{|g|\phi_0}{K_B T_C}\right)\right]=1+s_0 \tag{2.25}$$

from this latter equation, and taking into account all physical variables are experimentally known with the exception of ϕ_0, we can obtain its value. Then, the expression of the $\phi(r)$ of Eq (1.15) is completely established. However, the parameter which controls the asymptotic value of entropy is fundamentally the self-energy of the magnetic charges minus the chemical potential μ such as it is seen in Eq. (2.24).

Actually, for a decrease of a 20% in the self-energy in Eq. (2.24), we obtain a saturated value of the asymptotic entropy ($S=K_B\ln 2$) such as it is given in Fig. 13e. Therefore, in our model the relationships $|g|\phi_0/K_\beta T_C$ is what controls the asymptotic value of entropy. We want to note that in all cases given in Fig. 13, the entropy is a continuum functions with discontinuous derivative. On the contrary, when $|g|\phi_0/K_\beta T_V=2.4$ and $\Sigma_0-\mu\approx 1$ which are values close but different to those used for obtaning Fig. 13, the phase transition is of a first order, since, the entropy is discontinuous for 0.17 K, such as it is given in Fig.14a. In Fig.14b, we give entropy of Eq.(2.24) with the same parameter values of Fig.14a. This result being coherent with recent experimental measurements in Ref.[55]. We slightly vary in Figs. 14c,14d and 14e the parameters of the different energies that have influence in the determination of expressions (2.13) and (2.24).

In the case of these figures, we show that the thermodynamical transition is a phase transition of first kind. We have elongated in these curves the T-interval toward lower temperature which that of the temperature of the first phase transition in the expression (2.24) and in the contrary direction toward higher temperature of this T-interval for the expression (2.13), and we find which never find the cut point both entropy expressions. Therefore, entropy is discontinuous, although, the evolution of entropy is similar from Eq. (2.13) and Eq. (2.24), but its value is larger for fermionic phase than that for bosonic phase, such as shown in Fig. 14c and 14e.
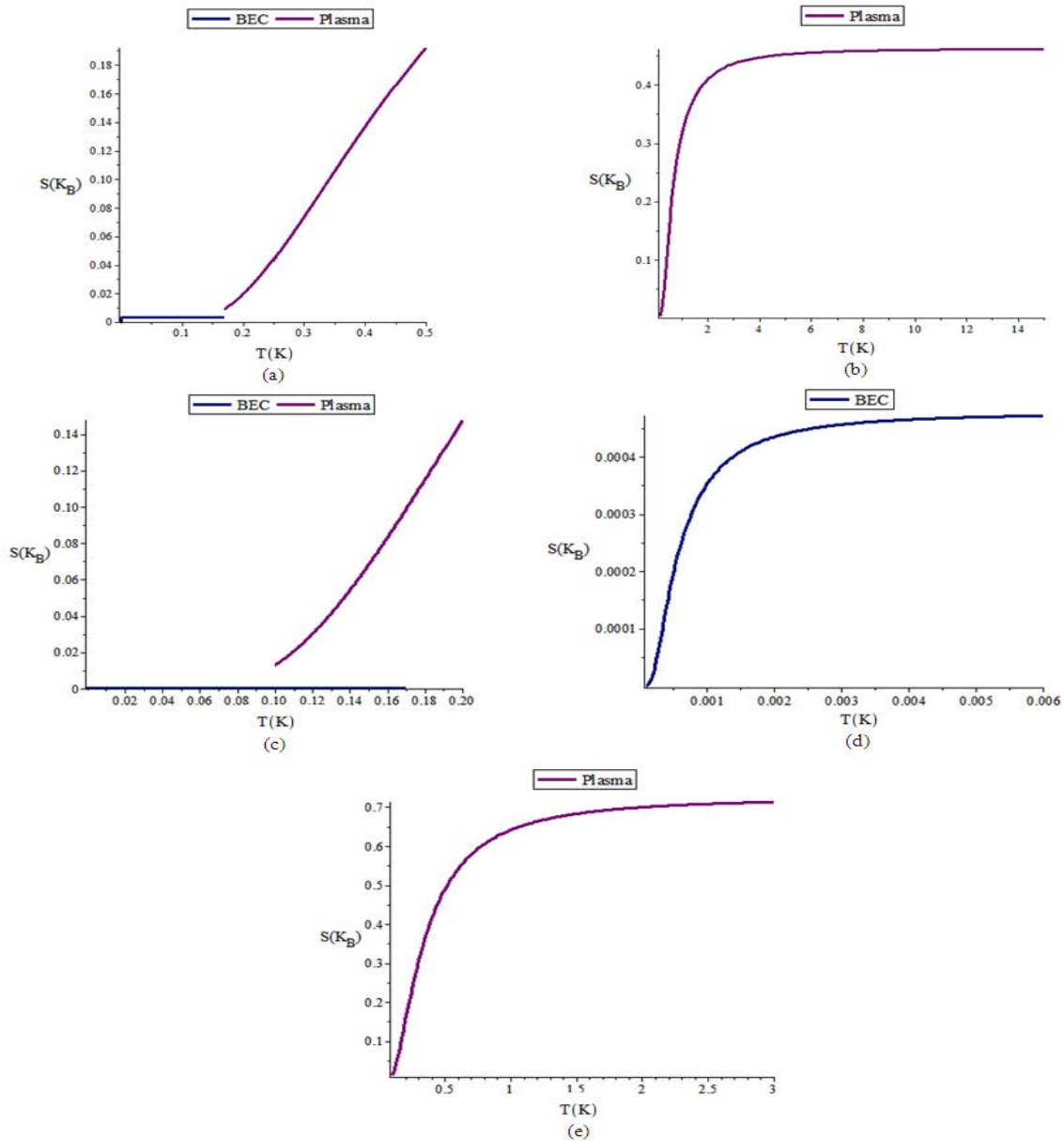
Figure 14. Evolution with temperature of entropy in a case of first order phase transition.

In this figure the two entropy expressions does not have any cut and it shows the asymptotic evolution in the so-called plasma state, being this value $\sim 0.43\text{K}$. The units on the axes as in Fig. 13, the Figs 14a and 14b are obtained with the following parameter of Eq. (2.7): $a\beta = 1$, $|g|\phi_0/K_\beta T_C = 2.4$ and $n_0 = 0.095$; and with the following parameters of Eq. (2.5): $|g|\phi_0/K_\beta T_C = 2.4$, $b\beta = -0.001$ and $n_0 = 0.95$. The Figs. 14c, 14d and 14e are obtained of Eq. (2.16) with $a\beta = 0.6$, $|g|\phi_0/K_\beta T_C = 2.4$ and $n_0 = 0.05$ and Eq. (5) with $|g|\phi_0/K_\beta T_C = 2.4$, $b\beta = -0.001$ and $n_0 = 0.95$.
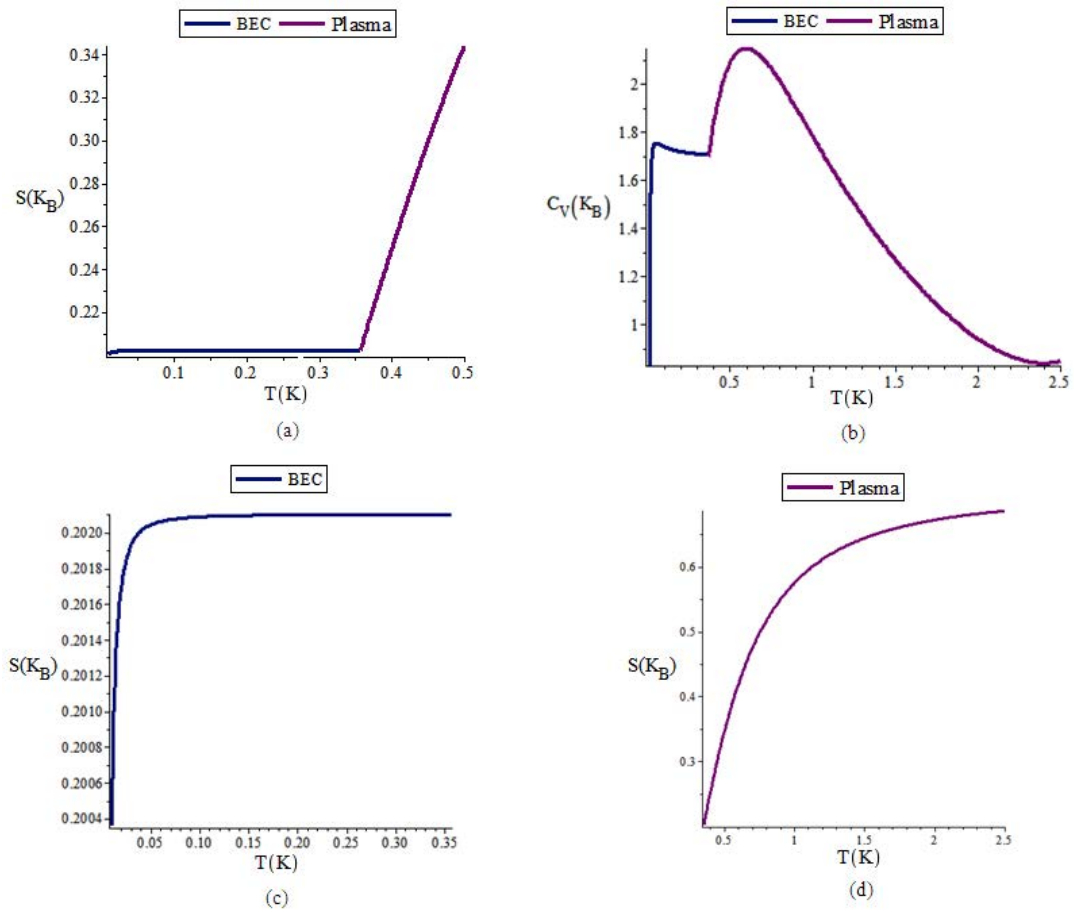
Figure 15: The evolution of entropy with temperature when its asymptotic values are the Pauling residual entropy.

The saturated value value, $K_B(\ln 2)$, in the plasma state. These expressions are obtained with the following values of different parameters of Eq. (2.24): $a\beta = 0.1/K_B T$, $|g|\phi_0/K_\beta T_C = 0.1$ and with the following parameters of Eq. (2.13): $|g|\phi_0/K_B T_V = 0.1$, $b = 0.001$. In Figs. 12-15, the evolution of macroscopic quantum states is analyzed from thermodynamic functions and their derivatives, such as entropy and specific heat which depend on the parameters that have dimensions of energy and define those states. The purpose of these results given in figures 12 and 15 is the evolution of the entropy and the specific heat varying energies a, b, Σ_0, effective attractive interaction in the bosonic phase and n_0.

The features of the entropy of the spin-ices given in Fig. 15 are that when the temperature rises far above the phase transitions, the entropy reaches saturation values, $NK_B \ln 2$, and when the temperature is in values for which the state is a boson condensate, entropy is limited to the residual value of $\frac{N}{2}K_B \ln(3/2)$.

56

On the other hand, when the temperature tends to zero, the entropy decreases and is lower than the residual one. Fig. 15a shows the entropy in the range from zero to 0.50K. In this range, the entropy varies at very low temperatures, is constant until the phase transition to the state of plasma magnetic and from then increases rapidly. Figs. 15c and 15d show the entropy evolution with temperature in the boson condensate state and magnetic plasma, respectively. The Fig.15b show the specific heat values using the same parameters used in the calculation of entropy. One point that is necessary to comment is that when considering the values of the parameters that allow us to obtain the asymptotic entropy per particle equal to $K_B (0.5\ln1.5)$ in the bosonic phase and $K_B \ln2$ in the fermionic phase, the phase transition temperature is $\approx 0.37K$ in our model. This temperature is also $\approx 0.37K$ in the specific heat. This dependence of the transition temperature with the asymptotic value of entropy is consistent with the results given in Fig. 13, and in general, these results given in Figs. 12-15 are in coherence with Refs. [30, 32,33,53,54].

Moreover, we want to comment that the similarities between the spin-ice systems with ice water is the reason for calling these compounds by this name. However, there is a clear thermal difference between them. These similarities fail in the entropy measures at temperatures close to 0 K, i.e. in states whose energy is close to the ground state. The evolution of entropy for these very low temperatures differs in the second compared to the first. Indeed, in ice water, probably by bimolecular association in the ground state, there is a residual Pauling entropy at 0 kelvins. On the contrary, the spin-ice systems at temperatures below mili-kelvins, entropy approaches zero when T=0, [32,53]. This could be due to the mentioned molecular associations existing in water at low temperatures do not exist in the case of spin ice. Since the only associations to this freezing temperatures are the pairs of pole-antipole which although they are interacting, they can also be considered independent bosonic particles. In our model, the components of the global system are pairs pole-antipole and the energy assigned to these is the constitutive energy of the pair plus the energy attractive interaction between the components thereof, without associations between several pairs.

Furthermore, the variation of entropy is continuous as continuous is the order parameter in the system and whose relationship with the energy of the magnetic charges can be deduced from Eq. (1.15) . The value of entropy is a function of the parameters which have been defined in Eqs. (2.13) and (2.24). As a consequence, this lost

entropy with respect to the Pauling residual one in the spin-ice systems can occur when temperature tends to zero. However, this problem of the loss of entropy of the spin ice systems respect to that of the water-ice is a matter that can give interesting surprises in future experiments. A similar question is whether the entropy has a continuous evolution with temperature or there is a discontinuous jump to temperature in which the phase transition of lowest thermal energy occurs, the main parameter that can discriminate this dilemma being ϕ_0 of Eqs. (2.13) and (2.24).

6. Comments

The origin of the content of the present chapter is the assumption based on the existence of two antagonistic situations within the spin-ice material at very low temperatures. On one hand, we consider that at more low temperatures, the system is constituted of the so-called pole-antipole pair condensation and on the other hand, the neutral magnetic plasma constituted of the quasi-free magnetic charges which appear when the temperature increase. The characteristic phase transition detected via measurements of specific heat, magnetic susceptibility and entropy behavior with temperature gives support to the existence of the mentioned states. These states correspond to two quantum macroscopic states whose thermodynamic development and electromagnetic propagation are inextricably linked to the density of free magnetic monopoles, to their masses and mobility within a quasi-particle gas such as we will see in chapter 4 and 5.

The phenomenology can be clearer when the successive appearance of the different transitions is commented by considering that temperature is descenddent. Therefore, we start from temperatures far from zero kelvin and far from the second phase transition in which the specific heat has a normal behaviour. In this temperature region, the magnetic charges, if their existence is possible, constitute a gas with a strong Coulomb interaction which competes with a large kinetic energy, whose result is the possible existence of quasi-crystallization of semi-periodic structures within the quasi-free magnetic charge system [56] (when this phase appears, the specific heat presents a wider and non-large peak). Following the cooling process of the spin-ice system, one finds a new clear phase transition when the magnetic charges are quasi-free and they constitute a neutral magnetic plasma where the electromagnetic interaction can become completely dominant. Continuing the decrease of temperature, the kinetic energy decreases and the attractive Coulomb interaction can provoke a gas of pole-antipole pair configuration similar to the excitonic condensation which is a coherent macroscopic quantum

state, similar to the Bose-Einstein condensate. This latter situation is for the lowest temperature and corresponds to the sharper peak in both the specific heat and magnetic susceptibility measurements. However, this low temperature state (in which the pole-antipole pairs are in the lowest energy state of double-particle, whose linear momentum is zero) have a great theoretical and formal interest, but its possible application for transmitting as energy and information is more reduced. On the contrary, the magnetic plasma, maybe, has minor theoretical interest than that of the exciton condensate magnetic state, since its dual electric partner has a more known behaviour, however, the possible circuital applications for energy transmission are greater than the former antithetic state.

In this chapter we have presented a versatile, analytic model by considering the facts commented in the former paragraph that can explain the behavior of compounds called spin-ices at low temperatures where there are several phase transitions. We say that it is versatile because from determining the magnetic potential whose expression Eq. (1.15) is consistent with the dumbbell model and using methods of statistical mechanics have related this potential with the order parameter. This order parameter is the number of magnetic charges either in the form of pole-antipole pairs or free charges From this Eq. (1.15) we have obtained the internal energy of the system, the specific heat and entropy in two states that we have given by means of analytical formulas which allows us to carry out a general study of the thermodynamic evolution with temperature. In addition, our results are consistent with the experimental available data [12, 30, 32,33, 53-55, 62].

CHAPTER 3: Many-Body States as a Model of Two Fluids

1.   Two-fluid model of the excitation state of spin-ice

In the former chapter, we have presented two models for the low temperature excitation states of these systems. One concerns the BCS global state that we consider almost discarded by the inexistence of the presence a gap near the fermi level since this gap should be manifested in the specific heat and this feature does not appear in the experimental data. The second model of the chapter 2 is formalized from the spin symmetry of its individual components. In this chapter 3, we give a structure for the global state based on the condensation of dipoles whose spin symmetry is bosonic and the posible phase transition is explained in terms of evaporation of this condensate of individual and quasi free magnetic charges. Therefore, we suppose that the low temperature states can be constituted of two fluids, one of them bosonic and another one whose components are fermions.

In the latter comments of the chapter 2, we give a summary of the phenomenology of the phase transitions by considering the temperature evolution in a cooling process. In this chapter we go to do a complementary visionage inciding in explanations of the same phenomenology in an inverse direction of increasing temperature, i.e. by considering that T starts in zero and it is progressively increasing. On the other hand, other novelty that we introduce in this chapter is the quantum formalization whithin the many-body wavefunction of the features of the creation and annihilation of the confined dipoles. The main physical objective being in this chapter the same of the chapter 2 and this is the description of the successive phase transition in this spin-ice materials in the first kelvin of temperature.

In the latter section of chapter 1, we explain the interpretation from the classic electrodynamics of the dumbell model. The basis of the explanation is the equality of the magnetic moment considered classically, that is to say an effective current of electric charges whose magnetic moment is perpendicular to the surface enclosed by it, by two magnetic charges $\pm g$ separated by a distance l, similar to the electric dipoles and their dipole moments coincided $\vec{m} = g\vec{l}$. There, we accept the demonstration by Castelnovo et al. described throughout the introduction and chapter 1 that the classical Hamiltonian of both models, the real one and the one of magnetic charges, is equivalent. In addition, we show in the aforementioned section that Maxwell's magnetic field continues to have zero

divergence. In this chapter 3, the main idea is to apply a version of the correspondence principle in order to formalize the dumbbell model within quantum mechanics and we will determine the phase transitions using the state functions obtained from the combination of Statistical Mechanics, Quantum Mechanics. and N-particle theory.

In this section, we consider a formalized theory of the spin state of each tetrahedron as well as the global many-particle state from the one component of each tetrahedron state, which is fixed by the following schematic form $|t>=|\uparrow,\uparrow,\downarrow,\downarrow>$. Where with the upward arrows we want to indicate that the magnetic moment has an exit direction of the tetrahedron and with the arrows in the opposite direction we indicate that the corresponding magnetic moments point towards the direction of the center of the tetrahedron. Therefore, all magnetic moments in the fundamental state of the global system have the direction pointing to the barycenter of each tetrahedron, two in direction toward out of tetrahedron and the other two in direction towards within it.

Consequently, the fundamental ground many-body state of the magnetic structure consists of tetrahedrons connected by a vertex in which there is a magnetic ion whose magnetic moment is shared by two connected tetrahedrons. In this situation, if in one of the tetrahedron the magnetic moment points to the center of the tetrahedron and in the other one, obviously, points in the opposite direction. This situation is identical for each vertex of each tetrahedron. The dumbbell model [7,8] associates at each magnetic moment the existence of two virtual magnetic charges, $q_m = \pm\dfrac{|\vec{\mu}|}{l}$, a negative charge at the origin of the magnetic moment vector and a positive one at the end of that vector, in a dual image analogous to the electrical dipole momentum. Therefore each tetrahedron in the ground state of the system contains two negative, $-\dfrac{|\vec{\mu}|}{l}$ charges and two positive ones, $\dfrac{|\vec{\mu}|}{l}$.

When the temperature increases slightly there is a probability that a magnetic moment of a vertex undergoes a change of direction of its magnetic moment, which by the dumbbell model would imply that one of the connected tetrahedrons should have three positive magnetic charges and one negative and the corresponding connected tetrahedron should have three negative magnetic charges and one positive. This would lead us to the effective image that for each pair of tetrahedra in which there was an inversion of the magnetic moment in a shared vertex,

in a tetrahedron of the pair there is a magnetic charge, $g = 2\,|\,q_m\,|$, constituted of two original virtual charges, in the another one there is a negative magnetic charge, $g = -2\,|\,q_m\,|$.

These resulting magnetic charges are those that the Bramwell et al. [11,12] have discovered that can be moved inside the magnetic structure when the inversion of the magnetic moment travels over the magnetic structure. Therefore, the fundamental state is formed by $|\Phi_0> = \prod_i^N |\,t_i,t_i'>$, where i-index runs over al vertexes of the tetrahedrons of the crystal; t_i is the tetrahedron in which the magnetic moment enters its interior and $t_i' >$ is the tetrahedron in which the magnetic moment points outside of the tetrahedron.

2. Principles of the lowest energy of excitation states

The spin-flips among the pairs of contiguous tetrahedrons occur with a reduced energy expenditure. When they run over through the crystal, modifying the local magnetic moment of each tetrahedron, the Castelnovo et. al's model [7] interpreted as resulting interacting magnetic charges forming weak crystalline structures that have similarities with the Dirac strings [1,3]. The elemental excitation state can be analytically described by the expression $S_i^- |\,t_i,t_i'>$, where $S_i^- = S_i^x - jS_i^y$, with $S_i^x\,(S_i^y)$ being the x(y) components of the $\vec{S}$-spin of i-atom located in the shared vertex of two tetrahedrons of each pair. When the spin-flips travel within the crystal, then the length of these strings increases and in the limit, the resulting magnetic monopoles can be considered quasi-free magnetic charges [1,3,7]. In this way, the state $S_i^- |\,t_i,t_i'>$ can be written as:

$$S_i^- |\,t_i,t_i'> = |\,p> \times |\,a> = |\,p,a> \tag{3.1}$$

where $|\,p>\,(|\,a>)$ is the definition of a positive(negative) magnetic charge whose absolute value is $g = 2\,|\,\vec{\mu}_0\,|/L$, where L is the length separation between the two centers of the corresponding tetrahedrons of the pair. These structural entities require the existence of a magnetic structure such as that of the spin-ice compounds and they are different from the magnetic monopoles which the high energy physics researchers justified their existence since forty four years ago [4,5] and several laboratories try insistently to find (see for instance, Refs.[2,63,64]).

Within the solid state magnetic structure scheme, we can define fermion operators $p^{\dagger}|0>=|p>$ and $a^{\dagger}|0>=|a>$, and then the many-body state of the gas constituted of confined magnetic dipoles can be given in similar way to different many-body states in which pairs of particle-antiparticle are associated in a condensate such as the exciton bubble [57-59] by means of the following many-body wave function:

$$|\Phi_0>=\prod_{i}^{N}\left(\alpha_i+\beta_i p_i^{\dagger}a_i^{\dagger}\right)|0,0>$$
(3.2)

where β^2 is the probability of obtaining the pair of magnetic charges, $\pm g_i$ in two contiguous tetrahedrons generated by a spin-flip in a vertex and, in addition, $\alpha_i^2+\beta_i^2=1$. The difference between this global wavefunctions from that of BCS of chapter 2 is that while this is static and confined dipoles, those of chapter 2 are associations or coupling between two monopoles which travel inside the crystal with k and -k linear momentum. In addition, the hamiltonian which governs the system is in this case exclude the posibility of several charges of the same sign within any tetrahedon since the repulsive interaction whitin the space of a tetrahedron is very large, therefore, this Hamiltonian can be the following:

$$H=\sum_{i}^{N}\varepsilon(p_i^{\dagger}p_i+a_i^{\dagger}a_i)+\sum_{i}^{N}\sum_{j}^{N}V_{ij}p_i^{\dagger}a_i^{\dagger}a_j p_j+U\sum_{i}n_i^{p}n_i'^{p}+U\sum_{j}n_j^{a}n_j'^{a}$$
(3.3)

where $V_{ij}<0$ corresponds to the attractive pole-antipole interaction. We, without losing generality and for the sake of simplicity, consider the isotropic version which can be simplified by $V_{ij}=-|V_0|$, and this version will be conciliated with a many body state of Eq. (3.2) based on N-bosons where each one body state is a fermion pair. The two latter terms of the Hamiltonian can be interpreted as Hubbard-like terms which hinder two magnetic charges of the same sign could be within the same tetrahedron. The great repulsive energy U forbids the existence of two charges of equal sign within a same tetrahedron. In these two Hubbard-like hamiltonian terms, n_i and n_i' are two magnetic charges of the same sign arising from two spin-flips within the same tetrahedron.

These two Hubbard-like terms imply that only one of the seven vertexes of each pair of contiguous tetrahedrons can initially have a spin flip into the many-body excited condensate state of above wavefunctions. The average energy of the isotropic version of Hamiltonian considering the many-body wave-function (3.3) is :

$$E = \sum_{i}^{N} 2\varepsilon_i \beta_i^2 - |V_0| \sum_{i}^{N} \sum_{j}^{N} \alpha_i \beta_i \alpha_j \beta_j = 2N\varepsilon\beta^2 - \frac{\Delta_0^2}{|V_0|} \tag{3.4}$$

where $\Delta_0 = |V_0| \sum_{i}^{N} \alpha_i \beta_i$, the energy ε is the necessary energy for obtaining the required spin-flip which is the cause of the magnetic charges appearance. This energy is deduced from the Casselnovo et al's dumbbell model and given the characteristic features, we have drawn from a recent paper, [65], and whose deduction is in chapter 1 [Eqs. (1.15)] whose expression is:

$$\varepsilon_i = KT \ln \frac{n_0}{n_i} + \frac{|g_i| \phi_0}{T_V} T \tag{3.5}$$

where T_V is the transition temperature in which the many-body excitation state is in the maximum semblance with a Bose-Einstein condensate and whose consideration have been experimented in several works [34,46-49,66,62]. From Eq. (5), it is clear that for $T=0$, $n_i = 0$ and then, $\varepsilon_i = 0$. This BEC-like state should be coherent with the first and narrow peak in the specific heat. When the number of pairs n_i is close to the maximum value, the spin-flips runs over the crystal and then the lengths of the Dirac strings increases; then the probability of evaporating charges of the condensate increases and the new many-body state of higher temperature excitation starts to be formed.

3.   Transition from BEC towards a magnetic plasma state

The form that has the experimental temperature evolution of the specific heat at constant volume of the lanthanide compounds crystallizing as spin-ices is characterized by the existence of a very narrow and intense peak between 0.05 and 0.2 K. This seems an unequivocal empirical result and leads us to the idea that the formation of pole-antipole pairs can reach its maximum value. This maximum has to have a limit value taking into account that the Hamiltonian of the Eq. (3) implies that any tetrahedron can only be associated with a single contiguous tetrahedron of the four possible in which it shares a spin-flip. Therefore only a vetex of the seven of each pair of tetrahedons can be implied in a spin-flips.

Exceeding this temperature of about 0.2 K, the length of the dipoles increases due to the evolution of the spin-flips such as we have mentioned in the previous paragraphs. Then, the number of free magnetic charges can progressively increase taking into account that it is equally probable the creation of positive and negative charges.

This tends to create a gas of positive and negative charges in such a way that the total charge will remain zero. As a result, a state in the form of a magnetic plasma is progressively generated [25,65,67], which can initially share space with the gas of pole-antipole pairs. Having in mind this idea, we go to consider the analytical principle of the fermion gas formation by means of the creation of fermion particles from the $|\Phi_0\rangle$-state of Eq. (3.2). This idea requires to establish analytically the evaporated states (evaporated particles) of the condensate [61,68] whose evaporation process can be defined by means of the following creation operators applied to the $|\Phi_0\rangle$ - state:

$$\begin{aligned} u^\dagger &= \alpha p^\dagger - \beta a \\ v^\dagger &= \alpha a^\dagger + \beta p \end{aligned}$$

(3.6)

definitions determine the corresponding annihilation operators, in such a way that we have the following operations over the ground state of the condensate: $u_j^\dagger |\Phi_0\rangle = |p_j\rangle \prod_{i\neq j}^{N}\left(\alpha_i + \beta_i p_i^\dagger a_i^\dagger\right)|0,0>$, simplifying the notation, we can write $u^\dagger |\Phi_0>=|p>$, $v^\dagger |\Phi_0>=|a>$, $u|\Phi_0>=0$ and $v|\Phi_0>=0$, where $|p>$ ($|a>$) is an excited state respect to the BEC-like ground state $|\Phi_0>$ corresponding to the creation of a positive (negative) free magnetic charge and which are the magnetic charges evaporated from the condensate. The many-body state with M/2 free positive magnetic charges, a M/2 free negative ones and M' confined dipoles till inside the condensate is:

$$|\Phi> = \prod_i^{M/2} u_i^\dagger \prod_j^{M/2} v_i^\dagger |\Phi_0> = \prod_i^{M/2} |p_i> \prod_j^{M/2} |a_j> \prod_l^{M'}\left(\alpha_l + \beta_l p_l^\dagger a_l^\dagger\right)|0,0>$$

(3.7)

where $M+M'=N'$, N' being the number of vertexes of the tetrahedons, taking into account that the two last terms of Hamiltonian (3.3) hinder the double occupation in any tetrahedron of magnetic charges, g of the same sign. This above wave-function state (3.7) is that of system of the two fluids. The variational procedure of obtaining the average value of hamiltonian Eq. (3.4) yields an energy whose expression can be easily determined via the definitions of the actions of creation and destruction operators defined, this expression is the following:

$$E \approx 2\sum_i^{M'}\left[\varepsilon_i \beta_i^2 - \frac{\Delta_0^2}{2M'|V_0|}\right] + \sum_i^{M}\left[\varepsilon_i(1-2\beta_i^2) + \frac{\Delta_0^2}{\sqrt{<\varepsilon>^2+\Delta_0^2}}\right]$$

(3.8)

where the one body energy ε_i corresponding to free magnetic charge of Eq. (3.5). In order to describe the temperature evolution of the extensive state functions and their corresponding first and second temperature derivatives, in this scenario, we have considered the statistical thermodynamic theory in order to determine the

specific heat and entropy starting from the thermodynamic potential or Helmholtz free energy F. We determine the thermodynamic Hemholtz potential for a mixed fluid forming two channels one of them as a boson gas and another one constituted of fermions [69] described by the many-body functions of Eq. (3.7):

$$F = -\frac{1}{\beta}\left\{2\sum_j \ln\left[1+\exp\left(-\beta(e'_j-\mu')\right)\right] - \sum_j \ln\left[1-\exp\left(-\beta(e_j-\mu)\right)\right]\right\} \qquad (3.9)$$

where, e'_j and e_j are the one body energies of the fermions and bosons, respectively i.e. the monopoles and dipoles respectively corresponding to the mixed fluids of many-body wavefunctions of Eq. (3.7), whose expressions are given by:

$$e_j = 2\left(K_\beta T\ln\left(\frac{n_0}{n_j}\right) + T\frac{|g|\phi_0}{T_V}\right)n_j + \Sigma_0 - \frac{\Delta^2}{|NV_0|} \qquad (3.10)$$

$$e'_j = \left(K_\beta T\ln\left(\frac{n_0}{n_j}\right) + T\frac{|g|\phi_0}{T_V}\right)(1-2n_j) + \Sigma_0 + \frac{\Delta^2}{(<e_j>^2+\Delta^2)^{1/2}} \qquad (3.11)$$

then, the Helmholtz free energy per channel can be given by the following expressions (see Appendix B):

$$F_{BEC} = N'\frac{K_B T}{2n_0}\int_0^{2n_0}\ln\left|1-\left(\frac{t}{2n_0}\right)^t e^{-at}e^{-b\beta}\right|dt \qquad (3.12)$$

$$F_{Plasma} = -N'\frac{K_B T}{2m}\int_{1-2m}^1 \ln\left[1+\left(\frac{1-t}{2n_0}\right)^t e^{-at}e^{-b'\beta}\right]dt \qquad (3.13)$$

where, $a = \frac{|g\phi_0|}{K_B T_V}$, $b = \Sigma_0 - \frac{\Delta_0^2}{N|V_0|} - \mu$, $b' = \Sigma_0 + \frac{\Delta_0^2}{\sqrt{<\varepsilon>^2+\Delta_0^2}} - \mu$, n_0 is the probability that a magnetic dipole is created in each pair tetrahedron in the BEC-like state, m is the probability of appearing a free magnetic charge coming from a confined dipole of the BEC-like state. Having in mind these definitions, the entropy in the boson channel per each vertex in which a spin-flip is possible, taking into account that all vertexes have the same probability for suffering an identical spin-flip due to the temperature variation, is given by:

$$s_{BEC}(T) = -\frac{1}{N}\frac{dF_{BEC}}{dT} \qquad (3.14)$$

and the entropy for each dipole of the bosonic phase when it is decaying and is becoming the fermionic phase of free charges can be given by the following expression:

$$s_{Plasma}(T) = -\frac{2}{M'}\frac{dF_{Plasma}}{dT} \tag{3.15}$$

and the specific heat in the boson channel corresponding to the BEC-like global estate per dipolar component is:

$$c_{BEC}(T) = -\frac{1}{M'}T\frac{d^2F_{BEC}}{dT^2} \tag{3.16}$$

On the other hand, the specific heat of the fermionic channel of the magnetic plasma state per each free magnetic charge is given by:

$$c_{Plasma}(T) = -\frac{1}{M'}T\frac{d^2F_{Plasma}}{dT^2} \tag{3.17}$$

An important characteristic of the bosonic channel, not present in the fermionic one, is according to Eq. (3.12), the possibility of presenting divergences both in the thermodynamic potential and in its derivatives regarding the temperature. These divergences define first-order transitions in the thermodynamic potential, internal energy and the specific heat. This is not a minor issue neither from the theoretical point of view nor much less from its empirical consequences. Indeed, in the Eq. (3.12) of the bosonic channel, the possibility of infinite values appears at a certain temperature when the following equality is fulfilled in the integrals:

$$1 = \left(\frac{t}{2n_0}\right)^t e^{-at}e^{-b\beta} = \left(\frac{n}{n_0}\right)^{2n} e^{-2an}e^{-b\beta} \tag{3.18}$$

When this equality is satisfied for a value of temperature, the internal energy and the specific heat are representative of a first-kind phase transition. On the contrary, in the fermionic channel this possibility does not exist since in Eq. (3.13), the existence of any divergence is not possible. Therefore, the value of the interaction energies among magnetic charges plus their energy formation, defined as self-energy Σ_0 in the dumbbell model [7], are causes that collaborate in the generation in the spin-ices of a phase transition of either first or second order at T_V -temperature. In other words, this energy b and the parameters a and n_0 determine if in the specific heat there is an infinite or a simple cusp or possible discontinuity in the derivatives with respect to the temperature of the thermodynamic potentials.

We want to emphasize that the expressions of specific heat given in Eqs. (3.16) and (3.17) is specially sensitive to the variations of the energies, b, and b' as well as the parameters a, n_0 and m such as we have said in the last paragraphs of the previous section. This requires to have some idea about possible intervals in which the values of these in actual cases.

The dimensionless parameter a establishes the relationships between the "magnetronic" energy potential of the magnetic system interacting with the magnetic charges and the thermal energy at temperature corresponding to first maximum of the specific heat. This temperature at which the maximum appears is one in which the lowest energy state is dominant. This state, as above mentioned, may be similar to a Bose-Einstein condensate [34,46-49,62,66] and the temperature evolution leads to a system towards another low-excitation energy state which is similar to a plasma state where the currents of magnetic monopoles can be defined as $J_m = \partial M / \partial t$ [25,31,36,39,40,65,67]. The first of these states being the culminating point in the specific heat corresponding to the narrowest peak. The possible values of this a- parameter should be in the interval between the unity and the relation T_V / T_C whose value is around 0.1, since the two energy amounts of the corresponding fraction $a = |g| \phi_0 / K_B T_V$ is referred to energies typical of the corresponding states.

The parameters n_0 and m are the probabilities for the presence of the confined magnetic dipoles at T_V which is generated via the corresponding spin-flip and the probability for the breaking of each pair in the two magnetic charges confined in a dipole at T_C, respectively. The values of the n_0 and m can be obtained from indirect experimental results arising from the magnetic conductivity (see Refs.[67,70] and references therein) they may be between 0.25 and 0.75. The energies b and b' are those energies which do not depend on the increasing of the probability of appearance of the magnetic charges due to the temperature evolution but they are consequence of magnetostatic energies which comes from the gg' interactions [45]. And last, but not least important, μ is the chemical potential defined as $\mu = \partial F / \partial N$. The values of this chemical potential is more difficult to obtain by means of experimental data.

Then, we have considered free parameters whose fitting can be justified via the different results which afford to the specific heat and by means of their comparison with both the experimental data and other theoretical researches. Therefore, if the other assumptions and hypotheses of the model are justified, the coherence of the theoretical result yielded by the calculation can serve to justify the validity of the values given in these energies. However, we recognize that the study of a more consisting theory for the assignation of values for these energies can be important to be developed.

4. Results and comments

As it is empirically well evidenced, and such as it is explained in the introduction and throughout the text of this chapter, the first process that appears at low temperature is the creation of confined dipoles in contiguous tetrahedrons. These confined dipoles have complete similarity with microimagnets, or better said nanomagnets of dimensions of the height of each tetrahedron. When the temperature continues increasing the spin-flips of the magnetic moments are propagated along the magnetic structure. Then the length of the namomagnets increases until true free charges coexist (monopoles and antimonopoles) with confined dipoles. The confined dipoles have a structural resemblance to the mesons [43] with the difference that the quarks and anti-quarks that form the hadronic structure can not be released from each other, while the poles and anti-poles at spin-ices can be converted into effective free magnetic charges either under increasing temperatures or the presence of external magnetic fields. Then, there is coexistence between two quantum fluids, one of them corresponding to confined dipoles and another one to free monopoles. That is why we configure the model of two fluids in which the different form of Helmholtz free energy [69] corresponding to the bosonic fluid (of confined pole-antipole pairs) competes with the fermion gas constituted of positive and negative free charges.

In addition, the charges of different sign are quasi-particles with $+|g|$ and $-|g|$ which have the same energy. This energy equality is because their presence is simultaneously generated and whose energy is that necessary to produce the spin-flip. The physical bases of this model are Eqs (3.2)-(3.7) and (3.9)-(3.13) and the structural consequences of the temperature evolution of the low energy excitation states can be analyzed via Eqs (3.14)-(3.17) which correspond to the different specific heats and different entropies concerning the low temperature phases. These equations constitute the master formula for determining the phase transition in these

two quantum fluids. There exists the experimental doubt about whether the lowest-temperature phase transition in the spin-ices corresponds to either the first or second order.This doubt is logical since its existence occurs at very low temperature (between 0.05 and 0.17 K). When Eq. (3.18) ais satisfied, the specific heat suffers a divergence due the existence of an essential infinite for an intermediate value in integrals which define it. Having in mind this latter equation and given the meaning of these variables, the condition for the existence of a first-order phase transition is:

$$\frac{b}{KT_V} = 2n\left(\ln n - \ln n_0 - a\right) \tag{3.19}$$

where all constants of this equation have been defined and n is the variable of integration which defines a determined probability for the spin-flips to be generated in the corresponding state. If we represent this equation in a parameter space, considering a given T_V whose value can be between 0.05 and 0.17 K and a given value for the maximum n_0 , we can construct the parameter space with b as Z axis, a as Y axis and n the variable in the integrals as X axis. Then, Eq. (3.19) is represented in Fig. 16.
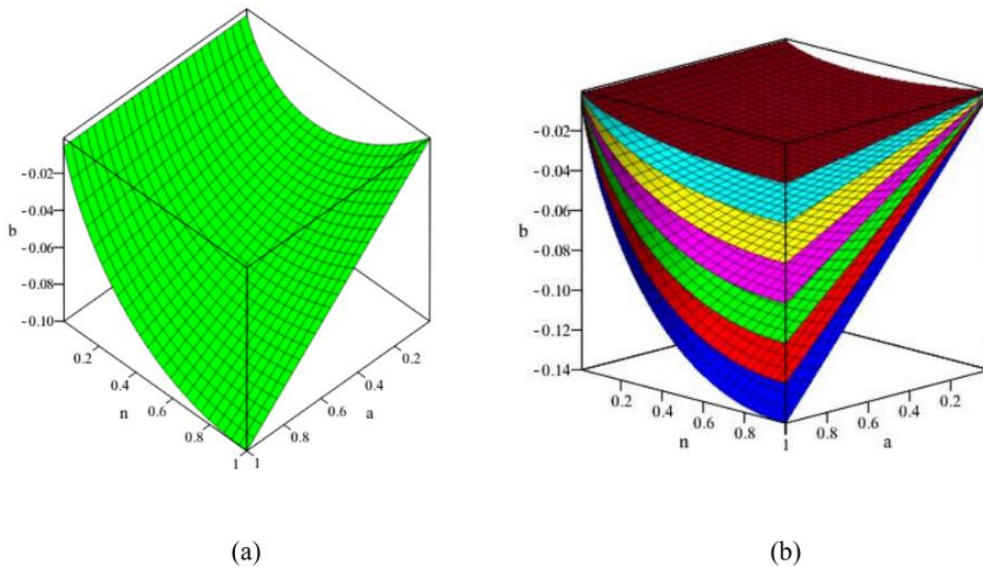
Figure 16.- Condition for a first-order phase transition.

In Fig.16a we give a surface corresponding to Eq.(3.18) for T_V =0.1 K and n_0 = 0.5 . For each point in this surface defined for its coordinates: the parameter a, energy b interaction and n- variable, there exist a divergence which implies the existence of a first-order phase transition, which is manifested in the specific heat for the given temperature T_V and a given probability of pair formation. n_0 . In Fig 16b, we given seven examples of the seven

surfaces corresponds to and $n_0 = 0.1$ (brown); $n_0 = 0.2$ (cyan), $n_0 = 0.3$ (yellow), $n_0 = 0.4$ (magenta); $n_0 = 0.5$ (green); $n_0 = 0.6$ (red) and $n_0 = 0.7$ (blue).

In this figure, we give a surface in the 3-dimensional parameter space whose points in this surface describe the physical situations in which the specific heat and internal energy has an essential infinite and therefore, the phase transition is of first order. The values of the energy b and the parameter a can imply the existence of a value of n which constitute a point in the parameter space located on the surface of Fig. 16a or on any other surface similar to those in Figure 16b. These values being actual parameters in real spin-ice compounds. If under normal conditions it is not possible, when the system is subjected to hydrostatic pressures or in the presence of external magnetic fields, then the divergences in the specific heat can appear.

The low temperature (between 50 and 170 mK), at which these first-order thermodynamic transitions must appear, are the cause for they have not been profusely detected, and although detected, the phase transition order is not known with total certainty. However, in 2016 an experimental result [55] detected structural modifications at temperatures below 1 K, with a transitions signature of first order without the existence of changes in the crystalline structure. The other points of the cube of the parameter space of Fig. 16, the phase transition, if any, will be of second order. This Fig. 16 can be made for different T_V and n_0 (see Fig. 16b) values but the shape being quantitatively different is qualitatively similar. By cuts of this surface with normal planes to the different axis, we obtain the different coordinates in the parameter space which give the necessary conditions for obtaining a first-order phase transition. With the results that we give below, we do not intend to give completely unknown results, but our intention is to compare them with those already in the literature. Our objective is to weigh the possibilities of our analytical model and first principles of double fluid by comparing our results with others performed either with Monte Carlo statistical models [30,33,54,71,72] or other experimental methods [32,53,73,74]. In our opinion the important thing of this chapter is in the ingredients of the model and the different analyzes that can be done with it. The results we present are examples without pretending that they are unique or the best that can be obtained, we only try to put the methodology into practice. We believe that our model goes a little further in the knowledge of the nature of the global excited states of the system and the possibilities of obtaining more approximate results by modifying the parameters that govern the fundamental equations.

Therefore, henceforth, we will stick and limit to the points of the parameter space in which there are no divergences, consequently we will concentrate on the situations which are outside the surfaces of Figs. 16a and 16b. These cases seem to correspond to thermodynamic situations whose signature is close to be a second-order phase transitions where a large number of experimental results agree with this feature for the spin-ice systems.
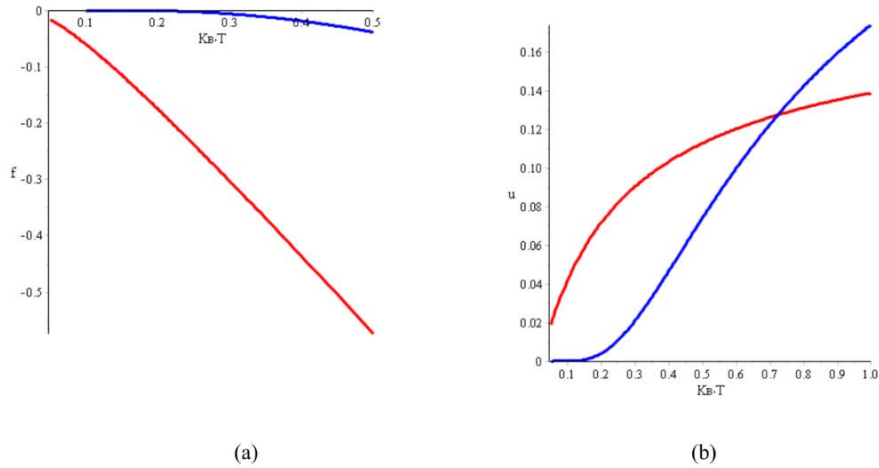
Figure 17.- Evolution with temperature of the thermodynamical potential and internal energy per particle.

In Fig. 17, with the red line, we represent the internal energy and the thermodynamical potential of the bosonic phase of confined magnetic dipoles as pairs of pole-antipole joined by the attractive interaction between both [48]. With the blue line we represent these two physical magnitudes per particle with magnetic charge in the free state. In Fig. 17a, we give the thermodynamic potential for the values of parameters $a = 0.1$, $n_0 = 0.5$, $m = 0.5$ and energies b and b' are energies such that the nondimensional sets of physical variables $b'\beta = \dfrac{1.00}{K_B T}$ and $b\beta = \dfrac{0.05}{K_B T}$. The blue line corresponds to the thermal evolution of the fermion channel of the thermodynamic potential and the red line corresponds to the boson channel of the same physical magnitude. The Fig. 17b corresponds to the thermal evolution of the internal energy with the same parameter and energies considered in Fig. 17a. The red curve is the boson channel and the blue one to fermion channel.

The different evolution of the thermodynamic potential and internal energy both at very low temperature and when it is growing is the reason for the existence of a possible discontinuity in the derivative and the other anomalies of the Helmholtz free energy which will lead, if any, to these possible phase transition of a second kind. The physical

reason for the different evolution with the temperature of both free energies is typical and due to the different nature of the thermodynamic potentials in the bosonic case with respect to the fermionic one. This difference being the fundamental reason that generates the features of the free and internal energies of the two phases, which in turn induces the special evolution of the specific heat detected experimentally. In the ground state the number of confined dipoles in each pair of two contiguous tetrahedrons must be zero and therefore the specific heat at zero kelvins should be null, as it appears in our results as well as in other investigations [30,33]. On the contrary, in other experimental results [32,73] and other obtained by statistical procedures as in references [54,71] this logic characteristic is not reflected in their results. Perhaps the low temperatures in the experimental results and the problems of establishing the specific heat when the growth of the internal energy is so intense at temperatures lower than 50 mK prevents obtaining results adjusted to the expected.The main characteristic difference in both the internal and Helmholtz energies between the two curves corresponding to the bosonic and fermionic states is in the temperature interval between 0 and 0.2K. In this narrow interval, the two energies corresponding to the fermionic phase is practically null, while that energy of the bosonic phase is fast increasing. This difference is the cause for the existence of the intense peaks in the specific heat of Fig. 18a and 18b and the possible discontinuity in the derivative versus temperature of the Figs. 18b, 18c and 18d.
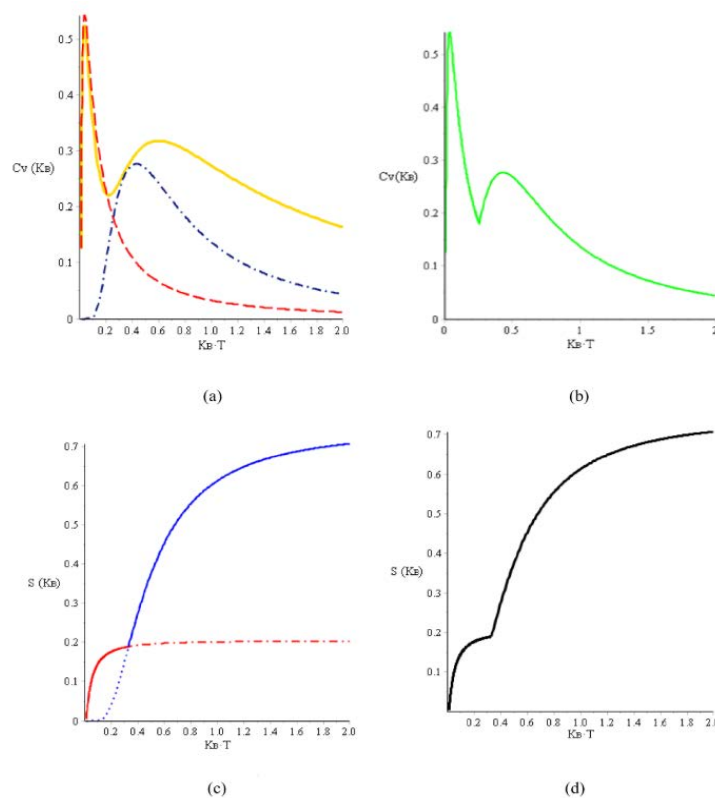

Figure 18.- Evolution with temperature of the specific heat and entropy.

In Fig.18a, we give the specific heat in the two first kelvins: the discontinuous red curve of narrow and intense peaks corresponds to specific heat $c_{BEC}(T)$ of the boson channel. This presents a rapid increase of the pole-antipole pairs and the also fast breaking of those dipoles via the prolongation of the splitting among the two poles but still considered partially confined dipoles. The discontinuous blue curve of $c_{Plasma}(T)$ of the fermionic channel which presents the second wider and less intense peak. The continuous yellow curve, we represent

$$c(T) = \left(1 - \frac{T}{T_c}\right)c_B(T) + 2\left(\frac{T}{T_c}\right)c_P(T).$$ This is the complete specific heat in which we suppose with this calculation

the idea of a progressive and continuous breaking of dipoles and formation the free magnetic charges.

In Fig.18b, we draw the curve of $c_{BEC}(T)$ until is cut with the curve $c_{Plasma}(T)$ which continue until 2 K. In Fig.18c, we represent the entropy per component, the blue curve is the corresponding entropy to the fermion channel and the red curve is that of the boson or confined dipole channels according to Eqs. (3.14) and (3.15). The discontinuous curves are the prolongation of the entropy to different channels. In Fig. 18d, we represent the entropy taking into consideration the change of Pauli symmetry within the the magnetic charge fluids. The first part of the curve up to 0.35 K corresponds to the bosonic contribution to the entropy and from this temperature value, the confined dipoles are progressively disappearing such as occurs in the specific heat. i.e. that corresponding to free magnetic charges. The values of parameters defined in Eqs. (3.12) and (3.13) which we have considered for obtaining the results of this figure are the following: $a = 0.1$, $b'\beta = \dfrac{1.00}{K_B T}$ and $b\beta = \dfrac{0.05}{K_B T}$, $n = 0.5$ and $m = 0.7$.

The responsible action reflected in this narrowest and intense peak is a quick massive generation of the confined pole-antipole states. Therefore, in this narrow interval of temperature between 0 and 70 mK the curve of specific heat is based on the fast increasing of components of the bosonic state. This abrupt growth reaches the peak, from which the number of dipole components abruptly decreases, beginning the creation of free magnetic charges. When the specific heat curve reaches the minimum this creation accelerates obtaining an evident growth of free charges but with less intensity than the most intense and narrow maximum. This image is the main characteristic of the spin-ices' specific heat and that it is perfectly compatible with the description of an initial transition of a second order and a continuous rupture or evaporation of the bosonic condensate forming carriers of

magnetic charge in freedom from this low temperatures [30,32,57,61,71,73]. The change of dominant state can be clearly seen at around 0.2 K, the narrow peak is centered at around 70 mK and the second wide maximum is at 0.6 K. These results being in concordance with that of experimental data of the literature (for instance, see Refs. [32,34,74]). When the curves of specific heat are cut, the boson channel can be disappearing and the dynamic is dominantly due to the fermionic free charges.

The figures of entropy deserve to be commented and related to those of specific heat. This behavior under temperature increasing in the entropy is the similar to that of the specific heat as well as the reasons for its similar evolution of entropy given in Fig.18c. In this figure, the red line refers to the growth of entropy with the increase in spin-flips and the corresponding creation of magnetic pole-antipole pairs and practically null presence of free magnetic monopoles. When this entropy of the bosonic channel no longer increases, the entropy arrives at a constant that approximately in Figure 18c is at around $T = 0.25K$ and a value around $0.20, [0.5\ln(1.5)]K_B$, that coincides with the residual Pauli entropy which is assigned to degeneration of the ground state. From this value, the bosonic phase disappears and the fermionic channel of free charges emerges. Then, entropy due to the fermionic gas grows until it reaches the value of entropy per free magnetic charge $K_B\ln2$, which is the saturation entropy of the fermionic gas.

Therefore the cut between the two entropy curves is done with a discontinuity in its derivative respect to the temperature. Therefore it may be consistent with the existence of a phase transition of states with different symmetry with respect to the spin of the individual components such as it is shown in Ref. [33]. Similar discontinuity appears in Figs. 18a and 18b when one joints the specific heat curves corresponding to the bosonic part (discontinuous red line) and the corresponding one of the fermionic channel (discontinuous blue line).

This cut, in our results which occurs at approximately the same temperature (0.35K similar to that of Fig 18c and 18d), in a similar qualitative way as that of Ref. [33]. The yellow solid line in Fig. 18a is identical to Fig. 18b. This continuous line is carried out by an alternative possible idea. This is in the sense that the change of spin symmetry between fluids may be continuous and not abrupt. In other words when one considers the conversion from the pairs in the creation of free charges in a continuous and progressive way, then we can represent a specific

heat by means of a continuous mixing between the boson and fermion channels, and this can be carried out by

means of the expression $c(T) = \left(1 - \dfrac{T}{T_C}\right) c_{BEC}(T) + 2\left(\dfrac{T}{T_C}\right) c_{Plasma}(T)$.

In this expression, typical of a two fluid model, $c_{BEC}(T)$ is the specific heat per pole-antipole pairs of the

boson channel and $c_{Plasma}(T)$ the specific heat per fermionic magnetic charge of the half of the fermion channel.

This idea of the mixing to establish a specific heat $c(T)$ based on the continuous sum of the two contributions has

a double motivation. A first physical reason is by change of spin symmetry from the boson channel to a fermion

gas might occur in a continuous and progressive way; and a second reason is thinking in to obtain a image for the

specific heat more similar to that of experimental curves [32,34,74].

Similar continuous expression between the two channels is not so much appropriated for entropy given the

constantly increasing value of this physical magnitude, but our results of Figs 18c and 18d reasonably agree with

the results of Refs. [32,34,73,74]. However, the discontinuity on the derivative with temperature in both specific

heat and entropy is very difficult to be experimentally observed given the extremely low temperatures in which they

should be obtained. The coherence between two results of Figs. 18a and 18c as well as the 18b and 18d may have

a certain importance since it gives certain support to the assumed hypotheses.

Otherwise, we want to emphasize the clear existence of a phase transition at 50mK determined in our results

of Figs. 16 and 18. This fact being perfectly coherent with the experimental results [32]. This phase transition may

be either a first order or a second order and although we have given unambiguous criteria for the discrimination of

its order with Fig. 16, unfortunately, there is not still a complete experimental consensus about this order due to the

extremely low temperatures which occurs this phase transition. In any case, it is clear that at T=0 K, the specific

heat should be null and at temperatures less than 0.2K there is a huge fast increasing such as it is given in our

results, this fact in concordance with previous data [30,32,54,73].

In summary, we start from a state of many quasi-particles, such that their individual energy explicitly depends

on the temperature, these quasi-particles have attractive interaction because they are magnetic charges of different

sign and for this reason we constructed a wave function corresponding to two fluids of different Pauli symmetry. One formed by magnetic pole-antipole pairs and another one of free charges that are evaporated from a condensed state of the same.

We construct the thermodynamic potential corresponding to the two quantum fluids and determine the internal energy, specific heat and entropy. We give the condition that discriminates the situations defined by the parameters that lead to a first order transition in Figs. 16a and 16b. This condition for first order phase transitions being possible since it is within the interval of actual values for the parameters which govern these phase transitions. Given the greater tendency to accept the empirical evidence that in the spin-ices, the phase transition of the lowest temperature seems to be of the second kind, we obtain the thermodynamic characteristics of the same from the specific heat and entropy. We give examples of these physical variables that can be obtained empirically and that, on the other hand, agree fairly closely with the experimental results existing in the literature of these compounds.

CHAPTER 4: Dual Maxwell Equations and Lorentz Forces

1.　Electromagnetic propagation in the magnetic plasma state in spin-ice systems

From this chapter we change the methodology and we will study the behavior of the spin-ices before the electromagnetic interaction. That is, we are going to study the electromagnetic propagation within of the spin-ices or in any material that has structural entities that are effective magnetic charges. The prospective of possible applications are the reasons of the analysis developed in this chapter. This is carried out from the electromagnetic propagation phenomena in a quasi-particle system with magnetic charges submerged in a sea of magnetic dipoles and Dirac's strings of different lengths. Therefore, in this pattern, we have considered that there are two extreme states: the configuration of a magnetic condensed of pole-antipole pairs which can exist at low temperature [32,46-48,76,78], and a state of quasi-free magnetic charges which constitute a structure similar to aforementioned magnetic plasma [25]. Really, the actual situation can be any possible intermediate state between the two extreme states where the confined dipoles, Dirac's strings of different lengths and free magnetic charges can coexist.

Then, the electromagnetic propagation in both unlimited and confined substrates can put in evidence the different possibilities where the effective masses of the free charges and above all, the density of magnetic charges can be important parameters in the distinction of the different many-body states. In recent studies inertial effects of the movement of the charges under the extern magnetic field have been detected [75]. Consequently, in this part of the chapter, we carry out studies of electromagnetic propagation in order to suggest experimental indications for detecting these quantum macroscopic states. Besides with our analysis, we try to initiate a prospective about the possibilities of the spin-ices as devices able to propagate both information and energy. This is so, since when the system is constituted of pole-antipole pairs, the system under the action of external magnetic fields is different from that in which the individual magnetic charges can freely travel inside of crystal structure. Then, the electromagnetic propagation can discriminate which is the prevalent many-body state of any system.

We obtain linear response functions of unconfined plasma states of the spin-ices by means of transversal electromagnetic waves assisted by a constant and intense electric field whose direction is normal to the phase plane of the wave. This linear response allows to determine the effective mass of the magnetic charges by means

of a relationship with the absorption main frequency. This frequency is provoked by the precession oscillation of the magnetic charges under the action of the external electric field. In addition, in this first electromagnetic propagation process, we determine the plasmon frequency and the linear response function in the plasma phase.

On the other hand, we analyze the different modes within a wave guide which we suppose filled with this spin-ice material. This propagation is strongly dependent on the density of the magnetic charges. In addition, in this second study, we determine the dependence of the magnetic conductivity and the magnetization with the frequency and it allows to clearly discriminate each corporative state for a determined temperature according to the behaviour under the electromagnetic wave propagation.

The analysis and results of this chapter can be, in our opinion, interesting because we suggest experiments for determining the existence of magnetic currents in possible new materials and with these results, we intend to initiate the exploration of the possibilities for performing magnetronic devices, since although the concept of magnetic monopoles in spin-ices is clearly and conceptually consolidated, the mechanism of the mobility of the monopoles within the solid materials requires explanation in order to obtain knowledge of the technological advantages of possible future applications.

2. Transversal electromagnetic propagation in magnetic plasmas

The T-evolution of the magnetic structure of the spin-ices can be a mixture of confined magnetic dipoles, Dirac-like strings of different lengths and magnetic charges of both signs. In this scheme the neutral magnetic plasma state [25] in dual similitude to the electric plasma such as the jellium system and the Bose-Einstein condensation of pole-antipole pairs can appears in an inextricable mixing [32,46-48,76,77]. The procedure for distinguishing these two states via the different electromagnetic propagation is one of the ideas of this and the next section. One of the main objectives of the next sections is to establish an electromagnetic propagation method for describing properties which allow discriminating the corporative states which can be present within the magnetic charge gas in the spin-ices or in any material with similar circumstances. In any case, we want to emphasize that

all main variables of the system in both extremal global states depend on the effective masses of the magnetic charges as well as on their density.

The transversal electromagnetic propagation in the plasma state can be an experimental methodology for obtaining the inertial phenomena in magnetic charges as well as the increase of kinetic energy coming from the interaction of external magnetic field in a parallel direction to the velocity of these magnetic monopoles. These have been recently measured as inertial effects under magnetic field [75] and their knowledge allows us to determine the mobility and therefore one of the most important physical magnitudes for using these materials as devices for the electromagnetic propagation.

The first case of electromagnetic propagation which we analyze is the perturbation generated in the state with magnetic charges by means of a transversal wave. In addition, this analysis serves for detecting the existence of magnetic charges in new possible materials. The corresponding experiment in the case of electric plasmas (which is the dual situation of the case of our study) is based on the incidence of a transversal electromagnetic wave over the electronic-protonic plasma with the additional assistance of a sufficiently intense magnetic field in the direction of propagation of the electromagnetic wave. The result of this experiment based on the standard Maxwell and Lorentz force equations is a clear birefringence of the levorotatory and dextrorotatory circular polarizations of the electromagnetic waves along with anisotropy with respect to the direction of the constant magnetic field [36]. The dual experiment which can serve as a test for the existence of magnetic charges in a determined material is the incidence of transversal electromagnetic waves assisted by a sufficiently intense and constant electric field (in dual rule to the magnetic field in the electric plasma) in the electromagnetic direction of the transversal wave. However, there is a crucial difference between the magnetic plasma with respect to the electric ones. Actually, in the electric plasmas, the positive charge current vanishes with respect to the value of the negative charge current due to great difference between the masses of the ions in front of the electrons. On the contrary, in the magnetic plasma the masses of negative charges are strictly equal to that of the positive magnetic charges. This is due to the completely symmetric structural presence of both charges, positive and negative, such as explained in the introduction. We focus our attention on the effect of the dynamics of the magnetic charges and magnetic currents on electromagnetic propagation and for the sake of simplicity we will consider that the system is

isotropic and homogeneous. Therefore, the extended electromagnetic equations for the magnetic charge system can be the following:

$$\nabla \wedge \vec{H} = \varepsilon_0 \frac{\partial \vec{E}}{\partial t}$$

(4.1)

$$\nabla \wedge \vec{E} = -\mu_0 \left(\vec{J^+} + \vec{J^-} \right) - \mu_0 \frac{\partial \vec{H}}{\partial t}$$

(4.2)

$$\frac{d\vec{J^+}}{dt} + \gamma \vec{J^+} = \frac{\mu_0 g_m^2 N^+}{m} \vec{H} - \frac{gE_0}{mc^2} \vec{J^+} \wedge \vec{e_z}$$

(4.3)

$$\frac{d\vec{J^-}}{dt} + \gamma \vec{J^-} = \frac{\mu_0 g_m^2 N^-}{m} \vec{H} + \frac{gE_0}{mc^2} \vec{J^-} \wedge \vec{e_z}$$

(4.4)

where g is the effective magnetic charge which may take values according to the dumbbell model around $g \approx 4.3 \times 10^{-13} \, JT^{-1}m^{-1}$ for the spin-ices based on the Dy and Ho compounds [31]; $N^\pm = n(T)$ are the densities of magnetic charges $(\pm g)$ that we have analyzed its evolution with temperature in chapter 2 and 3; E_0 is the constant absolute value of the external and constant electric field whose direction is in the z-axis; $\vec{J^+}$ and $\vec{J^-}$ are the current density of the positive and negative charges, respectively. From Eqs. (4.1-4.4) we can deduce that the dual Electrodynamics with magnetic charges bases its differences with the standard classical Electromagnetism in three fundamental facts. First, the generation of the electric field, Eq. (4.2), is due to the existence of magnetic current term in addition of the temporal variation of the magnetic field. Secondly, the action of the electric and magnetic fields on the motion of the magnetic charges due to the dual and generalized Lorentz force, Eqs. (4.3) and (4.4), which exerts its action on those structures which resemble in behaviour the magnetic monopoles. In a third place, the existence of a dual Ohm law, which we consider in the following section of this chapter, and that can be immediately deduced from Bramwell's experiments initiated in 2009 [12]. These experiments relate the magnetic current with the magnetic field through the conductivity which in this case is coined as magnetricity.

There are two simple examples that allow to understand in a simple way the essence of the dual Electromagnetism of the fields created by the movements of magnetic charges and the action of these fields over the corresponding magnetic monopoles, as well as its difference with standard Electromagnetism. These examples

could be analyzed in a better way in an artificial spin ice which is a frustrated magnetic two-dimensional layered nano-material [77] that can present effective magnetic structures (monopoles) even at higher temperature [79].

2.1. Illustrative simple phenomena

The first of these phenomena could be the so-called electric braking that is the dual effect of the well-known phenomenon of magnetic braking in conductor materials. Electric braking occurs when a material with free magnetic monopoles (the disk of Fig. 19a) enters with a velocity in an area where there is an electric field, $\vec{E}$. After a small period of time, Δt , under the effect of electric field, the velocity of the magnetic charge, $\vec{u}$, undergoes a variation

$$\Delta\vec{u} = -\frac{g}{mc^2}\vec{u}\wedge\vec{E}\Delta t$$, due to the dual Lorentz force over the g magnetic charge and this variation of velocity implies

a braking force [39,41] per each magnetic charge which is given by the following expression

$$\Delta\vec{F} = -\frac{g^2}{mc^4}\Delta t\left|\vec{E}\right|^2\vec{\omega}\wedge\vec{r}$$. The torque corresponding to this force becomes per each g magnetic monopole

$$\Delta\vec{\tau} = -\frac{g^2}{mc^4}\Delta t\left|\vec{E}\right|^2 r^2\vec{\omega} = I\frac{d\vec{\omega}}{dt}$$. If the number of particles is sufficiently large, the assembly will undergo a braking

whose expression depends on the number of magnetic charges existing inside of material, the electric field and the effective masses of the magnetic charges. If one considers a density of magnetic charges n_0 and a volume (Ω) of the disk exposed to the electric field $\vec{E}$, the corresponding torque suffered by the macroscopic disk becomes

$$\Delta\vec{N} = -\frac{n_0\Omega g^2}{mc^4}\Delta t\left|\vec{E}\right|^2 r^2\vec{\omega} = I\frac{d\vec{\omega}}{dt}$$.

With these data, the disk presents a rotation braking whose the decreasing law is given by the expression

$$\omega(t) = \omega_0\exp\left[-\frac{n_0\Omega g^2\tau\left|\vec{E}\right|^2 <r>^2}{Imc^4}t\right]$$, where ω_0 is the initial angular velocity, $<r>$ is the average radius respect

to the disk center evaluated in volume under electric field action, and I is the inertial moment of the disk. Therefore, the electric braking is exponential and the lower the greater is the mass of the magnetic charges. The determination of this masses is one of the goals of this section and it is explained in the following paragraphs.

The second example is dual Ampère law with magnetic currents which produce electric-field lines in inverse direction to that of magnetic field created by the normal Ampère law of the Standard Electromagnetism.

(a)

$$\nabla \wedge \vec{E} = -\mu_{o}\vec{J}_{m}$$

(b)
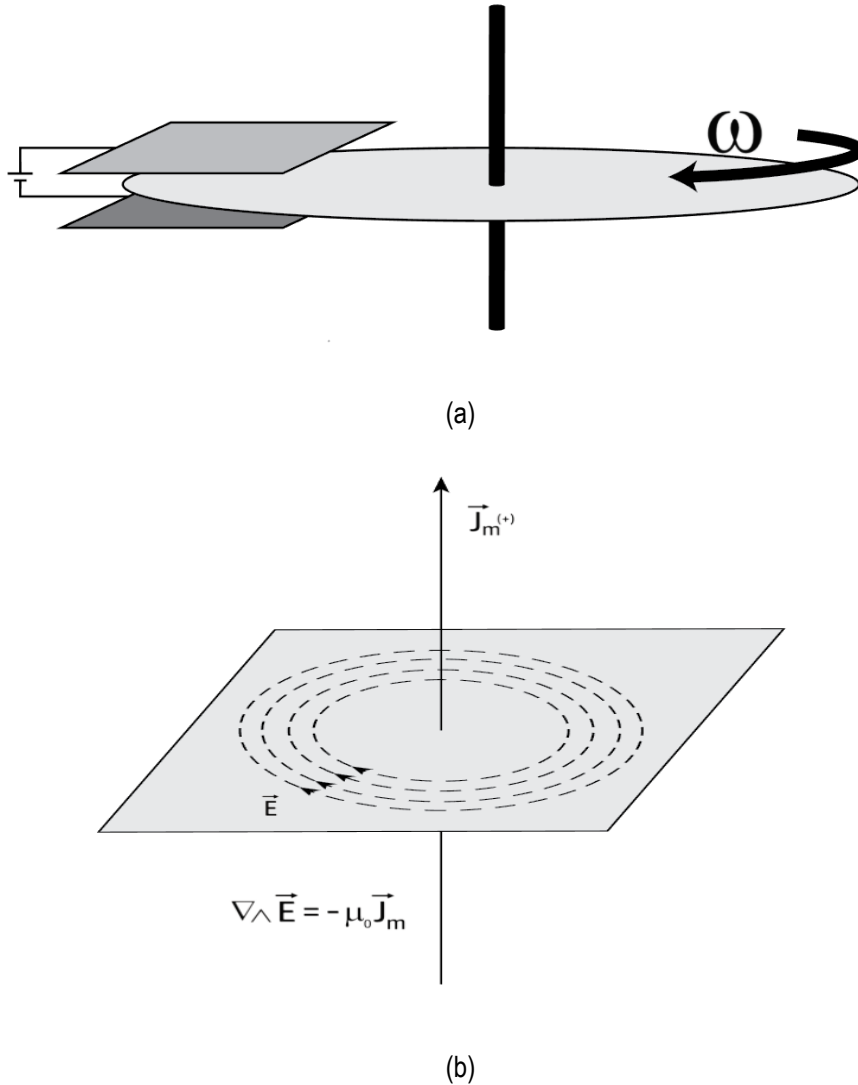
Figure 19.- Examples of electric braking and dual Ampère law with magnetic currents.

The schematics of the Fig.19 show in a simple way the fundamental keys of the dual Electrodynamic applicable to the spin-ice systems in the plasma state by means of two simple examples, a) we represent the electric braking due to a statics electric field over the gyratory movement of a disk constituted of a material that contains inside magnetic charges, b) in this figure, we show a schematic drawing of the generation of the electric field lines when the external magnetic field oscillates to very low frequency in a dual way to that obtained in the Ampère law of classical electromagnetism when the electric field also oscillates to low frequency.

In the Fig.19b, each magnetic positive charge (of the current whose density is $\vec{J}_M^+ = J_0 \vec{e}_z$), whose speed is $v_g \vec{e}_z$, generates an electric field which is located in a normal plane to the movement of the charges and its expression is: $\vec{E}_g(\vec{r}) = -\dfrac{|g|}{4\pi\varepsilon_0 c^2} v_g \vec{e}_z \wedge \dfrac{\vec{r}-\vec{r}_g}{|\vec{r}-\vec{r}_g|^3} = -\dfrac{|g|}{4\pi\varepsilon_0 c^2} v_g \dfrac{(-y,x,0)}{\left(x^2+y^2+z^2\right)^{3/2}}$, and the total field of an infinite line, with the corresponding magnetic current intensity I_M, is as shown in Fig. 19b, $\vec{E}(\vec{r}) = \dfrac{I_M}{2\pi\varepsilon_0 c^2 \left(x^2+y^2\right)^{1/2}}\left(-\vec{e}_\varphi\right)$, where v_g is the magnitude of the charge velocity.

3. Magnetic current

Otherwise, one way of defining, not the only, but one that best describes the formation of magnetic currents in spin-ice systems is the temporal derivative of magnetization [31] due to spin-flips between contiguous tetrahedra when these spin-flips progress spatially throughout the crystalline structure of the material. Therefore, the magnetic current can be defined as: $\vec{J}^\pm = \dfrac{\partial \vec{M}^\pm}{\partial t}$. If one considers this latter definition of the magnetic currents and it is included in Eqs. (4.3) and (4.4), we obtain the following time evolution for the magnetization:

$$\frac{d^2\vec{M}^+}{dt^2} + \gamma \frac{d\vec{M}^+}{dt} = \frac{\mu_0 g^2 N^+}{m}\vec{H} - \frac{gE_0}{mc^2}\frac{d\vec{M}^+}{dt} \wedge \vec{e}_z \qquad (4.5)$$

$$\frac{d^2\vec{M}^-}{dt^2} + \gamma \frac{d\vec{M}^-}{dt} = \frac{\mu_0 g^2 N^-}{m}\vec{H} + \frac{gE_0}{mc^2}\frac{d\vec{M}^-}{dt} \wedge \vec{e}_z \qquad (4.6)$$

These two latter equations correspond to the movement of the charges by means of the generalized Lorentz equation [36-42]. We have to remark that the spin-ices are electric insulators, and this is the reason for which in these equations we do not consider electric currents. In addition, we suppose that the movement of the plasma charges under the interaction of the electromagnetic wave is circumscribed in its phase plane, since the intensity of the constant electric field is much greater than that of the EM wave.

We also assume that the transversal condition of the EM wave is conserved in the propagation within the magnetic plasma. All these assumptions seem to be reasonable and they are similar to those considered in the dual propagation of the electric plasma experiment. The trial functions of the fields, currents and magnetizations become:

$$\vec{E} = E_0 \left(\vec{e_x} \pm i\vec{e_y} \right) \exp\left[i\left(kz - \omega t \right) \right]$$
$$\vec{H} = H_0 \left(\vec{e_x} \pm i\vec{e_y} \right) \exp\left[i\left(kz - \omega t \right) \right]$$
$$\vec{M}^+ = M_0^+ \left(\vec{e_x} \pm i\vec{e_y} \right) \exp\left[i\left(kz - \omega t \right) \right]$$
$$\vec{M}^- = M_0^- \left(\vec{e_x} \pm i\vec{e_y} \right) \exp\left[i\left(kz - \omega t \right) \right]$$

(4.7)

The solution $-(+)$ of unitary vectors corresponds to dextrorotatory (levorotatory) polarization which implies a clockwise (counter-clockwise) of time evolution of the resulting electromagnetic wave. The inclusion of these trial functions in the Eqs. (4.1)-(4.4), leads to the following algebraic equations:

$$\pm kE_0 - i\mu_0\omega H_0 - i\mu_0\omega M_0^+ - i\mu_0\omega M_0^- = 0$$

(4.8)

$$\pm kH_0 + i\varepsilon_0\omega E_0 = 0$$

(4.9)

$$\left(\pm\omega\frac{gE_0}{mc^2} - \omega^2 - i\gamma\omega \right) M_0^+ = \frac{\mu_0 g^2 N^+}{m} H_0$$

(4.10)

$$\left(\mp\omega\frac{gE_0}{mc^2} - \omega^2 - i\gamma\omega \right) M_0^- = \frac{\mu_0 g^2 N^-}{m} H_0$$

(4.11)

and the solution of this homogeneous equation system requires the condition:

$$\begin{vmatrix} \pm k & -i\mu_0\omega & -i\mu_0\omega & -i\mu_0\omega \\ i\varepsilon_0\omega & \pm k & & \\ & \dfrac{\mu_0 g^2 N^+}{m} & \pm\omega\dfrac{gE_0}{mc^2} - \omega^2 - i\gamma\omega & \\ & \dfrac{\mu_0 g^2 N^-}{m} & & \mp\omega\dfrac{gE_0}{mc^2} - \omega^2 - i\gamma\omega \end{vmatrix} = 0$$

these two latter equations imply following refractive index and magnetic permeability due to these conditions:

$$n^2(\omega) = \mu_r(\omega) = 1 + \frac{\omega_p^2}{\omega}\left(\frac{1}{\omega_E - \omega - i\gamma} - \frac{1}{\omega_E + \omega + i\gamma} \right)$$

(4.12)

where $\omega_p = \left(\mu_0 N g^2 / m\right)^{1/2}$ is the so-called plasmon frequency which is a characteristic frequency of the magnetic

plasma, and $\omega_E = \dfrac{gE_0}{mc^2}$ is the precession frequency due to the external electric field normal to the phase plane.

These two frequencies have prevalent roles in the electromagnetic propagation and are crucial in the properties of

magnetic charge gas [25,75] since both frequencies can be determined via relatively simple experimental

procedures whose theoretical explanations are given in this chapter. Once one knows these two frequencies, the

mass of magnetic charges and their spatial density are totally determined.

In order to show the frequency variation of the magnetic permeability in the simplest form we will assume

that the characteristic system frequencies of plasmon and precession are quantitatively similar. Then, the relative

permeability of Eq. (4.12) is negative for a narrow frequency interval equal and larger than the ω_E frequency and

positive for frequencies less than this precession frequency.
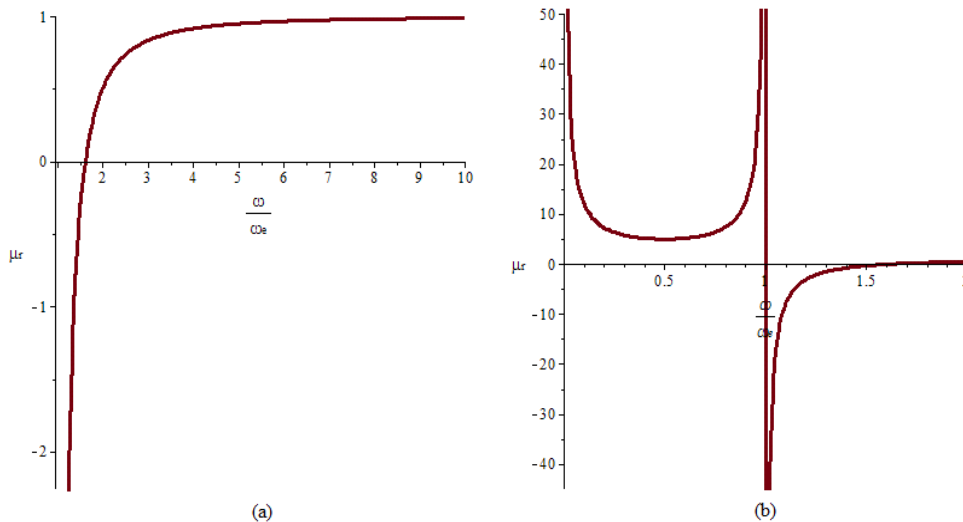
Figure 20.-Relative permeability in infinite media.

The Fig. 20a is extended interval of frequencies and the Fig. 20b shows detailed results in a defined interval

for smaller values of these frequencies. In this figure, we represent the relative permeability in function of

$x = \omega / \omega_E$. From this figure and Eq. (4.12), we deduce that the material is diamagnetic for any frequency greater

than ω_E . This frequency ω_E , which depends on the external electric field, produces the precession effect that acts

as an induced oscillation of the system. The precession frequency, ω_E of the magnetic charges implies the spin around the direction of the constant electric field in its normal plane. For an EM wave whose frequency is equal to ω_E, the system presents a complete electromagnetic absorption when the γ-parameter in Eq. (4.12) tends to zero. In addition, the electromagnetic absorption frequency allows us to determine the effective mass of the magnetic charges since for the frequency of the maximum absorption, the mass of these magnetic charges become $m = gE_0 / \omega_E c^2$. In this equation, ω_E can experimentally be determined via EM absorption and E_0 and g are starting data of this experiment. This EM propagation experiment can be a single test for detecting the presence of mobile magnetic charges in electric insulators.

On the other hand, we want to emphasize that in the magnetic plasma, the birefringence, which is present in the dual experiment with the electric plasma [36], does not appear, since both dextrogyre and levogyre polarizations present the same linear response, i.e. they have the same complex refraction index. However, the dependence of this electromagnetic propagation on the direction of the external field remains in the magnetic plasma, since the linear response depends on this direction.

The analysis of this type of EM propagation is valid for determining the possibilities of spin-ice materials for utilizing them as devices of information transmission. If we assume the results for the experimental masses of magnetic charges of reference [77] which are in the interval between 1.6×10^{-27} and 2×10^{-27} Kg and, for instance, the value of the magnetic charges corresponding to 3.3 Bohr magnetons, then ω_E frequency of Eq. (4.12) is related with the external electric field by means of the expression $\omega_E \approx 0.4 \times 10^{-3} E_0$. This expression implies that for obtaining a frequency of 10 KHz (frequency obtained in the field susceptibility of reference [51]), we require an external field of $E_0 \approx 2.5 \times 10^5$ volts/cm.

4. Propagation in confined magnetic plasmas

Another parameter which has a capital importance in the knowledge of the magnetic plasma is the characteristic plasma frequency, ω_p of Eq. (4.12); this depends on the density of magnetic charge carriers whose expression is given in chapter 2 and 3. This plasmon frequency has a relevant role in the propagation not only in

the quantitative determination of the refractive index and the propagation in transversal wave that is analyzed in this section but it is also crucial in the electromagnetic propagation in confined waves such as we show in this section. Here, we deal with the propagation of magnetic modes within wave guides filled with materials containing magnetic charges such as either spin-ices, topological insulators or any materials which one suspects it contains magnetic monopoles which can freely travel inside them. We suppose that there are positive and negative magnetic charges freely moving in the many-body state. These charges can coexist with confined dipoles which do not generate magnetic currents, but there are not electric charges in this magnetic plasma state. The algebraic field equations are obtained introducing expressions for the fields as that of Eq. (4.7) in Eqs. (4.1)-(4.4). Then, it allows us to determine the frequency dependent conductivity of the plasma state of these systems. In the right side of equality of the time evolution of the current densities, Eqs. (4.3) and (4.4), there are two dynamical terms which come from the generalized Lorentz force [36,40-42]. One can observe in the above equations, (4.3) and (4.4) that if the absolute values of these two terms are quantitatively equivalent, the positive and negative current densities hold different dynamics and therefore, there is an asymmetry in the responses of these currents. However, this quantitative equivalence can be analyzed by comparison of the respective absolute values of these two terms:

$$\left| \frac{\mu_0 g^2 N^\pm}{m} \vec{H} \right| \times \left| \frac{g\vec{J^\pm} \wedge \vec{E}}{mc^2} \right|^{-1} \approx \frac{N^\pm gc}{J^\pm} \tag{4.13}$$

where c is the light speed in the vacuum. The right-hand terms of the equality are quantitatively equivalent if and only if the corresponding positive and negative current densities correspond to magnetic charge particles travelling with light speed which is a very restrictive condition. As a consequence, the asymmetry between positive and negative current densities in Eqs. (4.3) and (4.4) can be neglected. Thus, we can consider that $N^+ = N^-$ and by addition of the two equations of these current densities, we have:

$$\frac{d\vec{J}}{dt} + \frac{\gamma}{m}\vec{J} = \frac{\mu_0 g^2 N}{m}\vec{H} \tag{4.14}$$

where $N = N^+ + N^-$ is the total current density of magnetic charges, Eq. (4.14) leads the definition of the frequency dependent conductivity of the spin-ices under the presence of magnetic field. If one considers a mono-chromatic wave, the above differential equation is converted in the following:

$$\vec{J} = \frac{\mu_0 N g^2}{\gamma - im\omega}\vec{H} = \frac{\omega_p^2}{\gamma/m - i\omega}\vec{H} \tag{4.15}$$

where ω_p is the plasmon frequency of the spin-ice system in the plasma state. Therefore, the conductivity depending on frequency is this case:

$$Z_1 = \sigma(\omega) = \frac{\omega_p^2}{\gamma/m - i\omega} \tag{4.16}$$

This equation, for $\omega \to 0$ should give the magnetricity, σ_0 which is: $\sigma_0 = \mu_0 N g^2 / \gamma$. Obviously, this expression should be coherent with the experimental magnetricity which allows us to determine a relationship between the density of magnetic charges and the viscosity parameter. In these sections, we give EM propagation procedures for determining the monopole mass and its density and therefore one can determine the viscosity parameter. Besides, it is also demonstrated that the diffusion of these free magnetic charges within the Dirac's strings which constitutes a dilute magnetic plasma implies that these systems in this state can transmit information from alternating currents, this being a source of circuital applications of these materials [31]. In any case, we have to emphasize that the conductivity crucially depends on the charge, the density of carriers and the magnetic masses which we have analyzed in the previous section.

Concerning the conductivity in function of frequency, we have modified Eq. (4.16) considering the following dimensionless magnitude, $x = m\omega / \gamma$ and then, we have the optical conductivity:

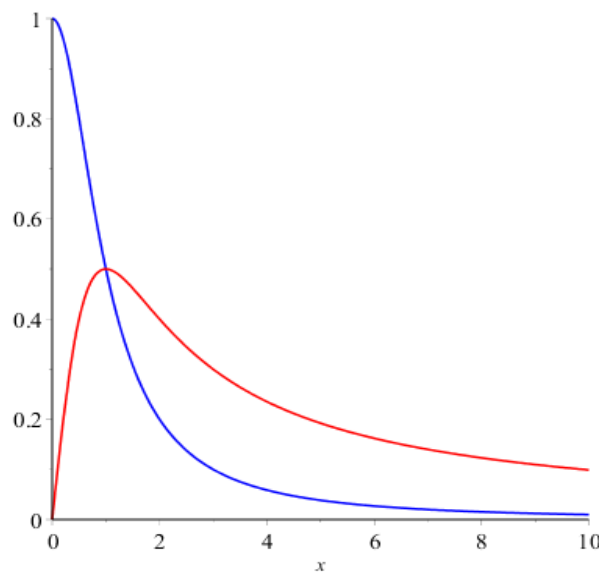$$\sigma(x) / \sigma_0 = \left(1 + x^2\right)^{-1} + ix\left(1 + x^2\right)^{-1} \tag{4.17}$$

Figure 21. – Magnetic conductivity in confined media.

The real part of $\sigma(\omega)/\sigma_0$ in blue and the imaginary part in red. The real part follows a parabolic form and decreases with increasing frequencies. The imaginary part presents an increasing value for the interval between zero and $\omega = \gamma/m$, a maximum for this specific frequency, a parabolic decreasing value with increasing frequencies and tends to zero when the frequency tends to infinite. The representation of this conductivity is coincident with previous experimental results [80].

5. Generalized wave equations in confined media

Any solution of the generalized Maxwell equations in confined guides requires to the knowledge of the wave functions which are solutions of the generalized wave equation. Thus, we obtain these equations from Eqs (4.1) and (4.2). We multiply Eq. (4.1) by $\nabla \wedge$ to both sides of equality and carrying out a similar procedure to that of standard electromagnetism, and considering that the divergence of the Maxwell magnetic field continue being zero in the spin-ices such as we have shown in latter section of chapter 1 that $\nabla \cdot \vec{B} = 0$, which is concordant with Refs. [25,41], $\vec{B}$ being the averaged induction magnetic vector or Maxwell magnetic vector of the Electromagnetic wave. Then we have:

$$\nabla^2 \vec{H} - \frac{1}{c^2}\frac{\partial^2 \vec{H}}{\partial t^2} = \frac{\sigma(\omega)}{c^2}\frac{\partial \vec{H}}{\partial t} \tag{4.18}$$

where $\sigma(\omega)$ is defined by Eq. (4.16). Operating in a similar form for the electric field, we obtain:

$$\nabla^2 \vec{E} - \frac{1}{c^2}\frac{\partial^2 \vec{E}}{\partial t^2} = \frac{\sigma(\omega)}{c^2}\frac{\partial \vec{E}}{\partial t} \tag{4.19}$$

An important characteristic, which is not present in the electric conductors, is that the terms in the right-hand sides of Eqs. (4.18) and (4.19), for monochromatic wave, are real numbers which multiply to the electric and magnetic fields if the dissipative forces accounted by the γ-parameter tend to zero. This crucial characteristic is important since it allows to obtain oscillating functions for the longitudinal components of the electric and magnetic fields and as it is determined in the next section, the transversal components of these fields are fixed from these longitudinal ones. In addition, if one considers the nonexistence of superficial magnetic currents in the limits of the wave guide, the edge conditions of generalized Maxwell equations are equal to those of standard

electromagnetism. Thus, we have that $E_z = 0$ and $\partial B_z / \partial \vec{n} = 0$. Then, the trial wave functions for E_z and B_z depends on the geometry of the guide. For instance, for a waveguide of rectangular cross section whose sides are a and b, the trial wave functions of the longitudinal components (z-components) of the fields can be given by the following functions:

$$E_z = E_0 \sin(k_x x) \sin(k_y y) \exp(\pm ik_z z - i\omega t) \tag{4.20}$$

$$H_z = H_0 \cos(k_x x) \cos(k_y y) \exp(\pm ik_z z - i\omega t) \tag{4.21}$$

where, $k_x = m\pi/a$ and $k_y = n\pi/b$. Therefore, including these trial wave functions in the above generalized equations of waves, Eqs. (4.18) and (4.19) when $\gamma \to 0$, we have that k_z, should accomplish the following condition:

$$k^2 = \frac{\omega^2 - \omega_p^2}{c^2}; \quad \vec{k} = \left(\frac{m\pi}{a}, \frac{n\pi}{b}, k_z\right) \tag{4.22}$$

This relationship has a clear physical interpretation since k is the module of the "wave vector" $\vec{k}$. Therefore, for electromagnetic frequencies less than ω_p, the EM propagation is not possible. Thus, ω_p is a true cut off frequency since for frequencies less than ω_p, the corresponding k module is complex, and then the corresponding longitudinal components of Eqs. (4.20) and (4.21) are evanescent.

The determination of this ω_p frequency along with the precession frequency, ω_E, given in the former section are two important physical magnitudes which are determinant by the electromagnetic propagation inside the plasma state. These two frequencies can be obtained via two simple experiments and with them we can obtain the values of the masses of the magnetic charges and the density of magnetic charges in any system.

Consequently, the determination and analysis of the electric and magnetic modes inside a guide can be considered another good test for determining these two magnitudes which characterize the many-body plasma state of the spin-ice materials.

6. Transversal field components

The objective of this subsection is to reach relationships of the transversal components in function of the longitudinal components of magnetic and electric fields, E_z and H_z, obtained in the former subsection, obviously, in a material with magnetic currents and without electric currents. The first step is the breakdown of the ∇ operator in a transversal part plus another longitudinal part [36,37], in such a way that we have the following

$\nabla = \nabla_t + \vec{e}_z \dfrac{\partial}{\partial z}$ and we also consider that the gradient of the longitudinal part of the fields can be given by:

$$\nabla E_z = \nabla\left(\vec{e_z}\cdot\vec{E}\right) = \left(\vec{e_z}\cdot\nabla\right)\vec{E} + \vec{e_z}\wedge\left(\nabla\wedge\vec{E}\right) = \frac{\partial\vec{E}}{\partial z} + \vec{e_z}\wedge\left(\nabla\wedge\vec{E}\right) \tag{4.23}$$

and following the transformation of this equation, we obtain:

$$\nabla_t E_z - \frac{\partial\vec{E}}{\partial z} = \nabla_t E_z - \frac{\partial\vec{E_t}}{\partial z} = \vec{e_z}\wedge\nabla\wedge\vec{E} \tag{4.24}$$

$$\nabla_t H_z - \frac{\partial\vec{H_t}}{\partial z} = \vec{e_z}\wedge\nabla\wedge\vec{H} \tag{4.25}$$

and using Eq. (4.1) and Eq. (4.2), we have the following relationships between the longitudinal and transversal components of the fields:

$$\nabla_t E_z = \frac{\partial\vec{E_t}}{\partial z} - \mu_0\vec{e_z}\wedge\vec{J} + i\mu_0\omega\vec{e_z}\wedge\vec{H_t} \Rightarrow \nabla_t E_z = \frac{\partial\vec{E_t}}{\partial z} - \mu_0\vec{e_z}\wedge\vec{J_t} + i\mu_0\omega\vec{e_z}\wedge\vec{H_t} \tag{4.26}$$

$$\nabla_t H_z = \frac{\partial\vec{H_t}}{\partial z} - i\varepsilon_0\omega\vec{e_z}\wedge\vec{E_t} \tag{4.27}$$

and the trial functions for these two equations are:

$$\vec{E_t}\left(\vec{r},t\right) = \vec{E_t}\left(x,y\right)\exp\left(\pm ik_z z - i\omega t\right) \tag{4.28}$$

$$\vec{H_t}\left(\vec{r},t\right) = \vec{H_t}\left(x,y\right)\exp\left(\pm ik_z z - i\omega t\right) \tag{4.29}$$

and then, the above Eqs (4.26) and (4.29) are utilized for calculating direct relationships between the transverse part of the electric and magnetic fields depending on the longitudinal ones. Multiplying $\vec{e_z}\wedge(4.26)$, we have:

$$\vec{e}_z \wedge \nabla_t E_z = \pm i k_z \vec{e}_z \wedge \vec{E}_t - \mu_0 \vec{e}_z \wedge (\vec{e}_z \wedge \vec{J}_t) + i\mu_0 \omega \vec{e}_z \wedge (\vec{e}_z \wedge \vec{H}_t)$$
$$= \pm i k_z \vec{e}_z \wedge \vec{E}_t + \mu_0 \vec{J}_t - i\mu_0 \omega \vec{H}_t$$

(4.30)

Therefore,

$$\vec{e}_z \wedge \vec{E}_t = \frac{\vec{e}_z \wedge \nabla_t E_z}{\pm i k_z} - \frac{\mu_0 \sigma(\omega)}{\pm i k_z}\vec{H}_t + \frac{i\mu_0 \omega}{\pm i k_z}\vec{H}_t$$

(4.31)

and considering then that:

$$-i\varepsilon_0 \omega \vec{e}_z \wedge \vec{E}_t = \mp \varepsilon_0 \omega \frac{\vec{e}_z \wedge \nabla_t E_z}{k_z} + \frac{\omega \sigma(\omega)}{\pm k_z c^2}\vec{H}_t - \frac{i\omega^2}{\pm k_z c^2}\vec{H}_t$$

(4.32)

and using Eq. (4.27), we have:

$$\nabla_t H_z \mp i k_z \vec{H}_t = \mp \varepsilon_0 \omega \frac{\vec{e}_z \wedge \nabla_t E_z}{k_z} + \frac{\omega \sigma(\omega)}{\pm k_z c^2}\vec{H}_t - \frac{i\omega^2}{\pm k_z c^2}\vec{H}_t$$

(4.33)

In addition in this section, we consider that the dissipation small, i.e. $\frac{\gamma}{m} \ll \omega_E$ an then, taking into account

the expression of $\omega\sigma(\omega)$ in this non too-much-restrictive case, we obtain the relationships whose deduction is

relatively easy between the transversal components in function of the longitudinal ones of both electric and

magnetic field of the electromagnetic wave which become:

$$\vec{H}_t = i\frac{\mp k_z \nabla_t H_z - \varepsilon_0 \omega \vec{e}_z \wedge \nabla_t E_z}{k_z^2 - \frac{\omega^2 - \omega_P^2}{c^2}}$$

(4.34)

where E_z and H_z in a rectangular waveguide are determined via expressions (4.20) and (4.21) and therefore the

general $\vec{H}(\vec{r},t)$ -solution in this rectangular waveguide is completely determined.

The calculation of the transversal components of the electric field can be initiated from Eq. (4.27) which

under small exact transformations, multiplying both sides by $\vec{e}_z \wedge (4.27)$, is: $\vec{e}_z \wedge \nabla_t H_z = \pm i k \vec{e}_z \wedge \vec{H}_t + i\varepsilon_0 \omega \vec{E}_t$, from

this expression, we have: $\vec{e}_z \wedge \vec{H}_t = \frac{\vec{e}_z \wedge \nabla_t H_z}{\pm i k_z} \mp \frac{\varepsilon_0 \omega}{k_z}\vec{E}_t$, and including this latter expression in Eq. (4.26), we

easily arrive to the transversal components of the electric field in function of the longitudinal components of the

electric and magnetic field and the transversal components of the magnetic field given in Eq. (4.34), obtaining as

final results for the transversal components of the electric field of the electromagnetic wave in any confined waveguide of any transversal geometry, the following expression:

$$\vec{E}_t = i\frac{\mp k_z \nabla_t E_z + \mu_0 \omega \vec{e}_z \wedge \nabla_t H_z \mp k_z \mu_0 \sigma(\omega)\vec{e}_z \wedge \vec{H}_t}{k_z^2 - \dfrac{\omega^2}{c^2}}$$

(4.35)

The Eqs. (4.34) and (4.35) are the general expressions of the transversal components of the electric and magnetic field within a guide filled with the magnetic plasma. Now, we can explicitly determine the electric and magnetic fields in a rectangular waveguide in which the longitudinal components are those given in Eqs. (4.20) and (4.21). These results lead to the fact that the existence of magnetic monopoles are the main agents of the EM propagation. Hence, our goal in this section is not to determine all possible solutions that can be analyzed in other works. In this chapter, we carry out some examples of calculations in which one can see the differences between the electromagnetic propagation with the existence of magnetic monopoles respect to the solution of the normal Maxwell equations in the same material without magnetic charges. We can consider, for example, a spin-ice in which predominantly there are free magnetic charges and that same material below the first phase transition when there are only magnetic dipoles and not free magnetic charges.

Henceforth, we will call to this last material empty material of magnetic monopoles (EMMM). Within the general solution given in the former section, there are several cases that may seem conflicting, since, in the resulting transversal components of the magnetic and electric fields there could appear possible divergences in Eqs. (4.34) and (4.35). When $k_z^2 = (\omega^2 - \omega_P^2)/c^2$, the possible values of the z-component of $\vec{H}_t$ fields of Eq. (4.34) seem to be divergent and then, the numerator of Eq. (4.34) should be zero, in order that these equations have valid solutions. Therefore, $\mp k_z(-\vec{e_X}k_X g_1 - \vec{e_Y}k_Y g_2) = \varepsilon_0 \omega(-\vec{e_X}k_Y g_1 + \vec{e_Y}k_X g_2)$, g_1 and g_2 are the basic functions which define all transversal components of magnetic and electric fields and whose expressions in a rectangular waveguide are:

$$g_1 = H_0 \sin(k_X x)\cos(k_Y y)\exp(\pm ik_z z - i\omega t)$$

(4.36)

$$g_2 = g_1 \cot g(k_X x)tg(k_Y y)$$

This implies that $\pm k_z k_X = -\varepsilon_0 \omega k_Y$ and $\pm k_z k_Y = \varepsilon_0 \omega k_X$. Thus, k_X and k_Y are null, which implies that:

$\vec{E} = 0$ and $\vec{H} = H_z \vec{e}_z = H_0 \vec{e}_z \exp(\pm i k_z z - i\omega t)$. Therefore, under these conditions there is no EM propagation and then a perfect diamagnetism depending on frequency appears in accordance with Maxwell's equation by considering the annulment of the electric field curl. This same conclusion can be reached, perhaps more easily through equation (4.25). The other special case is for $k_z^2 = \omega^2 / c^2$. This condition could imply that the solution of the expression (4.35) explodes, however, it is only possible when $k_X = k_Y = 0$ and $\omega_p = 0$, then the electric field is zero and this also implies the non-existence of electromagnetic propagation in the guide. From Eqs (4.34) and (4.35), it is trivial determine the TM and TE modes of the electromagnetic field within the rectangular waveguide. The TM modes, i.e. $H_z = 0$, these relationships take the following form:

$$\left[\vec{H}_t = -i \frac{\varepsilon_0 \omega \vec{e}_z \wedge \nabla_t E_z}{k_z^2 - \frac{\omega^2 - \omega_P^2}{c^2}} \right] \qquad (4.37)$$

$$\left[\vec{E}_t = i \frac{\mp k_z \nabla_t E_z \mp k_z \mu_0 \sigma(\omega) \vec{e}_z \wedge \vec{H}_t}{k_z^2 - \frac{\omega^2}{c^2}} \right] \qquad (4.38)$$

and the TE modes, i.e. $E_z = 0$:

$$\left[\vec{H}_t = i \frac{\mp k_z \nabla_t H_z}{k_z^2 - \frac{\omega^2 - \omega_P^2}{c^2}} \right] \qquad (4.39)$$

$$\left[\vec{E}_t = i \frac{\mu_0 \omega \vec{e}_z \wedge \nabla_t H_z \mp k_z \mu_0 \sigma(\omega) \vec{e}_z \wedge \vec{H}_t}{k_z^2 - \frac{\omega^2}{c^2}} \right] \qquad (4.40)$$

We want to emphasize that when the the magnetic charges are different from zero, by means of Eqs (4.34) and (4.35), and the four above expressions of the TM and TE modes all components, of the magnetic and electric fields are modified, since $\sigma(\omega)$ and ω_p are null. On the other hand, as these physical magnitudes depend on the density of magnetic charges with these six expressions, we can deduce the density of monopoles which can be produced vía the increase with temperature and magnetic fields.

7. Results of confined EM propagation

The information which we can yield in this section is for the case of a rectangular waveguide; any other geometry does not modify the systematic and will only affect the mathematical solution of the general wave equations (4.20) and (4.21). A point that we want to emphasize is that when the density of free magnetic charges is null, the results of Eqs. (4.34) and (4.35) coincide with those of the standard Maxwell equations.

We have selected some results corresponding to the magnetic and electric fields of the transversal components in function of the longitudinal ones in systems with magnetic charges and to establish the differences with the cases in which the density of these are zero. The main parameter governing these differences is the frequency of plasmon which in turn is drastically dependent on the density of monopoles. Therefore, we have to look at equation (4.22) that controls the cutoff frequency and in equations (4.34) and (4.35) to justify the differences between the results when $\omega_P = 0$ with respect to the same cases with $\omega_P \neq 0$. Let us consider an average density of magnetic charges 10^{-4} with respect to their maximum value that would be either the number of tetrahedra [7,8,12] if it is the case of the spin-ice materials or the vertices if we consider a spin-ice type artificial material [78,79]. With this data and equations (4.22), (4.34) and (4.35), we can obtain the complete values of the electric and magnetic fields of the general wave propagated in a square-section waveguide of 10 cm of side.

In the propagation results, there are two physical variables which depend on the plasmon frequency and therefore on the density of monopoles in the material. These magnitudes are the cut-off frequency from which electromagnetic propagation is possible in the wave-guide and the wave vector, Eqs. (4.34) and (4.35), corresponding to the phase common to all the components of the fields, as seen in Eqs. (4.20), (4.21), (4.28), (4.29) and (4.36). The expressions of these variables are as follows:

$$\omega_C^{(m)} = \left[\omega_P^2 + \frac{c^2\pi^2}{a^2}(m^2+n^2) \right]^{1/2} \tag{4.41}$$

$$k_z^{(m)} = \pm \left(\frac{\omega_P^2}{c^2}(x^2-1) - \frac{\pi^2}{a^2}(m^2+n^2) \right)^{1/2} \tag{4.42}$$

where $x = \omega/\omega_P$. In the case that the waveguide contains the same EMMM, these expressions become

$$\omega_C^{(0)} = \frac{c\pi}{a}(m^2 + n^2)^{1/2} \text{ and } k_z^{(0)} = \pm\left(\frac{\omega_C^2}{c^2}x^2 - \frac{\pi^2}{a^2}(m^2 + n^2)\right)^{1/2}.$$

In Fig. 22, we represent the transversal electric field in a guide filled with natural (or artificial) material inside the waveguide with magnetic charges and an EMMM in order to show the effect of magnetic charges on electromagnetic propagation.
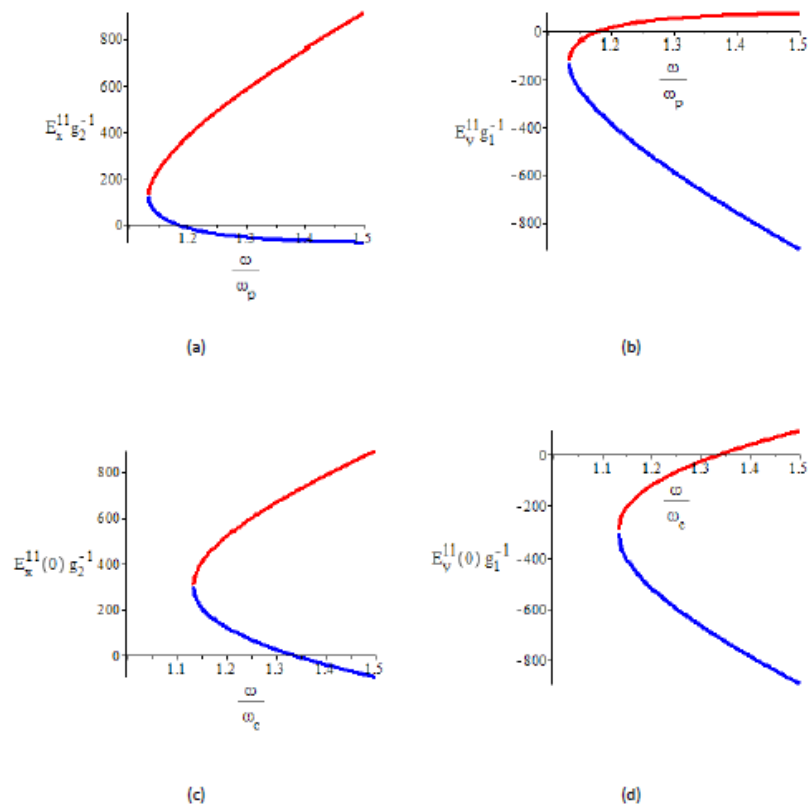

Figure 22.– Transversal electric components of the mode m=1 and n=1 in function of frequency.

In the vertical axis, we represent $E^{11}_{(x,y)}g^{-1}_{(2,1)}$. In horizontal axis, the variable is dimensionless, ω/ω_P. In Fig.22a, the X-component of this mode $E^{11}_x g^{-1}_2$ for negative k_z in Eq. (4.42) is represented in blue and for positive ones in red. In Fig.22b, $E^{11}_y g^{-1}_1$ is coloured in red for positive k_z and in blue for negative ones. In Figs. 22c and 22d, the same with former graphic but considering the same EMMM inside waveguide. The horizontal axis is the dimensionless variable ω/ω_C, being ω_C the corresponding cutting frequency in the waveguide. Besides a phase difference of $3\pi/2$ should be added to the phase of the Z-component of this electric field of Eqs. (4.20) and (4.32).

In this Fig. 22, the effect that the magnetic charges produce in the electromagnetic propagation can be appreciated. Although the curves appear deceptively equal, there is a significant quantitative difference in the case of electric fields propagating in spin-ice materials (both in natural and artificial spin-ice compounds) and in the EMMM. At the vertex of the curves, where the Z component of the wave vector changes sign, there is a strong damping in case of magnetic charges due to the negative induction character of the electric field produced by the magnetic currents. This effect is similar to that coming from the law of Lenz, which is explained in Fig. 20b.

Otherwise, in the case of the existence of magnetic charges there is an electric field of approximately 100 electric field units, while in the EMMM it is 300. Then the evolution of the field with frequency is faster in systems with monopoles than in EMMM. In addition, in the cut with the horizontal axis, when the field is cancelled, there is also a remarkable quantitative difference, since in figures 22a and 22b this field is cancelled for substantially different frequencies.
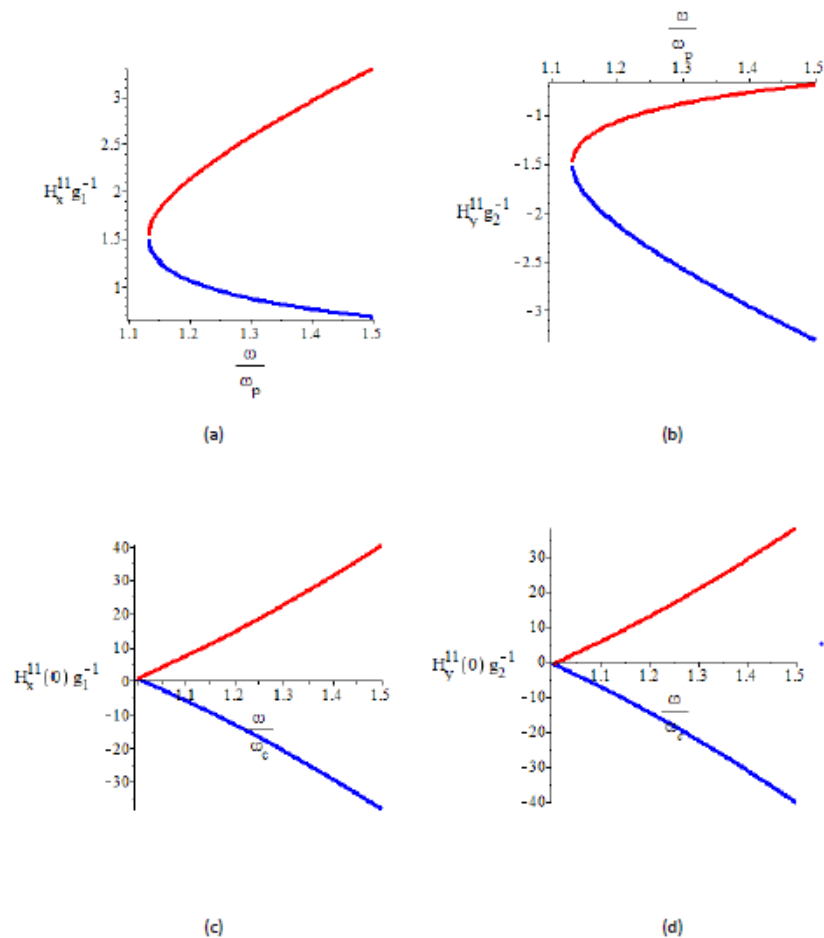

Figure 23 – Transversal magnetic components of the mode m=1 and n=1 in function of frequency.

In Figs. 23a and 23b, we show $H_X^{11}g_1^{-1}$ and $H_Y^{11}g_2^{-1}$, respectively with magnetic charges within the material that fulfils the waveguide, and in Figs. 23c and 23d, $H_X^{11}(0)g_1^{-1}$ and $H_Y^{11}(0)g_2^{-1}$, when the EMMM is inside the guide. The red curves correspond to the respective magnetic field with positive k_z in the phase of longitudinal and transversal components and blue for negative values of k_z. The magnetic fields present differences (both quantitative and qualitative points of view) between the two different systems: EMMM and spin-ices inside the waveguide. In the case of spin-ice the solutions both the X and Y components in the apex where there is the sign change are symmetric with respect to the horizontal axis components. The symmetry in the EMMM case is complete, such as one can see in Figs. 23c and 23d. In addition, a physically relevant characteristic is the decreasing values of the magnetic field due to the presence of the magnetic currents. These currents seem to screen the magnetic fields of the electromagnetic modes which are propagated through the waveguide. Although from a mathematical point of view this screening is clear, the phenomenological aspects are very interesting since one should think in the direction of a negative sign of inductive magnetic field created by these magnetic currents due to change of sign in the dual Maxwell equation corresponding to the curl of the electric field.
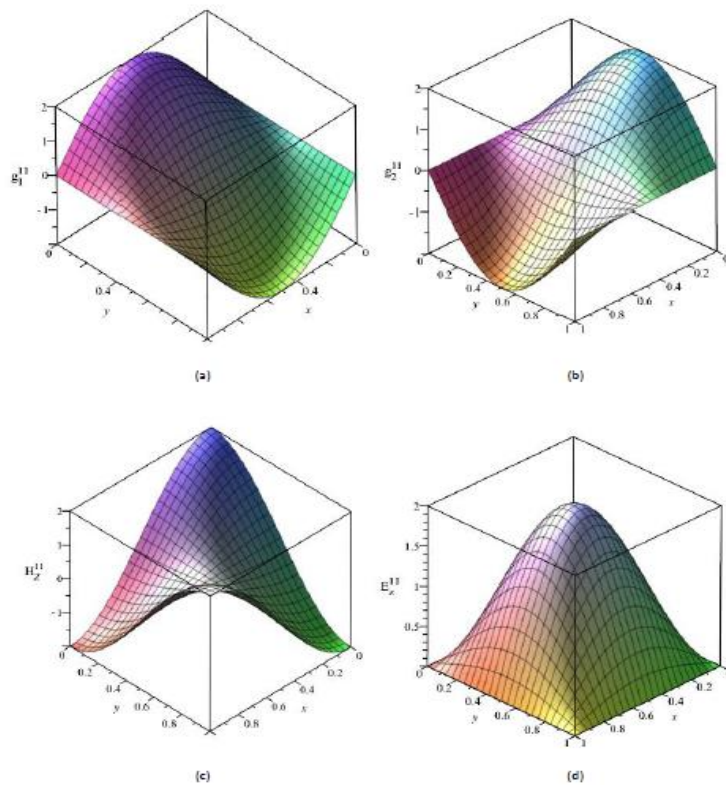

Figure 24 – Several mode functions. (a) $g_1^{11}(x,y)$ of Eq. (4.36). (b) $g_2^{11}(x,y)$ see also Eq. (4.36). (c) The part of longitudinal magnetic field H_z^{11} [see Eq. (4.21)] which depends on x and y. (d) Same as in (c) but E_z^{11} [see Eq. (4.20)].

In Figs. 24a and 24b, we represent the parts of the functions $g_1^{11}{}'(x,y)$ and $g_2^{11}{}'(x,y)$ that depend on x and y. These functions have to be multiplied by the results given in Figs. 22 and 23 to obtain the corresponding transverse components of the electric and magnetic fields. In Figs. 24c and 24d the graphs of the parts of the longitudinal components of fields which depend on x and y are shown. In all four cases, the part of the phase that depends on the frequency and the component k_z of the wave vector must be included. With the results of Figs. 22, 23 and 24, we have completely obtained the results of the electromagnetic propagation in the waveguide of the mode m=1 and n=1 both when inside there are spin-ice material and EMMM. This allows the knowledge of the effect in the corresponding electric and magnetic fields under the presence of magnetic charges and magnetic currents.

8.   Comments

The origin of the interest and inspiration for the content of this chapter is based on the existence of two antagonistic situations within the spin-ice material: on one hand the so-called pole-antipole pair condensation and on the other hand, the neutral magnetic plasma. The characteristic phase transition detected via measurements of specific heat and magnetic susceptibility give support to the existence of these two states which are deeply analyzed in our previous paper [65]. These two states correspond to two quantum macroscopic states whose thermodynamic development and electromagnetic propagation are inextricably linked to the density of free magnetic monopoles, to their masses and mobility within a quasi-particle gas whose components are: confined dipoles, Dirac's strings of more or less elongation and mainly the quasi-free magnetic charges. One of the main goals of this chapter is the analysis of the electromagnetic propagation in order to establish experimental tests for detecting similar phenomenology in other compounds whose structural properties imply the possibility of existence of effective magnetic charges. The low temperature state (in which the pole-antipole pairs are in the lowest energy state of double-particle, whose linear momentum is zero) can have a great theoretical and formal interest, but its possible application for transmitting energy and information can be more reduced.

Otherwise, the magnetic plasma, maybe, has minor theoretical interest than that of the exciton condensate magnetic state, since its dual electric partner has a more known behaviour, however, the possible circuital applications for energy transmission are larger than the former state. This interest is based on the new form of

electromagnetic propagation which is different from that existing in its dual electric plasma. These differences in the propagation in the electromagnetic spectra can offer advantages over the EM propagation in electronic devices if the effective masses of the magnetic charge carriers are different from those of the electronic carriers. But in addition of the practical interest, there exists the theoretical interest about the knowledge of the Electrodynamics with magnetic monopoles, since, the inexistence (up to 2008) of effective magnetic charges has implied the underdevelopment of the dual Electrodynamics and the engineering for transmission of energy and information of devices with materials containing magnetic charges.

Obviously, we have followed a plot line of thought inspired by the standard Electromagnetism by modifying the Maxwell equations for explaining the new phenomenology. According to our analysis, the EM field interaction with the spin-ices system is very sensitive to both the mobility of the charges (the masses of the charges is then an important parameter) and the density of quasi-free magnetic charges. The EM propagation depends on the macroscopic state of the system, therefore, it is a good test for determining its evolution with temperature. The density of charge magnetic carriers is the decisive order parameter in the thermodynamic properties and therefore, this physical variable is a true order parameter for the existence of the different phases.

Concretely, in a first stage, we analyze the transversal electromagnetic waves assisted by an intense and constant electric field in a parallel plane to the wave phase plane. In this analysis, we determine the linear response in the plasma state. In addition, we find a relationship between the effective magnetic masses of the magnetic charges and the absorption frequency. This main absorption is given for the precession frequency due the oscillation of the magnetic charges caused by the external electric field. In a second part, we determine different properties of the macroscopic states through the electromagnetic confined propagation. When the state is in a magnetic plasma state, the cut off frequency in the confined wave-guided propagation is approximately the plasmon frequency. This being a clear indication for the experimental determination of the density of magnetic charges in any system. On the other hand, we find new relationships of the intensity of the different fields which depends on the density of free magnetic charges. Eqs. (4.34) and (4.35) constitute a compendium of the EM propagation in rectangular microwave guide which is strongly dependent on the order parameter. On the contrary, when the state is a pole-antipole condensate, the behaviour under the electro-magnetic propagation in a confined system is

sensibly different. This analysis can discriminate the different states and their temperature evolution. In summary, electromagnetic propagation in unconfined structure and confined   more important many-body states coming from the dumbbell model: the coupled magnetic dipole phase and the magnetic plasma state. This latter propagation in waveguides is a simple and illuminating study in order to determine the magnetic charge density, and the mobility such as it was determined eight years ago [12,13] in the discovery of the magnetricity in the spin-ices.

This chapter attempts to make a contribution to the analysis of the electromagnetic behavior with two objectives: to give a methodology for discovering new materials with magnetic charges, and, in turn, to initiate a prospective for using these materials for "electronic devices" (maybe, to name them "magnetronic devices"). However, the fundamental problem of finding applications to obtain magnetronic devices with the spin-ice materials is the low temperature of magnetricity phenomenon. Precisely, in ref. [78], the authors analyze a proposal for the design and realization of a three-dimensional artificial spin ice by means of the superposition of layered nano- two-dimensional structures which afford the same topological equivalence that the tetrahedrons in a pyrochlore lattice.

On the other hand, in Ref. [79], the authors express the confidence that in these artificial spin-ices can obviate the difficulties of the natural spin-ices in which Bramwell et al. [12] found magnetricity since this magnetic charge conductivity requires pure spin ice crystals operating around 0.36 K. Therefore, appropriate candidates to try to carry out magnetronic devices are the so-called artificial spin-ices [78], avoiding the difficulty inherent to extremely low temperatures.

In summary, in this chapter, we have presented a generalization of the solutions for the extended Maxwell equations with presence of currents of magnetic charges in isotropic and homogeneous systems. These magnetic currents coming from the time dependence of the magnetization generates electric fields and interact with it. Besides, we determine the temporal and spatial evolution of the magnetic and electric fields when there is presence of magnetic charges. We think that these results may be used for obtaining new technological ideas in order to obtain "magnetronic" devices.

We would like to emphasize the following points that have been described in this chapter and that, in our opinion, are crucial in the electromagnetic propagation in the spin-ice systems with magnetic charges,

i.   The determination of effective mass of the magnetic charges via the electromagnetic absorption to the precession frequency, ω_E, and described in section 3 of this chapter.

ii.   The plasma frequency, ω_P, also described in sections 3 and 4 and whose experimental detection can be obtained by means of the measurement from the cut-off frequency in a microwave guide.

iii.   From these two frequencies can be obtained the density of magnetic monopoles and their effective masses.

iv.   The frequency dependent conductivity under action of the magnetic field which is in reasonable agreement with recent experimental results and which depends on the plasmon frequency.

We have the idea that these points are keys the electromagnetic propagation in both confined and unconfined enclosures of spin-ice systems. Given the possible values of the plasmon frequency and the precession frequency, one may think that the electromagnetic propagation of the devices based on spin-ices may be in both the RF and microwave regions of the electromagnetic spectrum depending on the density of magnetic charges and their magnetic masses.

CHAPTER 5: Complete Solutions of Maxwell and Lorentz Equations

1.   Electrodynamics in cylindrical symmetry in the magnetic plasma state

Throughout the text, we have proposed the existence of a "metallic" behavior called jellium system for the excited state above 0.35 K in the spin-ice materials generated naturally. In some artificially obtained materials whose magnetic structure is similar to spin-ices being this temperature extraordinarily higher. In this jellium state the charges evolve freely since the repulsive interactions between magnetic charges of the same sign are compensated by the attractive interactions with charges of the opposite sign. This jellium model, as we have said, behaves like a magnetic plasma in which, although the charges can move, local interactions cause frictions (dissipative forces) that arise when the magnetic charge densities are sufficiently large. Therefore, in this state the density of magnetic charges is decisive in the electromagnetic wave propagation in both open media and confined systems (waveguides) filled with materials. In the chapter 4, we have considered that the dissipative forces are negligible. This is an actual case when concentration of quasiparticles which mimic to magnetic monopoles is small. In this case, the electromagnetic propagation is without losses. However, the specific heat presents a peak that announces the existence of an increasing presence of monopoles in a state of freedom within a jellium format. In this situation it is difficult to accept that the interaction between these magnetic charges does not produce friction forces. Therefore, we consider the electromagnetic propagation by considering these dissipative forces in the fundamental Eqs, (4.3)-(4.6), (4.18), (4.19) and (4.35), which are decisive in the operation and development, both from a quantitative and qualitative point of view in order to be the system able to transmit information and energy.

Other important novelty in this chapter respect to the chapter 4 is the consideration of the terms in the magnetic conductivity, Eq. (4.14), coming from the interaction of the electric field. These terms of interaction of the electric field on the magnetic charges moving both in Eqs (4.3) and (4,4) and in the evolution of time space of the magnetization: Eqs. (4.5) and (4.6) have been neglected quantitatively in the study of chapter 4, when we determine the magnetic conductivity to deduce the Eq. (4.14). However, in the study that we do in this new chapter we see that in the case of high concentrations, this interaction has a great and decisive incidence both qualitative and quantitative. This interaction exerts its function in the frequency of absorption which comes to be the frequency of precession in the normal plane to the axis of the waveguide there being a large multiplicity in these frequencies. A

third difference between what was done in chapter 4 with respect to this chapter 5 is that in this chapter in a complementary way to the previous one we carried out the study of the propagation in a cylindrical symmetry since it is a symmetry so frequent in real devices as is the rectangular.

As mentioned throughout the text the EM propagation analysis is addressed to obtain theoretical results about magnetic responses and frequency-dependent magnetricity. The key physical magnitudes again are the plasmon frequency (ω_P) which is related with the cut-off frequency in the wave guide and the effective inertial masses (m) of these magnetic charges. All properties of the electromagnetic propagation in these compounds with effective magnetic monopoles depend on ω_P and m. In this chapter, this electromagnetic propagation is, as above mentioned important in the case of increasing density of magnetic charges. In this case, the electromagnetic propagation adquires new features which are described in this chapter 5.

The properties that present the materials when the density of magnetic charges is close to saturation show interesting characteristic features that could imply these compounds to be serious candidates for circuital and functional devices able for propagating both information and computational memories. Since Bramwell et al. [12] analysed in 2009 the mobility of these entities with the presence of external crystal magnetic fields whose effects were coined as magnetricity there is an attempt to find these and another now-unknown new applications.

In this scenario, we have considered the electromagnetic propagation of the different transversal magnetic modes, magnetic responses of the spin-ice materials and energy electromagnetic losses due to the existence of dissipative forces within a cylindrical wave-guide which we suppose it is filled with this spin-ice material. This propagation is strongly dependent on the effective inertial masses. Through the values of the absorption frequencies that are in turn those of precession, we can determine the inertial masses of the charges as well as their energies of formation or energies at rest of these magnetic charges [75]. The temperature variation analysis of this density of free magnetic monopoles in the magnetic plasma state is carried out in Ref. [65]. We think that these analyses and the results of this work can be interesting in order to detect the existence of magnetic currents in possible new materials.

2.   Paradigm of classical electrodynamics with magnetic charges

The conductivity properties of magnetic charges systems in zero frequency is the first in being measured and it is illuminating phenomenon based on the mobility of these magnetic charges under the interaction with the magnetic fields. We consider that this property allows the finding of applications even considering these magnetic monopoles as classical objects. This Classical-Physics analysis is based on the fact that although the origin of the entities that emulate the behaviour of magnetic charges has a quantum nature, the increase of technological interest may come from the possible applications for transmitting the electromagnetic signals in a better way than the electronic devices. Experiments in this sense have been interpreted with classical models in recent literature [76] obtaining a good agreement between the classical theories and experiences with these spin-ice materials.

The T-evolution of the plasma state as well as the phase transition between the two many body states are analized in the three first chapters of this work. In addition, we have the theoretical elements for concluding that the applications of the electromagnetic propagation are dramatically different in the BEC state in front of the plasma state due to the presence of a number of magnetic monopoles whose production is due to the successive generation of Dirac's strings and posterior creation of two magnetic charges of different sign in a quasi-free state. In a synthetic argument, the density of magnetic monopoles, N(T), is clearly depending on temperature due to the symmetry of the crystal and we obtained [66] the following solution for this density:

$$N(T) = n(T_C) \exp[\phi(T) - \phi(T_C)] \tag{5.1}$$

with, $n(T_C)$ is experimentally obtained for $T = T_C$ and $\phi(T_C)$ is related with the asymptotic entropy [65]. The above equation is important since it represents a relationship between the scalar magnetic potential for a determined temperature with the density of monopoles for this temperature.

The conductivity at zero frequency is, as we have shown in the previous chapter, inversely proportional to the dissipative factor and directly proportional to the density. This implies that although with the concentration can increase the conductivity, it is not linear with it, since when increasing this concentration, the dissipative forces also increases, although this is also not linear. In next sections, we analyse the EM transmission with a given monopole density of positive magnetic charges in the plasma state metallic devices containing magnetic charges. There are

still controversies respect to the Lagrangian function that must provide both the field equations and the corresponding dynamics of the electric and magnetic charges under these fields. However, there is a consensus general enough concerning with generalized "Maxwell" equations and the generalized forces that these fields exert on electric and magnetic charges. These equations are those given in chapter 4, Eqs. (4.1)-(4.4).

On the other hand, the divergence magnetic field is also null such as it is explicitly explained in Ref. [25] and also in chapter 1. In these introductory equations g is the effective and positive magnetic charge which may take values for each unity around $\approx 4.3 \times 10^{-13} \, JT^{-1}m^{-1}$ for the spin-ices based on the Dy and Ho compounds [75]. From Eqs. (4.1)-(4.6), we can deduce that the dual Electrodynamics for the spin-ices in the state with free magnetic charges bases its differences from the standard classical Electromagnetism on three fundamental facts. First, the generation of the electric field, Eq. (4.2), is due to the existence of magnetic current term in addition to the temporal variation of the magnetic field. Secondly, the action of the electric and magnetic fields [36,81-85] on the motion of the magnetic charges is due to the dual Lorentz force, Eqs (4.3)-(4.6). This produces its action on those structures which resemble in behaviour the magnetic monopoles. In third place, the existence of a dual Ohm law for zero frequency, which is fruit of Bramwell's experiments initiated in 2009 [12].

3. Magnetricity

We suppose that there are positive and negative magnetic charges freely moving in the many-body state and that can coexist with confined dipoles which do not generate magnetic currents. In addition, we suppose that there are not electric charges in this magnetic plasma state. However, in chapter 5, we study the qualitative and quantitative effects of second terms of the right-hand side of the equalities (4.5) and (4.6).

In order to compare the actions of the two terms of the right-hand side of equality of these equations, we go to consider these two terms and to establish the incidence of the second one in the two cases, i.e. in a first case we do not consider the second one and after considering it. The first case, there is an equal symmetry of the different distribution of positive magnetic charges distribution $N^+ = N^-$ and therefore, we have by addition to the two Eqs. (4.5) and (4.6) of these current densities, we obtain (4.14): and the magnetic conductivity (4.15), and by dual analogy to the electric plasma we have the conductivity in function of the magnetic charges concentration is:

$$\sigma(\omega, N) = \frac{\omega_P(N)^2}{\gamma/m - i\omega}$$

(5.2)

This equation implies, for $\omega \to 0$, the Bramwell's magnetricity, which is:

$$\sigma_0 = \mu_0 N g^2 / \gamma$$

(5.3)

We give, in Figs. 25 and 26, the results of the real and imaginary parts of optical magnetricity, Eq (5.2), in function of frequency for different values of density of magnetic monopoles whose variation is given in the expression of plasmon frequency. Our results of Fig. 25 being in concordance with experimental results of other previous works [44,85]. The objective of these figures is to give a simple graphic representation of the expression of magnetic conductivity, Eq. (5.2). Therefore, these results are not presented as definitive results of magnetic conductivity, which we treat with more care and details in the results in this chapter, but they give an idea of what is the evolution of this dynamical magnetricity in terms of frequency and variation with the density of magnetic charges. Besides, These calculations done excluding, the term of the electric field of the generalized Lorentz force, will allow us by comparison the action of the electric field of the electromagnetic wave on magnetic conductivity of the magnetic charges.

On the other hand, the existence a magnetricity out the frequency dependence given in Eq. (5.3) implies that the dissipation forces can have an importance in the general magneticity depending on this frequency. Therefore, we start a study of this magnetricity in function of the density of magnetic charges. These results of Fig. 25 have been made with a value of the dissipative forces coming from the parameter γ and a mass assigned to the monopoles, coming from Ref. [76], $m = 2 \times 10^{-27}$ such that the relaxation rate is $\frac{\gamma}{m} = 0,105 \times 10^{12}$.

The plasmon frequency assigned in these calculations is $\omega_P = 0.48 \times 10^{12}$. These results of magnetic conductivity are in good qualitative agreement with those of Ref. [80]. The quantitative differences can be justified since we have used a less adjusted expression than the one we use in the following sections of this chapter where we include the generalized Lorentz force in a complete way. The importance of these results comes from the fact

that the longitudinal and transversal components of both electric and magnetic fields depend on this optical conductivity of magnetic charges under the action of the frequency dependent magnetic field.
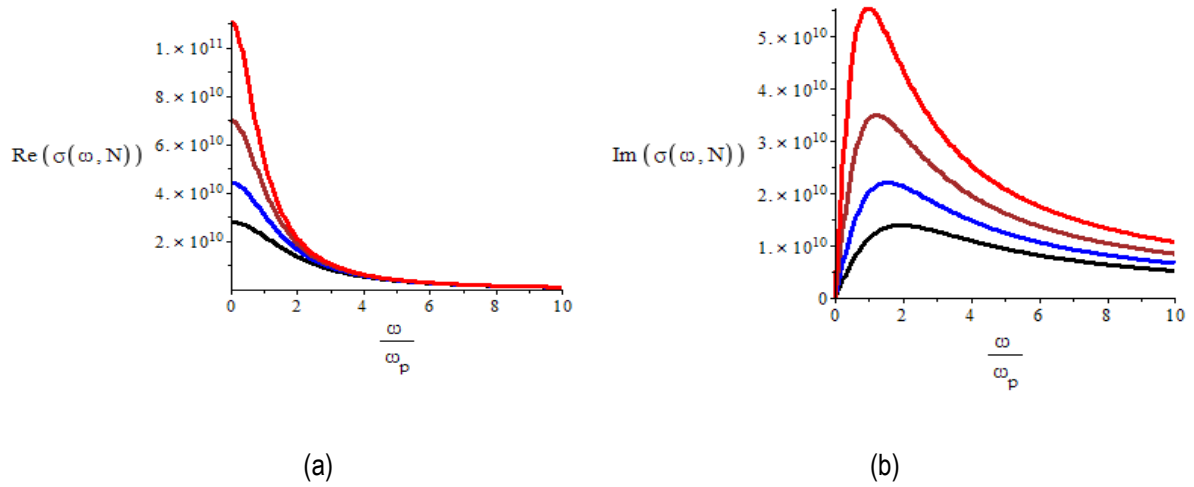

(a)   (b)

Figure 25.- Real part (a) and imaginary part (b) of optical for four values of the density of magnetic charges. (N=10^y , where y=26 , in red; y=25.8 , in brown; y=25.6 , in blue; y=25.4 , in black, all N values in number charges/ m^3).

If one considers a continuous variation of the density of magnetic monopoles, we have the following representation:

(a)   (b)

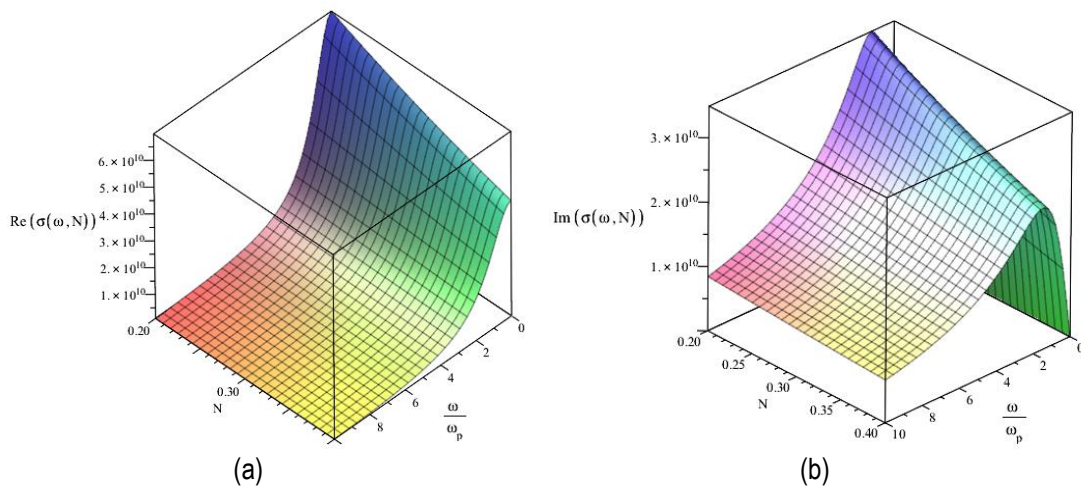Figure 26.- Real part (a) and imaginary part (b) of optical magnetricity (frequency dependent magnetricity) in function the density of monopoles $N = 10^{26-y}$, where y is the second planar axis.

The continuous variation of the density of magnetic monopoles yields a plausible approximation to the temperature variation of the magnetic conductivity. In this figure, for zero frequency, the Bramwell magnetricity reaches the

110

maximum values and increasing this frequency, the conductivity decreases, and this also decreases with the magnetic charge number. It is important to give the variation of the electromagnetic propagation with the density of magnetic monopoles. Therefore, in a next section (section 5), we give the results of the transversal components of both electric and magnetic fields. On the other hand, from Eq. (5.2), we deduce the expression of the complex magnetic permeability:

$$\mu_r^* = 1 + i\frac{\sigma(\omega, N)}{\omega} = 1 - \frac{m^2\omega_p(N)^2}{\gamma^2 + m^2\omega^2} + i\frac{m\gamma\omega_p(N)^2}{\gamma^2 + m^2\omega^2} \tag{5.4}$$

Therefore, the real part of this complex permeability could be negative for frequency values which satisfy the inequality $\omega \leq \left(\frac{m^2\omega_p^2 - \gamma^2}{m^2}\right)$, and the real part of the complex magnetic susceptibility is:

$$\chi_r = -\frac{\omega_p(N)^2}{\frac{\gamma^2}{m^2} + \omega^2} \tag{5.5}$$

This implying that the magnetic plasma state is diamagnetic for all-frequency. This magnetic susceptibility is obtained with Eq. (5.4). A characteristic of the compounds with magnetic charges is that if one considers the nonexistence of superficial magnetic currents in the limits of the wave guide, the edge conditions of generalized Maxwell equations are equal to those of standard electromagnetism. Thus, we have:

$$E_z = 0 \ ; \ \partial B_z / \partial \vec{n} = 0 \tag{5.6}$$

Then, the trial wave functions for E_z and B_z depend on the geometry of the guide.

4. TM longitudinal modes in a cylindrical cross section

The solutions of the wave equation with considering Eq. (5.6) that can best describe the phenomenology of systems with magnetic charges are the magnetic transverse modes (TM) because in this case there are no magnetic currents in the longitudinal direction. The magnetic current is normal to symmetry axis of the system. Then there is only longitudinal component of the electric field, and since the spin-ices, both natural and artificial, are electrical insulators, the complete electric and magnetic fields can have an oscillating shape in the direction of the cylinder axis. The longitudinal component of the electric field satisfies the following equation which can obviously be deduced from wave equation:

$$\nabla^2 E_z + \left(\varepsilon_0 \mu_0 \omega^2 - \frac{1}{1+i\dfrac{\gamma}{m\omega}} \frac{\omega_P(N)^2}{c^2} \right) E_z = \left(\nabla^2 + \alpha^2 \right) E_z = 0 \tag{5.7}$$

The solution of this equation in cylindrical symmetry is it is necessary in order to know the true electromagnetic propagation as well as determining the parameters which define it. The way to solve the differential equation (5.7) is vía the separation of variables in such a way that, we have $E_z = E_0 \phi(r,\varphi,z) = E_0 \phi_1(r)\phi_2(\varphi)\phi_3(z)$ in cylindrical system of coordinates, being $\alpha^2 = \dfrac{\omega^2}{c^2} - \dfrac{m\omega}{m\omega + i\gamma} \dfrac{\omega_P^2}{c^2}$, and ω_P is the plasmon frequency. Then, Eq. (5.7) is:

$$\frac{1}{\phi_1}\left(\frac{\partial^2 \phi_1}{\partial r^2} + \frac{1}{r}\frac{\partial \phi_1}{\partial r} \right) + \frac{1}{r^2 \phi_2}\frac{\partial^2 \phi_2}{\partial \varphi^2} + \frac{1}{\phi_3}\frac{\partial^2 \phi_3}{\partial z^2} = -\alpha^2 \tag{5.8}$$

and considering the variable separation, Eq. (5.8) implies which each summand of the left-hand side of equality are constant. Therefore,

$$\frac{1}{r^2 \phi_2}\frac{\partial^2 \phi_2}{\partial \varphi^2} = -u^2 \Rightarrow \frac{\partial^2 \phi_2}{\partial \varphi^2} = -r^2 u^2 \phi_2 \tag{5.9}$$

$$\frac{1}{\phi_3}\frac{\partial^2 \phi_3}{\partial z^2} = -k_z^2 \Rightarrow \phi_3(z) = \exp(\pm ik_z z - i\omega t) \tag{5.10}$$

and these latter equations allow us to transform Eq. (5.8) as follows:

$$\frac{r^2}{\phi_1}\frac{\partial^2 \phi_1}{\partial r^2} + \frac{r}{\phi_1}\frac{\partial \phi_1}{\partial r} + \frac{1}{\phi_2}\frac{\partial^2 \phi_2}{\partial \varphi^2} = (-\alpha^2 + k_z^2)r^2 \tag{5.11}$$

and in addition, the solution in ϕ_2 is $\dfrac{1}{\phi_2}\dfrac{\partial^2 \phi_2}{\partial \varphi^2} = -\nu^2 \Rightarrow \phi_2 = \cos(\nu\varphi)$, and Eq. (5.11) is converted in the following differential equation:

$$\frac{r^2}{\phi_1}\frac{\partial^2 \phi_1}{\partial r^2} + \frac{r}{\phi_1}\frac{\partial \phi_1}{\partial r} = \left[\nu^2 - \left(\alpha^2 - k_z^2\right)r^2 \right] \Rightarrow \frac{\partial^2 \phi_1}{\partial r^2} + \frac{1}{r}\frac{\partial \phi_1}{\partial r} = \left[\frac{\nu^2}{r^2} - \left(\alpha^2 - k_z^2\right) \right]\phi_1 \tag{5.12}$$

and now, we have done the variable change $x = (\alpha^2 - k_z^2)^{1/2}r$ on Eq. (5.12):

$$x^2 \frac{\partial^2 f_\nu(x)}{\partial x^2} + x \frac{\partial f_\nu(x)}{\partial x} = (\nu^2 - x^2)f_\nu(x) \tag{5.13}$$

This latter equation is the Bessel equation in real variable and jointing all parts of the primitive equation, we have:

$$E_z = E_0 f_\nu \left[(\alpha^2 - k_z^2)^{1/2} r \right] \cos(\nu\varphi) \exp\left(\pm ik_z - i\omega t \right) \tag{5.14}$$

and taking into account the edge condition which is in the cylindrical waveguide $E_z = E_0 \phi(R,\varphi,z) = 0$, the simpler solution is:

$$E_z = E_0 f_{1/2} \left[(\alpha^2 - k_z^2)^{1/2} r \right] \cos\frac{\varphi}{2} \exp\left(\pm ik_z - i\omega t \right) \tag{5.15}$$

and from Eq. (5.12)-(5.14), we have the relation $f_{1/2}(x) = \left(\dfrac{2}{\pi x} \right)^{1/2} \sin x$ is the minimal Bessel function, with

$(\alpha^2 - k_z^2)^{1/2} = \dfrac{n\pi}{R}$, and R being the radius of the cross section of the guide. Therefore, we have:

$$k_z(\omega,N) = \pm \left(\frac{\omega^2}{c^2} - \frac{m\omega}{m\omega + i\gamma} \frac{\omega_p(N)^2}{c^2} - \frac{n^2\pi^2}{R^2} \right)^{1/2} = \pm \frac{\omega}{c} n(\omega,N) \pm ib(\omega,N) \tag{5.16}$$

$$n(\omega,N) = \frac{c\,\mathrm{Re}\left[k_z(\omega,N) \right]}{\omega} \tag{5.17}$$

$$b(\omega,N) = \mathrm{Im}\left[k_z(\omega,N) \right] \tag{5.18}$$

$$v_g(\omega,N) = \mathrm{Re}\left[\left(\frac{dk_z(\omega,N)}{d\omega} \right)^{-1} \right] \tag{5.19}$$

These Eqs. (5.16)-(5.19) are important in the electromagnetic propagation since from it, we can deduce the effective refractive index corresponding to phase velocity, Eq. (5.17), of the EM wave, the extinction coefficient, Eq. (5.18), and the group velocity, Eq. (5.19). In the following, we give some results deduced from Eq. (5.16). In first place, we give, results of the extinction parameter varying with frequency defined in Eq. (5.18):
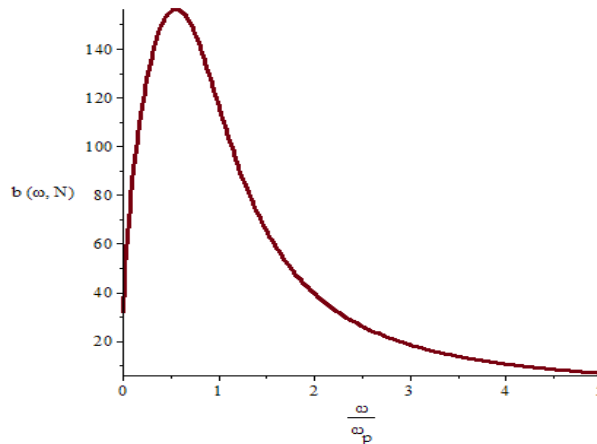

Figure 27. Extinction parameter.

113

This figure represents in horizontal axis a non-dimensional variable $x = \omega/\omega_P$ and vertical axis, we give the extinction parameter, defined in Eq. (5.16). For a value of $N = 10^{26}$ magnetic charges/m^3. In this Fig. 27, we suppose that the plasmon frequency is that corresponding to a value of the magnetic charges close to the maximum one. Then, the extinction value is maximum around $\omega \approx 0.75\omega_P$, and from $\omega \approx 5\omega_P$, the corresponding mode is completely oscillating; therefore, the electromagnetic propagation is total without losses. This behaviour is almost independent on magnetic conductivity (magnetricity) value, including when this is large. This being antithetic to the case when the electric conductivity is different from zero, since then the extinction parameter is increasing with frequency. Other results of this extinction parameter are given in Fig 28:
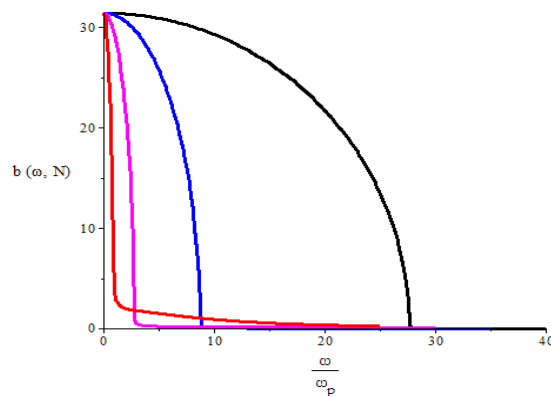
Figure 28.-Extinction parameter for different density of magnetic charges

At Fig. 28, we can see that the cut-off frequency, from which the electromagnetic propagation has not any energy losses, is decreasing according to the density of magnetic monopoles increases in the corresponding material, therefore, the electromagnetic propagation improves with temperature since if this increases the magnetic monopoles also increase.

Figure 29.-Refraction index corresponding to the phase velocity.

In the figure, $n(\omega, N) = \dfrac{c}{v_f}$, where v_f is the phase velocity of the EM wave depending on frequency within the microwave

guide for values $N = 10^{-5}$ (black); 10^{-4} (blue); 10^{-3} (magenta); 10^{-2} (red) respect to the maximum value of magnetic charges. The Fig. 29, shows the refraction 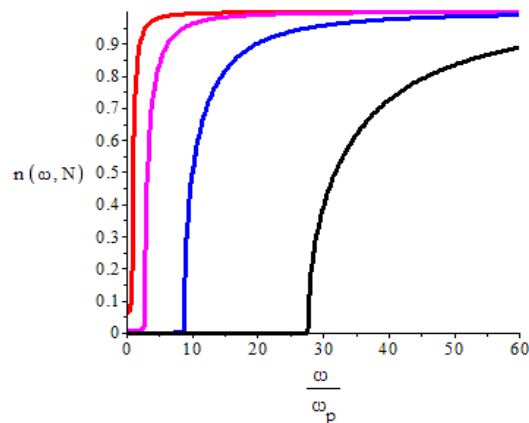index corresponding to the phase velocity within the guide. This index is complementary with the results of extinction parameter given in Fig. 28. The asymptotic values for all curves are 1, which corresponds to light velocity in the vacuum. However, the frequency for reaching this asymptotic value is increasing for decreasing values of density of magnetic charges and the greater cut-off frequency is when the plasmon frequency is lower. For lower frequencies imply less dissipative forces among magnetic charges and then the magnetricity increases.

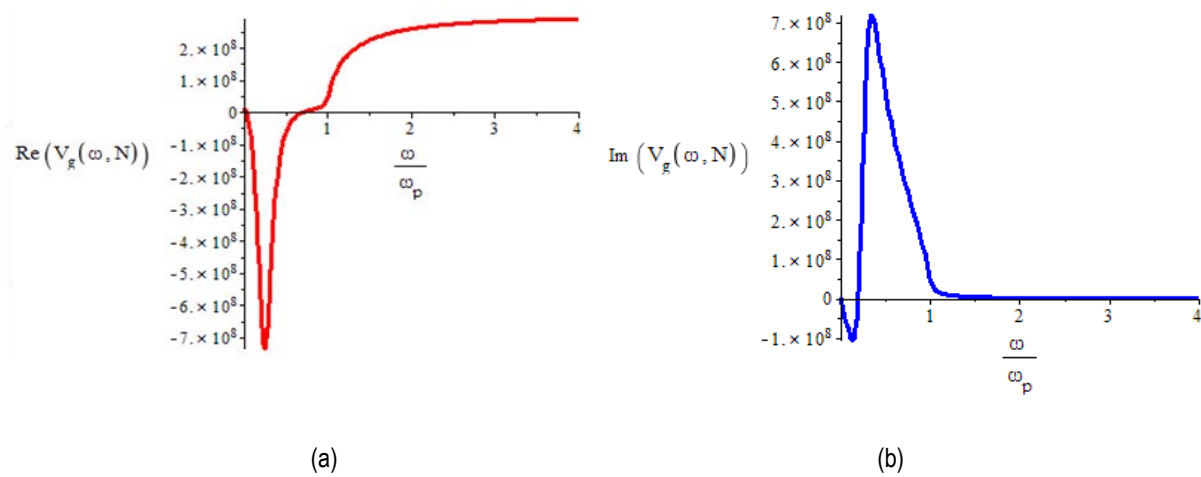(a)   (b)

Figure 30.- Real and imaginary parts of group velocity of EM wave.

The real part of the group velocity is one which determines the information speed transmitted via the electromagnetic signal, therefore, only can be a real positive number and less than the light speed in vacuum. Then, only the part (a) of this figure has a clear physical meaning and only when this curve is located in the positive zone of the vertical axis from $\omega \approx 0.75\omega_P$ and for $\omega \approx 4\omega_P$, this group velocity reaches its asymptotic value of c. The frequency zones in which this real part is negative would correspond to values for which the causality principle is violated, and it corresponds for large values of the imaginary part of the group velocity. This zone is the abnormal dispersive electromagnetic radiation zone of the linear response.

The most important conclusion of this section is that for a magnetic neutral plasma whose magnetic charges present mobility with small dissipative forces, i.e. small resistance and therefore great magnetricity, the

electromagnetic signal propagation in a cylindrical waveguide is possible. Some properties of the electromagnetic propagation in a "magnetic metallic phase" of a system with free monopoles are shown in Figs. 28-30 The most relevant characteristic is the existence of a cut-off frequency which is larger when smaller is the concentration of magnetic charges and consequently the dissipative forces due the interaction of the magnetic charges is smaller. For the smaller density of free magnetic monopoles corresponds the greater critical cut-off frequency.

These characteristic features of this behaviour being exclusive of magnetic charge system and it is contrary to that of any electric system under the electromagnetic propagation in electric metallic phase whose electric and magnetic fields are evanescent and whose extinction parameter is greater for large frequencies than for small ones. Another important conclusion deduced from Eq. (5.5) is the diamagnetic condition of the magnetic plasma state for all-frequencies and for $\omega = \left(\left(m^2 \omega_p^2 - \gamma^2 \right) \middle/ m^2 \right)^{1/2}$, this state is a perfect diamagnetic material in which the field $\vec{B} = 0$

These two latter properties are valid if and only if Eq. (5.5) is valid. In next sections of this chapter, we obtain other quantitatively different expressions for the susceptibility and permeability which quantitatively imply modifications in these two properties.

5. Transversal field components

The objective of this subsection is to reach relationships of the transversal components in function of the longitudinal components of the electric fields, E_z, in a material with magnetic currents and without electric currents. Given the longitudinal component of electric field, Eq. (5.15), the propagation and extinction are governed by the law defined by Eq. (5.16), and this E_z is a necessary determination in order to know the total electric and magnetic fields of the electromagnetic modes of the cylindrical waveguide.

The first step is the breakdown of the ∇ operator in a transversal part plus another longitudinal part [36,70], in such a way that we have the following $\nabla = \nabla_t + \vec{e}_z \dfrac{\partial}{\partial_z}$ and we also consider that the gradient of the longitudinal part of the fields can be given by $\nabla E_z = \nabla \left(\vec{e}_z \cdot E \right) = \left(\vec{e}_z \cdot \nabla \right) \vec{E} + \vec{e}_z \wedge \left(\nabla \wedge \vec{E} \right) = \dfrac{\partial \vec{E}}{\partial z} + \vec{e}_z \wedge \left(\nabla \wedge \vec{E} \right)$ and following

the transformation of this equation, we obtain $\nabla E_z - \dfrac{\partial \vec{E}}{\partial z} = \nabla_t E_z - \dfrac{\partial \vec{E_t}}{\partial z} = \overrightarrow{e_z} \wedge \nabla \wedge \vec{E}$ and

$\nabla_t H_z - \dfrac{\partial \vec{H_t}}{\partial z} = \overrightarrow{e_z} \wedge \nabla \wedge \vec{H}$. Then, by using the above auxiliary equations, we obtain the direct relationships

between the transverse part of the electric and magnetic fields depending on the longitudinal one of electric field.

These relationships, whose deduction is relatively easy, become:

$$\vec{H}_t(\omega, N) = i \frac{R^2 \varepsilon_0 \omega \vec{e}_z \wedge \nabla_t E_z}{n^2 \pi^2} \tag{5.20}$$

where E_z in a cylindrical waveguide is determined via expressions (5.15) and (5.16) by considering the edge

conditions for the longitudinal electric field, $E_z(r = R) = 0$. The smallest order Bessel function that can satisfy this

edge condition for a cylindrical symmetry can be for $\nu = 1/2$, and then, we have: $f_{1/2}(u) = \left(\dfrac{2R}{n\pi r}\right)^{1/2} \sin\left(\dfrac{n\pi}{R}r\right)$.

We can take into account any Bessel function that satisfies the edge condition of Eq (5.6) and then, we have

the corresponding TM mode. Therefore, the general $\vec{H}(\vec{r},t)$ -solution in this rectangular waveguide can completely

be determined with Eq. (5.20), and the transversal components of the electric field can be determined, and it

becomes:

$$\vec{E}_t(\omega, N) = -i \frac{\mp k_z \nabla_t E_z \mp k_z \mu_0 \sigma(\omega, N) \vec{e}_z \wedge \vec{H}_t}{\dfrac{m\omega}{m\omega + i\gamma} \dfrac{\omega_P(N)^2}{c^2} + \dfrac{n^2 \pi^2}{R^2}} \tag{5.21}$$

The Eqs. (5.20) and (5.21) are the general expressions of the magnetic and electric field within a guide filled

with the magnetic plasma. An important characteristic of these fields in the materials with presence of magnetic

charges is that while the magnetic fields only are modified by this presence via k_z given in Eq. (5.16), the second

term of the numerator of the transversal electric field depends in an explicit way on the magnet-optical conductivity

of the material within the guide.

On the other hand, the denominator is dependent on the material which fulfil this guide via its plasmon

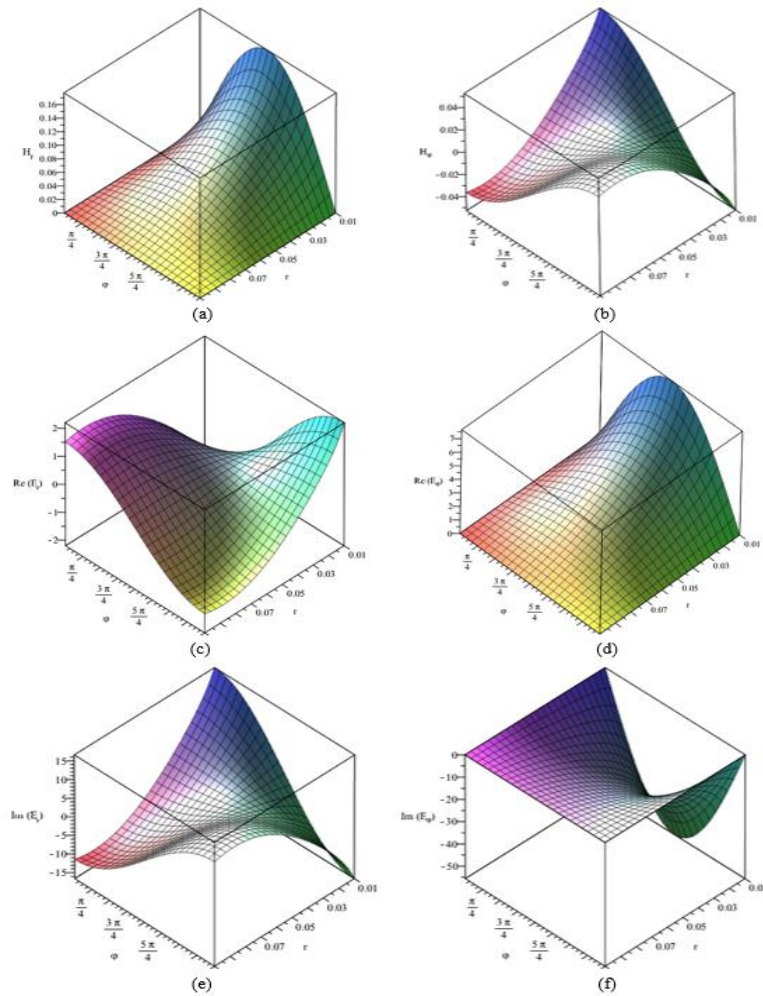frequency, $\omega_P(N)$, which depends on the density of entities which mimic the magnetic monopoles.

Figure 31.- Transversal components of magnetic and electric fields.

The first row: the left drawing is the real part of H_φ, the right figure is the real part of H_r. The second row on the left, the drawing corresponds to real part of E_r and on the right it is the real part of E_φ and the third row, we give the imaginary parts of E_r (left), and E_φ (right).

Therefore, in expressions (5.15)-(5.21), one can see that the transmitted electromagnetic fields are strongly depending on the frequency-dependent magnetricity which, in turn, depend on the plasmonic frequency whose values are crucially depending on the density of magnetic monopoles. In the Fig. 31, we give results concerning the transversal electric and magnetic field in which the oscillatory and extinction part of the z- component of the longitudinal electric field $E_z(r,\varphi,z) = E_0 f_\nu\left[(\alpha^2 - k_z^2)r\right]\cos(\nu\varphi)\exp\left(\pm ik_z z - i\omega t\right)$ is not considered since it affects

118

directly all results of other components of the fields, both electric and magnetic. From Figs. 27 and 28, one can deduce that the dissipative forces responsible of the extinction parameter imply losses of energy in the electromagnetic propagation. These energy losses can be deduced from the Poynting theorem. Furthermore, we can estimate that the cut-off frequency is a filter for frequencies close to plasmon frequency when the mode is of smallest order of the Bessel function.

6. Conductivity and susceptibility considering $\mp \dfrac{g}{mc^2}\vec{J}^{\pm} \wedge \vec{E}$.

One way of defining, not the only, the formation of magnetic currents in spin-ice systems is the temporal derivative of magnetization [31] due to spin-flips between contiguous tetrahedra when these spin-flips progress spatially throughout the crystalline structure of the material. Therefore, the magnetic current can be defined as: $\vec{J}^{\pm} = \partial\vec{M}^{\pm}/\partial t$. If one considers this latter definition of the magnetic currents and it is included in Eqs. (4.5) and (4.6), we obtain the following time evolution for the magnetization:

$$\frac{d^2\vec{M}^{\pm}}{dt^2} + \frac{\gamma}{m}\frac{d\vec{M}^{\pm}}{dt} = \frac{\mu_0 g^2 N^{\pm}}{m}\vec{H} \mp \frac{g}{mc^2}\frac{d\vec{M}^{\pm}}{dt} \wedge \vec{E} \tag{5.22}$$

These two latter equations correspond to the movement of the charges by means of the generalized Lorentz equation [80-84]. We must remark that the spin-ices are electric insulators, and this is the reason for which in these equations we do not consider electric currents. The analysis of this type of EM propagation is valid for determining the possibilities of spin-ice materials for utilizing them as devices of transmission of energy and information. If we assume the results for the experimental masses of magnetic charges of reference [75] which are in the interval between 1.6 and 2 x 10^{-27} Kg. The quantitative analysis of two terms on the right side of the equation in Eqs. (4.5)-(4.6) has allowed us to determine the frequency-dependent conductivity of Eq. (5.2). This equation is obtained by neglecting the electric term in equations (4.5), (4.6) and (5.22), and then, the conductivity and diamagnetic magnetic susceptibility are uniform and isotropic.

This term of the electric field, although it is quantitatively small with respect to the one corresponding to the magnetic field, introduces aspects of interest in the linear responses whose characteristics have been detected

experimentally in the systems with magnetic charges. These characteristics are fundamentally the non-linearity, non-uniformity and even anisotropy in the magnetic susceptibility.

The procedure to be followed is to consider the term of the electric field to be a perturbation in Eq. (5.22). Then, the fields that we will consider in thise equation are those obtained in previous sections and with them we will obtain magnetizations, magnetic susceptibilities and conductivities depending on the frequencies. For each monochromatic wave, the two equations (5.22) are converted to the following algebraic equations:

$$\left(-\omega^2 - i\frac{\gamma\omega}{m}\right)\vec{M}^{\pm} \mp \frac{ig\omega}{mc^2}\vec{M}^{\pm}\wedge\vec{E} = \frac{(\omega_P^{\pm})^2}{2}\vec{H} \tag{5.23}$$

where $(\omega_P^{\pm})^2 = \mu_0 g^2 N^{\pm}/m$, developing Eq. (5.23) by components, we have:

$$\left(-\omega^2 - i\frac{\gamma\omega}{m}\right)\left(M_r^{\pm}, M_{\varphi}^{\pm}, M_z^{\pm}\right) \mp \frac{ig\omega}{mc^2}\begin{vmatrix} \vec{e}_r & \vec{e}_{\varphi} & \vec{e}_z \\ M_r^{\pm} & M_{\varphi}^{\pm} & M_z^{\pm} \\ E_r & E_{\varphi} & E_z \end{vmatrix} = \frac{\left(\omega_P^{\pm}\right)^2}{2}\left(H_r, H_{\varphi}, 0\right) \tag{5.24}$$

and from z-components is

$$-\omega^2 M_z^{\pm} - i\frac{\gamma\omega}{m}M_z^{\pm} \mp \frac{ig\omega}{mc^2}(M_r^{\pm}E_{\varphi} - M_{\varphi}^{\pm}E_r) = (0,0) \tag{5.25}$$

and this Eq. (5.25) implies the following important consequences,

$$M_z^{\pm} = 0$$

$$M_r^{\pm}E_{\varphi} = M_{\varphi}^{\pm}E_r \tag{5.26}$$

The first of them can be more or less intuitive, but the second one is not intuitive, since it implies that the transversal components of the magnetization coming from the positive and negative magnetic charges maintain the same proportionality to the transversal components of the electric field of the electromagnetic wave in the waveguide. The following equations of other components are:

$$\left(-\omega^2 - i\frac{\gamma\omega}{m}\right)M_r^{\pm} \mp \frac{ig\omega}{mc^2}M_{\varphi}^{\pm}E_z = \frac{\left(\omega_P^{\pm}\right)^2}{2}H_r$$

$$\left(-\omega^2 - i\frac{\gamma\omega}{m}\right)M_{\varphi}^{\pm} \pm \frac{ig\omega}{mc^2}M_r^{\pm}E_z = \frac{\left(\omega_P^{\pm}\right)^2}{2}H_{\varphi} \tag{5.27}$$

and these two equations are grouped in a matrixial form of the following way:

$$
\begin{pmatrix} -\omega^2 - i\dfrac{\gamma\omega}{m} & \mp\dfrac{ig\omega}{mc^2}E_z \\[3mm] \pm\dfrac{ig\omega}{mc^2}E_z & -\omega^2 - i\dfrac{\gamma\omega}{m} \end{pmatrix} \begin{pmatrix} M_r^\pm \\[2mm] M_\varphi^\pm \end{pmatrix} = \dfrac{\left(\omega_P^\pm\right)^2}{2}\begin{pmatrix} H_r \\[2mm] H_\varphi \end{pmatrix}
\tag{5.28}
$$

and this implies the following equation where can be defined the magnetic susceptibility

$$
\begin{pmatrix} M_r^\pm \\[2mm] M_\varphi^\pm \end{pmatrix} = \dfrac{\dfrac{\left(\omega_P^\pm\right)^2}{2}}{\left(-\omega^2 - i\dfrac{\gamma\omega}{m}\right)^2 - \dfrac{g^2\omega^2}{m^2c^4}E_z^2}\begin{pmatrix} -\omega^2 - i\dfrac{\gamma\omega}{m} & \pm\dfrac{ig\omega}{mc^2}E_z \\[3mm] \mp\dfrac{ig\omega}{mc^2}E_z & -\omega^2 - i\dfrac{\gamma\omega}{m} \end{pmatrix}\begin{pmatrix} H_r \\[2mm] H_\varphi \end{pmatrix}
\tag{5.29}
$$

The complete solutions of equations (5.24) imply: i) there are neither magnetization nor current in the longitudinal component since the longitudinal component of magnetic field is null in the TM modes, and ii) we have the following relationship within transversal components of electric field and magnetization: $M_r^\pm E_\varphi = M_\varphi^\pm E_r$.

Otherwise, these components of the magnetization are related with the transversal magnetic field by means of the following expressions:

$$
\begin{pmatrix} M_r^\pm \\[2mm] M_\varphi^\pm \end{pmatrix} = \overset{\leftrightarrow}{\chi}\begin{pmatrix} H_r \\[2mm] H_\varphi \end{pmatrix} = \begin{pmatrix} \chi_{rr} & \mp\chi_{r\varphi} \\[2mm] \pm\chi_{r\varphi} & \chi_{\varphi\varphi} \end{pmatrix}\begin{pmatrix} H_r \\[2mm] H_\varphi \end{pmatrix}
\tag{5.30}
$$

where the matrix elements become:

$$
\chi_{rr} = \chi_{\varphi\varphi} = -\dfrac{1}{2}\omega_P^2\left(\omega^2 + i\dfrac{\gamma\omega}{m}\right)\left[\left(\omega^2 + i\dfrac{\gamma\omega}{m}\right)^2 - \dfrac{\omega^2 g^2}{m^2 c^4}E_z^2\right]^{-1}
\tag{5.31}
$$

$$
\chi_{r\varphi} = -i\omega\omega_P^2 g E_z\left[2mc^2\left(\omega^2 + i\dfrac{\gamma\omega}{m}\right)^2 - \dfrac{2\omega^2 g^2}{mc^2}E_z^2\right]^{-1}
\tag{5.32}
$$

Therefore, this magnetic susceptibility implies anisotropy, inhomogeneity and non-linearity magnetic properties. Hence, the transverse magnetization is not parallel to the magnetic field, since the matrix susceptibility elements depends on each point inside the waveguide via its dependence on the longitudinal component of the electric field. In addition, keeping in mind the definition of the magnetic current as the temporal derivative

magnetization, we can establish the conductivity of magnetic charges as a function of frequency by means of the following expression:

$$\begin{pmatrix} J_r^\pm \\ J_\varphi^\pm \end{pmatrix} = -i\omega \begin{pmatrix} \chi_{rr} & \mp\chi_{r\varphi} \\ \pm\chi_{r\varphi} & \chi_{rr} \end{pmatrix} \begin{pmatrix} H_r \\ H_\varphi \end{pmatrix} \tag{5.33}$$

and it must be remembered that the $\pm$ sign of $\begin{pmatrix} J_r^\pm \\ J_\varphi^\pm \end{pmatrix}$, $\begin{pmatrix} M_r^\pm \\ M_\varphi^\pm \end{pmatrix}$ and $\pm\chi_{r\varphi}$ concern the sign of the magnetic

monopoles, and this implies the anti-symmetry property of the magnetic susceptibility matrix. Then, the respective currents corresponding to positive and negative magnetic monopoles are different. Thus, if one considers the total

current $\vec{J} = \vec{J}^+ + \vec{J}^-$, given this anti-symmetric magnetic susceptibility, the resulting conductivity also corresponds to a non-lineal, non-uniform but isotropic material. This conductivity takes the form:

$$\vec{J} = \sigma(\omega,N)\vec{H} \tag{5.34}$$

where the frequency-dependent magnetricity which substitute that of Eq. (5.2), takes the form:

$$\sigma(\omega,\gamma,E_z,N) = \frac{\omega_P^2(N)}{\frac{\gamma}{m}f_+(E_z,\gamma,\omega) - i\omega f_-(E_z,\gamma,\omega)} \tag{5.35}$$

where, $f_+(E_z,\gamma,\omega) = 1 + \frac{g^2 E_z^2}{m^2 c^4}\left(\omega^2 + \frac{\gamma^2}{m^2}\right)^{-1}$, and $f_-(E_z,\gamma,\omega) = 1 - \frac{g^2 E_z^2}{m^2 c^4}\left(\omega^2 + \frac{\gamma^2}{m^2}\right)^{-1}$. Eq. (5.35) differs from Eq.

(5.2) in the expressions $f_+(E_z,\gamma,\omega)$ and $f_-(E_z,\gamma,\omega)$ which in this Eq. (5.2) are equal to 1 when the electric term of

Eq. (5.22) is considered vanishing. $f_+(E_z,\gamma,\omega)$ can be interpreted as a reinforcement of the dissipative forces and

$f_-(E_z,\gamma,\omega)$ the renormalization of the mass of the magnetic charges due both modifications to the interaction of the

electric field with the moving magnetic charges. This concept of this interaction being essential in the classic

treatment of the interaction among magnetic monopoles in both natural and artificial spin-ices. Eq. (5.35) implies

an isotropic, non-lineal and non-uniform frequency-dependent conductivity that should be introduced in expressions

of the components of the electric and magnetic fields in Eqs. (5.20) and (5.21).

This implies a methodology which allows to include the electric term of the generalized Lorentz force, Eqs.

(4.3), (4.4) and (5.22), in a first perturbation order using the same general Eqs. (5.15), (5.20), (5.21) and (5.34).

This conductivity is decisive in the electromagnetic propagation since all components of the electric and magnetic

fields depend on this physical variable. Therefore, this is the main finality of calculation of this section of the work and its plausibility is a signature of the same philosophical category for the complete theory deducible of Eqs. (4.3), (4.4) and (5.22) by considering a magnetic charge current defined as $\vec{J}^{\pm} = \partial \vec{M}^{\pm} / \partial t$.

This conductivity presents a maximum for the frequency $\omega_M = gE_Z / mc^2$ if electromagnetic wave frequency is one which satisfies the condition $\omega \approx \left(\omega_M^2 - \gamma^2 / m^2 \right)^{1/2}$. It must be remembered that the values of this maximum depend on the longitudinal component of the electric field which is a continuous function. Therefore, there are always spatial regions inside the guide whose conductivity is maximum unless we are in a frequency range below the cut-off frequency so that there is no electromagnetic propagation. A physical interpretation can be established from the action of the electric field term in Eq. (5.22). This produces a precession movement of the magnetic charges in the normal planes to the longitudinal axis of the cylindrical waveguide. In addition, this term forbids the magnetic charge movement in the axis symmetry direction.

This precession frequency depends on the z coordinate from the phase function $\exp(ik_z z - i\omega t)$, present in E_Z and also depends on r and φ spatial variables from the Bessel and $\cos(\nu\varphi)$ functions which appears in E_Z in Eq. (5.15). It implies a magnetic charge movement extremely complex in the electromagnetic propagation. Furthermore, this conductivity is depending on dissipative forces parameter γ which is a definition of the resistivity of the material. This parameter being also responsible for the features of the evolution space-time EM propagation in the waveguide. On the other hand, the conductivity of Eq. (5.35) satisfies all necessary conditions for being a correct expression of conductivity, since for $E_Z \rightarrow 0$ this expression of conductivity tends to that of Eq. (5.2). In addition, for $\omega \rightarrow 0$, Expression (5.35) tends to Bramwell et al's magnetricity, given in expression (5.3), and for $\omega \rightarrow \infty$ we have that $\sigma(\omega, N) \rightarrow 0$. Otherwise, carrying out appropriate and exact modifications of the diagonal matrix elements of the magnetic susceptibility, we obtain the following expressions:

$$Re(\chi_{rr}) = Re(\chi_{\varphi\varphi}) = \frac{-m^2 \frac{\omega_P^2}{2} f_-(E_Z, \gamma, \omega)}{m^2 \omega^2 f_-^2(E_Z, \gamma, \omega) + \gamma^2 f_+^2(E_Z, \gamma, \omega)} \qquad (5.36)$$

$$Im(\chi_{rr}) = Im(\chi_{\varphi\varphi}) = \frac{m\frac{\omega_P^2}{2}\gamma f_-(E_z,\gamma,\omega)}{m^2\omega^3 f_-^2(E_z,\gamma,\omega) + \gamma^2\omega f_+^2(E_z,\gamma,\omega)} \tag{5.37}$$

In this susceptibility it occurs as in the optical conductivity with respect to the factors $f_-(E_z,\gamma,\omega)$, $f_+(E_z,\gamma,\omega)$ and the similitudes and differences respect to Eq. (5.4) are equal to those of the frequency-dependent magnetricity between Eqs. (5.2) and (5.35). In addition, for dissipative forces tending to zero, but different strictly to zero, there is a continuum of maximum absorption frequencies and an essential discontinuity in the real part of magnetic susceptibility. These frequencies of maximum absorption are given by the expression: $\omega_M(\vec{r}) = \frac{gE_z(\vec{r})}{mc^2}$. Therefore, the absorption frequency coincides with the maximum optical conductivity.

On the other hand, these maximum absorption frequencies imply a precession rotation movement of the charges in normal planes to symmetry axis of the cylindrical waveguide and can easily be observed. Therefore, these frequencies allow us to determine the masses of the magnetic charges. Furthermore, with the achieving of the plasmon frequencies, we can determine within the same electromagnetic propagation experiment the determination of the density of magnetic charges.

7. Results of magnetic conductivity

The main results coming from Eq. (5.22) are those deduced from magnetic conductivity given in the expression (5.35). This conductivity which depends on frequency have four key physical magnitudes which are the characteristic features of the material in order to determine the main electrodynamical properties: the precession frequency, ω_M, the plasmon frequency, ω_P, whose value varies with temperature, the effective inertial mass of the magnetic charges, m, and the dissipation coefficient, γ. As mentioned in the text, ω_M can be determined by the maximum energy absorption and the maximum conductivity, ω_P controls the minimum frequency for which the waveguide is able to propagate the electromagnetic wave.

Once known ω_P, the inertial effective mass is the crucial parameter for obtaining the density of magnetic monopoles which is the order parameter in the phase transitions analyzed in Ref [65]. With these three magnitudes,

the dissipation parameter is univocally determined. Therefore, from a relatively simple experiment of the classical propagation of the electromagnetic fields in a guide of microwaves, we can know if a new material contains or not magnetic monopoles. In addition, we can estimate some circuital possibilities through determination of the response functions as material media. These being the goals and highlights of this work.

Otherwise, the present model has sufficient generality to obtain the objectives of explaining the electrodynamics of materials with magnetic monopoles that may have application in propagating energy and information. This generality along with a clear simplicity, in our opinion, contribute to the virtue and possible validity of the methodology. In addition, the results obtained from the expression (5.35) are in reasonable agreement with other models, perhaps more elaborated, but they do not have as this one a possible and simple experimental planning. These results can be seen in the Fig. 32 that represent the optical conductivity of systems with magnetic charges such as spin-ices in the interaction with electromagnetic fields.
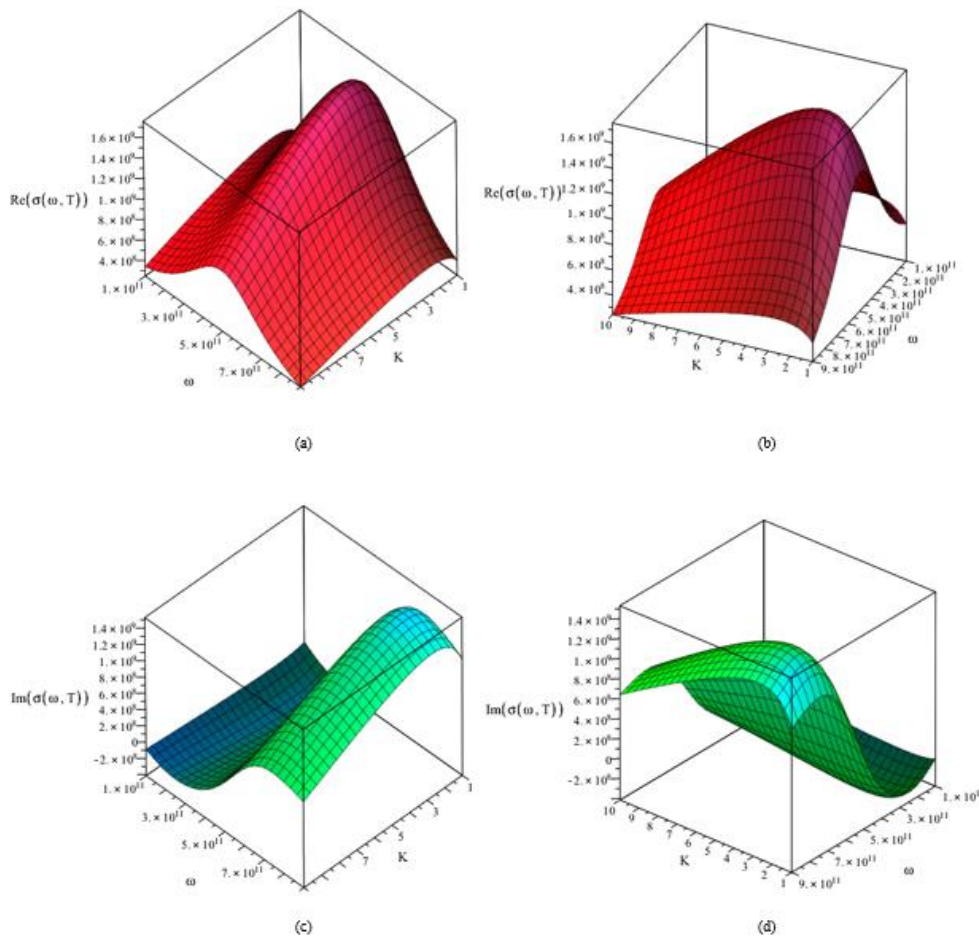
Figure 32.- Real and imaginary parts of the magnetic conductivity.

This figure shows the magnetic conductivity for frequency range between 0.1 to 0.9 THz. The X-axis is the electromagnetic frequency and the Y-axis is temperature. The Figs. 32a and 32b correspond to identical results of the real part in two different positions of the 3-dimensional figure. This is made in order to see the evolution at lower temperature than the maximum conductivity which in 32a is hidden. By cutting the figure with a plane perpendicular to the K axis, we can observe the frequency evolution curve of the conductivity for a given temperature. If we cut with a plane perpendicular to the axis of frequencies we have the evolution in temperature of the conductivity for a given frequency. In Figs. 32c and 32d, we represent the corresponding results concerning the imaginary part of the magnetic conductivity carried out with the same values for the relaxation parameters and temperature evolution of the plasmon frequency which are used for Figs. 32a and 32b.

In Fig. 32, the real part of the conductivity increases with temperature when this is lower than 2K. The variation of the real part of the conductivity presents a maximum for a frequency close to the precession one. The value of this maximum increases with T, when we consider the temperature evolution of $\omega_p(N)$ deduced from the internal energy such as in Ref. [65]. This increase can be seen in Fig. 32b.and occurs while the plasma state is progressively being formed. For temperatures upper the transition temperature for which this state is dominant, the temperature of maximum conductivity depending on frequency decreases such as one can see in Figs. 32a and 32b in congruent behaviour with the experimental data of Ref. [75]. This occurs since for upper temperatures than T_C (temperature of the plasma state transition), the free charges start to be recombined. In addition, the maximum conductivity appears to the same frequency for all temperatures. The imaginary parts present maximum for similar frequencies to those of the real part, and minima in a negative zone of this imaginary part (see our results of Figs. 32c and 32d as well as the experimental results of Ref. [75]). For the temperatures lower than $\approx 2K$, the conductivity decreases tending to zero since the density of free magnetic charges also tends to zero, existing only confined magnetic dipoles in rigid positions whose mobility is practically null. There is an apparent contradiction between the results of Figs. 25 and 26 with those of Fig. 32, since in the first ones, the maximum conductivity is for zero frequency and it is not so in Fig. 32.

In the results of Figs. 25 and 26, we have not considered the different thermodynamic transitions of the low energy states and that are reflected in the evolution of their internal energy and entropy. This structural modification

of the different states has been the main objective for the Ref. [65]. The use of the thermal evolution of the monopole density deduced from the aforementioned internal energy has been used in the results of this section and therefore the conductivity given in Fig. 32 differs from those in Figs. 25 and 26.This is the main reason for this difference since in the dynamical increase of free magnetic carriers with temperature is due to the breaking of confined dipoles and progressive conversion in free poles which we consider in results of Fig. 32 from the evolution with temperature of $N(T)$ taken into account from the internal energy of the low energy states [66]. As cited before, Figs. 25 and 26 are a simple representation of Eq. (5.2) for different values of density of free monopoles.

On the other hand, other reason which breaks the apparent contradiction is given in the results of Fig. 29 and in Eq. (5.16), since in both places it is shown that for frequencies smaller than a critical value whose expression

is: $\omega \leq \omega_c = Re\left[\omega^2 - \dfrac{m\omega}{m\omega + i\lambda}\omega_P^2(N) - \dfrac{n^2\pi^2 c^2}{R^2} \right]$, there is no propagation in a waveguide full of spin-ice materials

with free magnetic monopoles. These results of the conductivity present qualitative compatibility with those experimental results given in Ref. [75] in a similar way our results of Fig. 25 and 26 are in concordance with those of the theoretical analysis of Ref. [80]. This relative concordance is obtained although the theoretical analysis model carried out in this latter reference is different from our Classical-Physics procedure. Another compatibility of our results with recent theoretically analysis can be seen in Ref. [86] since although in this theoretical calculation, the authors give a gap in the conductivity respect to frequency, this gap is also compatible with our results. The idea of the gap of Ref. [85] can be explained within our method by the cut-off frequency showed in Figs. 28 and 29 since for lower frequencies than this cut-off there is not electromagnetic propagation in the microwave guide.

Otherwise, we believe as authors of Ref. [75] that there is not more contradiction in the use of the Classical Electrodynamics in excitation quantum states which produce the entities that mimics the magnetic monopoles than in the consideration of classical model for the optical conductivity in semiconductors. Actually, Lorentz-Drude model applied to the dielectric response and optical conductivity of semiconductors present excellent results in compatibility with the Random Phase Approximation theories of dielectric functions which are in the hard core of the many-body quantum physics. On the other hand, from results given in Fig. 32, one can easily deduce those coming from expressions (5.36) and (5.37), since these exactly are:

$$\chi_{rr} = \chi_{\varphi\varphi} = -\frac{\operatorname{Im}\{\sigma[\omega, N(T)]\}}{\omega} + i\frac{\operatorname{Re}\{\sigma[\omega, N(T)]\}}{\omega} \qquad (5.38)$$

In summary, the goal of this section is to present new results which give plausibility to the assumptions considered in our calculations given the reasonable concordance with experimental results of Ref. [75]. In addition, the achieved results allow the comparison our methodology with those of Refs. [35] and [86]. In our opinion, the method of this chapter presents certain advantages with respect to the previous literature due to the following points: i) Our method is inserted in the first principles in dual Electrodynamics applied to the materials with presence of structural excited states which mimic the magnetic monopoles. ii) The analysis is a reflection of a relatively simple experimental procedure which permits the finding of similar materials in which one can suspect the existence of magnetic charges. iii) This methodology allows the determination of magnetic conductivity, magnetic susceptibility in function of frequency and temperature as well as the main parameters of the magnetic plasma state: the plasmon frequency and inertial mass of the magnetic monopoles.

On the other hand, the possible disadvantages are that our methodology is within the Classical Electrodynamics since it is contemplated for prospecting and analyzing the possibility of finding circuital applications which transmit energy and information. Other quantum methods can serve for other more theoretical objectives such as the Ref. [86]. In any case, we are researching the determination of the response functions of material in different devices by using Quantum Electrodynamics in a continuation of previous paper [65], where we analyze the thermodynamics of the two phase-transitions occurred in the spin-ice materials.

8. Comments

The existence of two situations in both any artificial and natural spin-ice material provoke singular dichotomy in the corresponding phenomenology, on one hand the so-called pole-antipole pair condensation and on the other hand, the neutral magnetic plasma. The characteristic phase transition detected via measurements of specific heat and magnetic susceptibility give support to the existence of these two states which are profoundly analyzed in previous papers [31,65] and references therein. These two states are macroscopic states whose thermodynamic development and electromagnetic propagation depends on the density of free magnetic monopoles.

The objective of this analysis is in order to establish experimental tests for evaluating the influence of the dissipative forces due to the interacting action among magnetic charges in the electromagnetic propagation within the magnetic plasma state which is within a cylindrical waveguide. In this state the characteristic plasma frequency is not exactly the cut off frequency, since this cut off frequency also depends on the characteristic parameter of the dissipative forces. On the other hand, we find new relationships of the intensity of the different fields which also depends on the density of free magnetic charges. Eqs. (5.20) and (5.21) describe the EM propagation of the TM modes in a cylindrical cross-section microwave.

The real novelty in spin-ices regarding the existence or not of the magnetic monopole current is not so much in the generalized Maxwell, but in that the magnetic poles of the dipole can travel independently inside the solid under the presence of an external magnetic field not necessarily intense. Above all, given that if the magnetic charge current is defined [31], $\vec{J}^{\pm} = \partial\vec{M}^{\pm}/\partial t$, Eq. (4.2) becomes the standard equation Maxwell of the rotational of the electric field. Therefore, equations (4.3), (4.4) and (5.22) as the only novelty from the classical physics point of view. The solution of these equations allows us to establish more precisely the definition of the frequency-dependent conductivity and magnetic susceptibility including the exotic effects of the longitudinal component of the electric field such as discussed in section 6 of this chapter. Hence, this latter propagation in waveguides is carried out in order to determine the frequency dependent monopole conductivity in a complementary way to that determined eight years ago [12,13] in the discovery of the magnetricity in the spin-ices. On the other hand, our solutions of the electric and magnetic fields in these cylindrical guides allow us to conclude that there are intervals of frequencies for which there is electromagnetic propagation although there is mobility of the monopoles.

In summary, in this chapter, we have obtained the solutions for the extended Maxwell equations with presence of currents of magnetic charges, by considering the extended Lorentz force and dissipative forces in a cylindrical waveguide. We determine the frequency dependent magnetricity and the magnetic susceptibility whose characteristic features depend on the longitudinal component of the electric field. This dependence introduces great changes in the nature of these two physical responses of the material, since by considering the term $\frac{g}{mc^2}\vec{J}^{-}\wedge\vec{E}$ in Eq. (5.22), the magnetic susceptibility is non-uniform, non-linear and anisotropic; and the frequency dependent

conductivity is isotropic but non-uniform and non-linear. Whereas if we exclude this term in Eq. (5.21), both the conductivity and the frequency-dependent susceptibility are linear, uniform and isotropic. We also determine the temporal and spatial evolution of the magnetic and electric fields.

These results may be used for clearing new technological ideas in order to obtain "magnetronic" devices. However, the low temperature of magnetricity phenomenon is the fundamental problem of finding applications to obtain magnetronic devices with the spin-ice materials. Precisely, in Refs. [78,87], the authors analyze a proposal for the design and realization of a three-dimensional artificial spin ice by means of the superposition of layered nano-two-dimensional structures. These structures afford the same topological equivalence as the tetrahedrons in a pyrochlore lattice. Otherwise, in Ref. [79], the authors express the confidence that in these artificial spin-ices the difficulties found by Bramwell [12] in the measures of magnetricity in the natural spin-ices operating in pure crystals and around 0.36 K can be obviated.

Concluding remarks and perspectives

One of the most surprising facts of this subject of the electrodynamics of the spin-ices is that we spoke of magnetic monopoles and that this concept can be reconciled with the fact that the magnetic field maintained the characteristic of having zero divergence. Therefore, in chapter one of this thesis almost exclusively deals with the conciliation between the dumbbell model and the fact that we continue accepting that the flow of the magnetic field through a closed surface of elementary or infinitesimal dimensions is zero.

A second important achievement of this chapter 1 is equation (1.15) because with this expression of the magnetic potential we can obtain the energy of the magnetic charges whether in the free case or forming confined dipoles. This is important because it has allowed to do us the analysis inside of the statistical mechanics of chapters 2 and 3, in which these energies are utilized to do the thermodynamic study in order to describe the global excitation states at lower temperature.

In these chapters 2 and 3, we determine the evolution of the specific heat and the entropy that explains quite correctly the empirical behavior of these compounds from a thermodynamic point of view. In these chapters we give three models of structure and dynamic evolution with the temperature of the global excited states that are constructed for the entities that mimic the magnetic monopoles. We have explained in turn the phase transitions, emphasizing possible discrepancies existing, at the present time, in the literature and giving in chapter 3 a possible and plausible procedure to explain these differences.

We have established clear and unambiguous conditions in which there is a first phase transition at temperatures around 100 mK in the natural spin-ices materials, giving a criterion with which to discern the possible cases in which this transition is of the first order and in which it must be of the second kind. We have proposed that the rapid formation of free magnetic charges from confined dipoles can give rise to a second phase that if exists must be of a second kind, highlighting the empirical discrepancies existing in this point of interest. We have also obtained saturation entropy in the asymptote at the temperature of 1 K as well as the residual of Pauling at 0.3 K in the possible transition from the bosonic state of the pole-antipole pairs to the fermionic state of free charges.

If the first part consists in giving our version about the structure, spin symmetry and phase transitions, which is an issue within Many-Particle Physics and their thermodynamic evolution of the low-temperature excitation states, in the second, we consider free magnetic charges as classical charged objects and we study the dual electrodynamics, with free magnetic charges and magnetic currents and absence of electric charges and currents. This is carried out with two clear objectives i) to give clear and simple methodologies to detect magnetic charges in other new natural or artificial compounds, either at low temperatures (usually natural) or high temperatures artificial materials equivalent to spin-ices. ii) To initiate a prospective to determine the circuit possibilities of these compounds in both electromagnetic confinement devices and unconfined ones. In the first calculation we determine the frequency of precession that depends on the longitudinal electric field. In this way, we have given a procedure to determine the mass of the magnetic charges that under the conditions of the spins of Dysprosium and Holmium comes to be of the order of $10^{-27}\,\mathrm{Kg}$.

Also, in the second part of this first calculation in confined media with rectangular symmetry, we solve the generalized equations giving general formulas of electromagnetic fields when there are magnetic charges and there are no electrical charges. These fields are strongly dependent on the conductivity as a function of the frequency, and this one of the frequency of plasmon that depends its square of the density of magnetic charges per unit of volume. Density that can become of $N \leq \dfrac{10^{26}}{\mathrm{m}^3}$.

This first calculation of electromagnetic propagation has been carried out without considering the dissipative forces due to frictions. This supposition is legitimated with small densities of magnetic charges. This implies that we neglect interactions of the magnetic charges with either the network or with each other. In addition, we do not consider, in this chapter 4, within the Lorentz force the interaction of these moving charges with the electric field which has allowed to give an orienting idea of the electromagnetic propagation in finite and infinite media, always when the spin-ices are in the plasma state of low density of magnetic charges.

In the second calculation we have included the dissipative forces and the action of the electric field on the magnetic charges in motion. We have obtained the corresponding effects, determining a non-uniform behavior of

the frequency dependent conductivity but with spatial isotropy. However, the susceptibility is not uniform and leaves the system in anisotropic conditions. In the first case we determine that the cutoff frequency in the waveguide is univocally related to the plasmon frequency, and allows us to determine with this frequency, together with the precession frequency, the density of magnetic charges that is actually the parameter of thermodynamic order in the plasma state. A particularity of the second calculation of chapter 5 is that the frequency of precession as in the calculation in rectangular waveguide of chapter 4 is the frequency of maximum electromagnetic absorption. Besides, in the case of the second calculation in cylindrical symmetry this precession frequency is a variable and it depends on each point because it is proportional to the value of the longitudinal electric field in said point.

Concerning the perspectives for continuing the research in the direction established in this thesis, the natural prolongations are the following:

i) The first extension of the work presented in the thesis is to make an important qualitative leap by improving the thermodynamic potentials using the perturbation theories at a temperature different from zero. This supposes to enter in the formalism of thermodynamic potentials which can be deduced from the perturbation theories at finite temperature by means of the Matsubara method. Using as a perturbation the interaction Hamiltonian of Equation (3.3) of this document.

ii)A second natural extension is the determination of the magnetic responses of the conductivity and susceptibility of materials with magnetic charges within theories of the so-called Kubo formulas. In addition to determine possible quantum effects that emulate the Meissner effect in systems with magnetic dipoles which could correspond to the normal Meissner effect of electronic superconductivity under the dualness symmetry.

iii) A third investigation is the formalization of the Electrodynamics with dyons which are present in topological insulators following the directions presented in this thesis.

We are starting these three researches at the present time.

APPENDIX A

Determination of the formula:

$$\nabla\left\{\ln\left[n\left(\vec{r}\right)\right]+\beta\,|\,g\,|\,\phi\left(\vec{r}\right)\right\}=\vec{C}$$

We start from:

$$n\left(\vec{r}_i\right)=\frac{\exp\left(-\beta\left[g_i\phi\left(\vec{r}_i\right)+\Sigma_0\right]\right)}{\sum\limits_j\exp\left(-\beta\left[g_i\phi\left(\vec{r}_i\right)+\Sigma_0\right]\right)} \tag{A.1}$$

If one calculates $\nabla n\left(\vec{r}_i\right)$ of equation (A1.1), we have:

$$\nabla n\left(\vec{r}_i\right)=\frac{\exp\left(-\beta\left[g_i\phi\left(\vec{r}_i\right)+\Sigma_0\right]\right)\left[-\beta g_i\nabla\phi\left(\vec{r}_i\right)\right]}{\left[\sum\limits_j\exp\left(-\beta\left[g_j\phi\left(\vec{r}_j\right)+\Sigma_0\right]\right)\right]}-\frac{\exp\left(-\beta\left[g_i\phi\left(\vec{r}_i\right)+\Sigma_0\right]\right)\sum\limits_j\exp\left(-\beta\left[g_j\phi\left(\vec{r}_j\right)+\Sigma_0\right]\right)\left[-\beta g_j\nabla\phi\left(\vec{r}_j\right)\right]}{\left[\sum\limits_j\exp\left(-\beta\left[g_j\phi\left(\vec{r}_j\right)+\Sigma_0\right]\right)\right]^2}$$

$$=n\left(\vec{r}_i\right)\left[-\beta g_i\nabla\phi\left(\vec{r}_i\right)\right]+\beta n\left(\vec{r}_i\right)\frac{\sum\limits_j\exp\left(-\beta\left[g_j\phi\left(\vec{r}_j\right)+\Sigma_0\right]\right)\left[g_j\nabla\phi\left(\vec{r}_j\right)\right]}{\left[\sum\limits_j\exp\left(-\beta\left[g_j\phi\left(\vec{r}_j\right)+\Sigma_0\right]\right)\right]}$$

$$=n\left(\vec{r}_i\right)\left[-\beta g_i\nabla\phi\left(\vec{r}_i\right)+\beta\left\langle g_j^+\nabla\phi^+\left(\vec{r}_j\right)\right\rangle-\left\langle g_j^+\nabla\phi^-\left(\vec{r}_j\right)\right\rangle\right]$$

where $\nabla\phi^+\left(\vec{r}_j\right)$ and $\nabla\phi^-\left(\vec{r}_j\right)$ are the gradient of magnetic potentials for a positive and negative charge, respectively, whose absolute values can be considered equals. If one does not this assumption, we have the simplified Eq. (1.28):

$$\nabla\left\{\ln\left[n\left(\vec{r}\right)\right]+\beta\,|\,g\,|\,\phi\left(\vec{r}\right)\right\}=\vec{C} \tag{A.2}$$

APPENDIX B

In this appendix we will explain the mathematical derivations of the main formulas of chapter 2. We will start from the functions of the free energy of Helmholtz which is defined as:

$$F = -\frac{1}{\beta}\left\{2\sum_i \ln\left[1+\exp\left(-\beta(e_i'-\mu')\right)\right] - \sum_j \ln\left[1-\exp\left(-\beta(e_j-\mu)\right)\right]\right\}$$

(B.1)

and having in mind, the individual energy of respective components:

$$e_j = 2\left(K_B T\ln\left(\frac{n_0}{n_j}\right) + T\frac{|g|\phi_0}{T_V}\right)n_j + \Sigma_0 - \frac{\Delta^2}{|M'V_0|}$$

$$e'_j = \left(K_B T\ln\left(\frac{n_0}{n_j}\right) + T\frac{|g|\phi_0}{T_V}\right)(1-2n_j) + \Sigma_0 + \frac{\Delta^2}{(<e_j>^2+\Delta^2)^{1/2}}$$

we can obtain:

$$-\beta(e_j-\mu) = 2n_j\ln\left(\frac{n_j}{n_0}\right) - \frac{|g|\phi_0}{K_B T_V}n_j - \beta\left(\Sigma_0 - \frac{\Delta^2}{|M'V_0|} - \mu\right)$$

$$-\beta(e'_j-\mu) = (1-2n_j)\ln\left(\frac{n_j}{n_0}\right) - \frac{|g|\phi_0}{K_B T_V}(1-2n_j) - \beta\left(\Sigma_0 + \frac{\Delta^2}{(<e_j>^2+\Delta^2)^{1/2}} - \mu\right)$$

and defining the following physical variables $b' = \Sigma_0 + \frac{\Delta^2}{(<e_j>^2+\Delta^2)^{1/2}} - \mu$, $b = \Sigma_0 - \frac{\Delta^2}{|M'V_0|} - \mu$, and

$a = \frac{|g|\phi_0}{K_B T_V}$, we obtain:

$$F_{BEC} = M'\frac{K_B T}{n_0}\int_0^{n_0}\ \ln\left|1-\left(\frac{n}{n_0}\right)^{2n}e^{-a2n}e^{-b\beta}\right|dn, = M'\frac{K_B T}{2n_0}\int_0^{2n_0}\ln\left|1-\left(\frac{t}{2n_0}\right)^t e^{-at}e^{-b\beta}\right|dt$$

(B.2)

where for obtaining the right-hand side of equality, we have included the variable change $2n = t$. This being the corresponding Helmholtz free energy of the Bose-Einstein condensate. With a similar variable change $1-2n = t$, we obtain, the Helmholtz free energy of the plasma state:

$$F_{Plasma} = -2M\frac{K_B T}{m_0}\int_0^{m_0}\ \ln\left(1+\left(\frac{n}{n_0}\right)^{1-2n}e^{-a(1-2n)}e^{-b'\beta}\right)dn = -M\frac{K_B T}{m_0}\int_{1-2m_0}^1\ln\left[1+\left(\frac{1-t}{2n_0}\right)^t e^{-at}e^{-b'\beta}\right]dt$$

(B.3)

The final expressions of (B.2) and (B.3) are equal to (3.12) and (3.14).

References

[1] Dirac, P. A. M., "Quantized Singularities in the Electromagnetic Field", Proc. Roy. Soc., Vol. A133, 60, 1931.

[2] Cabrera, B., "First Results from a Superconductive Detector for Moving Magnetic Monopoles", Phys. Rev. Lett., Vol. 48, 1378-1381, 1982.

[3] Jordan, P., "The Dirac magnetic pole", Ann. Physik, Vol. 32, 66, 1938.

[4] Hooft, G., "Magnetic monopoles in unified gauge theories", Nuclear Physics 79, 276-284, 1974.

[5] Polyakov, A. M., "Particle spectrum in quantum field theory", JETP Lett., Vol. 20, 194-195, 1974.

[6] Balestra, S., G. Giacomelli, M. Giorgini, L. Patrizii, V. Popa, Z. Sahnoun, and V. Togo, "Magnetic Monopole Bibliography-II", arXiv: 1105.5587v1, May 27th, 2011.

[7] Castelnovo, C., R. Moessner, and S. L. Sondhi, "Magnetic monopoles in spin ice", Nature, Vol. 451, 42-45, 2008.

[8] Sondhi, S., "Wien route to monopoles", Nature, Vol. 461, 888-889, 2009.

[9] Fennel, T., P.P. Deen, A.R. Wildes, K. Achmalzl, D. Prabhakaran, A. T. Boothryod, R.J. Aldus, D.F. McMorrow, and S.T. Bramwell, "Magnetic Coulomb Phase in the spin ice", Science, 326,415-417, 2009.

[10] S.C. Qi, J. Zhang,"Topological insulators and superconductors" Rev. Mod. Phys., 83, 1057, 2011.

[11] Morris, D. J. P., D. A. Tennant, S. A. Grigera, B. Klemke, C. Castelnovo, R. Moessner, C. Czternasty, M. Meissner, K. C. Rule, J.-U. Hoffmann, K. Kiefer, S. Gerischer, D. Slobinsky, and R. S. Perry, "Dirac Strings and Magnetic Monopoles in the Spin Ice", Science, Vol. 326, 411-414, 2009.

[12] Bramwell, S. T., S. R. Giblin, S. Calder, R. Aldus, D. Prabhakaran, and T. Fennell, "Measurement of the charge and current of magnetic monopoles in spin ice", Nature, Vol. 461, 956-960, 2009.

[13] Giblin, S. R., S. T. Bramwell, P. C. W. Holdsworth, D. Prabhakaran, and I. Terry, "Creation and measurement of long-lived magnetic monopole currents in spin ice", Nature Phys., Vol. 7, 252-258, 2011.

[14] Bandyopadhyay S., and M. Cahay, "Introduction to Spintronics", CRC Press, 2008.

[15] Onsager L.J., "Derivations from Ohm's law in weak electrolytes", J. Chem.Phys. 2, 599-615, 1934.

[16] Mol L.A.S., W.A. Moura-Melo, and A.R. Pereira, "Conditions for the magnetic monopolesin nanoscale square arrays of dipolar spin-ice", Phys. Rev. B, Vol. 82, 054434-1-6, 2010.

[17] Mellado P., O. Petrova, Y. Shen, and O. Tchernyshyov, "Dynamics of Magnetic charges in artificial spin ice", Phys. Rev. Lett., Vol. 105, 187206-1-4, 2010.

[18] Tchernyshyov O., "No longer on thin ice", Nature Phys. Vol. 6, 323-324, 2010.

[19] Y. Perrin, B. Canals and N. Rougemaille, "Extensive degeneracy, Coulomb phase and magnetic monopoles in artificial square ice", Nature 540, 411, 2016.

[20] X.L. Qi, R. Li, J. Zang, and S.C. Zhang, "Inducing a magnetic monopole with topological surface States", Science, Vol. 323, 1184, 2009.

[21] Araque-Quijano J. L. and G. Vecchi, "Field and source equivalence in source reconstruction on 3D surfaces", Progress in Electromagnetics Research Vol. 103, 67-100, 2010.

[22] Ladak, S., D. E. Read, G. K. Perkins, L. F. Cohen, and W. R. Branford, "Direct observation of magnetic monopole defectsin an artificial spin-ice system", Nature Phys., Vol. 6, 359-363, 2010.

[23] Gingras, M.J., "Observing Monopoles in a magnetic Analog of Ice", Science, Vol. 326, 375-376, 2009.

[24] Mengotti, E., L. J. Heyderman, A. F. Rodriguez, F. Nolting, R. V. Hugli, and H.-B. Braun, "Real-space observation of emergent magnetic monopoles and associated Dirac strings in artificial kagome spin ice", Nature Phys., Vol. 7, 68-74, 2011.

[25] Bonitz, M., "A plasma of magnetic monopoles,"Nature Phys., Vol. 7, 192-194, 2011. F. F. Chen "Introduction to Plasma Physics" . Plenum Press (1977)..

[26] Jaubert, L. D. C., and P. C. W. Holsworth, "Signature of magnetic monopole and Dirac string dynamics in spin ice", Nature Phys., Vol. 5, 258-261, 2009.

[27] Ray M. W., E. Ruokokoski, S. Kandel, M. Mo¨tto¨nen2,3 & D. S. HallMilton K.A., "Observation of Dirac monopoles in a synthetic magnetic field", Nature, 505, 647, 2014.

[28] Bramwell S. T. and M. J. P. Gingras, "Spin ice state in frustrated magnetic pyrochlore materials", Science, Vol. 294, 1495-1501, 2001.

[29] Powell S, "Confinement of monopoles and scaling theory near unconventional critical points", Phys. Review B, 87, 064414, 2013.

[30] Borzi R. A, D. Slobinsky, and S. A. Grigera, "Charge Ordering in a Pure Spin Model: Dipolar Spin Ice", Phys. Rev. Lett. 111, 147204, 2013.

[31] Bovo L., J.A. Bloxsom, D. Prabhakaran, G. Aeppli & S.T. Bramwell, "Brownian motion and quantum dynamics of magnetic monopoles in spin ice", Nature Communications, February 26th, 2013.

[32] Pomaranski D., L. R. Yaraskavitch, S. Meng, K. A. Ross, H. M. L. Noad, H. A. Dabkowska, B. D. Gaulin, and J. B. Kycia, "Absence of Pauling's residual entropy in thermally equilibrated Dy2Ti2O7". Nat. Phys. 9, 353, 2013.

[33] Kato Y., and Shigeki Onoda, "Numerical Evidence of Quantum Melting of Spin Ice: Quantum-to-Classical Crossover", Phys. Rev. Lett. 115, 077202, 2015.

[34] Tercas H., D. D. Solnyshkov, and G. Malpuech, "TopologicalWigner Crystal of Half-Solitons in a Spinor Bose-Einstein Condensate", Phys. Rev. Lett. 110, 035303, 2013.

[35] Roukokoski E., V. Pietila, and M. Mottonen, "Ground state Dirac monopole", Phys. Rev. A, 84, 063627, 2011.

[36] Jackson, J. D., "Classical Electrodynamics", 3rd edition, John Wiley & Sons, Inc., 1999.

[37] Costa-Quintana y F. López-Aguilar, "Interacción electromagnética: Teoría Clásica", Ed. Reverté, 2007.

[38] Costa-Quintana, J. and F. López-Aguilar, "Extended classical electrodynamics with magnetic monopoles", F. E. Journal of Mechanical Engineering and Physics, Vol. 1, 19-56, 2010.

[39] Costa-Quintana J. and F. López-Aguilar, "Propagation of electromagnetic waves in material media with magnetic monopoles", Progress in Electromagnetics Research, Vol. 110, 267-295, 2010.

[40] Costa-Quintana J. and F. López-Aguilar, "Fresnel coefficients in materials with magnetic monopoles", Optics Express, Vol. 19, 3742-3757, 2011.

[41] Costa-Quintana and F. López-Aguilar, "Molecular EM fields and dynamical responses in solids with magnetic charges", Progress in Electromagnetics Research, Vol. 121, 159-179, 2011.

[42] Costa-Quintana J. and F. López-Aguilar, "Extended Lagrangian formalisms for dyons and some applications to solid systems under external fields", Annals of Physics (New-York) 327, 1948-1961, 2012.

[43] E. Witten, "Duality, Spacetime and Quantum Mechanics", Physics Today, May 28th, 1997.

[44] Shinichi Itoh, Yasuo Endoh, Tetsuya Yokoo, Soshi Ibuka, Je-Geun Park, Yoshio Kaneko, Kei S. Takahashi, Yoshinori Tokura & Naoto Nagaosa, "Weyl fermions and spin dynamics of metallic ferromagnet SrRuO3", Nat. Comm., 1, 2016.

[45] C. Paulsen, S. R. Giblin, E. Lhotel, D. Prabhakaran, G. Balakrishnan, K. Matsuhira and S. T. Bramwell, "Experimental signature of the attractive Coulomb force between positive and negative magnetic monopoles in spin ice", Nat. Phys, 12, 661, 2016.

[46] Conduit G. J., "Line of Dirac monopoles embedded in a Bose-Einstein condensate", Phys. Rev. A 86, 021605(R), 2012.

[47] Pietila V. and M. Mottonen, "Creation of Dirac Monopoles in spinor Bose-Einstein Condensates", Phys.Rev. Lett. 103, 030401, 2009.

[48] Solnyshkov D. D., H. Flayac, and G. Malpuech, "Stable magnetic monopoles in spinor polariton condensates", Phys. Rev. B 85, 073105, 2012.

[49] Masuda Shumpei, Utkan Güngördü, Xi Chen, Tetsuo Ohmi, and Mikio Nakahara, "Fast control of topological vortex formation in Bose-Einstein condensates by counterdiabatic driving", Phys. Rev. A 93, 013626, 2016.

[50] A. P. Sazonov, A. Gukasov, I. Mirebeau, and P. Bonville, "Double-layered monopolar order in the Tb2Ti2O7 spin liquid", Phys. Rev. B 85, 214420, 2012.

[51] M. J. Matthews, C. Castelnovo, R. Moessner, S. A. Grigera, D. Prabhakaran, and P. Schiffer,"High-temperature onset of field-induced transitions in the spin-ice compound Dy2Ti2O7", Phys. Rev. B 86, 214419, 2012.

[52] B. D. Gaulin, E. Kermarrec, M. L. Dahlberg, M. J. Matthews, F. Bert, J. Zhang, P. Mendels, K. Fritsch, G. E. Granroth, P. Jiramongkolchai, A. Amato, C. Baines, R. J. Cava, and P. Schiffer, "Quenched crystal-field disorder and magnetic liquid ground states in Tb2Sn2-xTixO7", Phys. Rev. B 91, 245141, 2015.

[53] Nic Shannon, "Entropy lost", Nat. Phys. 9, 326, 2013.

[54] McClarty P. A., A. O'Brien, and F. Pollmann, "Coulombic charge ice", Phys. Rev. B 89, 195123, 2014.

[55] S. Subhro Bhattacharjee, Erfanifam, E. L. Green, M. Naumann, Zhaosheng Wang, S. Granovsky, M. Doerr, J. Wosnitza, A. A. Zvyagin, R. Moessner, A. Maljuk, S. Wurmehl, B. Buhner, and S. Zherlitsyn, "Acoustic signatures of the phases and phase transitions in Yb2Ti2O7", Phys. Rev. B 93, 144412, 2016.

[56] Zhang Sheng, Ian Gilbert, Cristiano Nisoli, Gia-Wei Chern, Michael J. Erickson, Liam O'Brien, Chris Leighton, Paul E. Lammert, Vincent H. Crespi, and Peter Schiffer, "Crystallites of magnetic charges in artificial spin ice", Nature 500, 553, 2013.

[57] Jerome D., T.M. Rice, and W. Khon, "Excitonic Insulators", Phys. Rev. 158, 462, 1967.

[58] Keldich L.V., Y. V. Kopaev, "Possible Instability of the Semimetallic State Toward Coulomb Interaction", Sov. Phys. Sol. Stat. 6, 2219, 1965.

[59] Zhu X., P.B. Littlewood, M.S. Hybertsen, and T.M. Rice, "Exciton Condensate in Semiconductor Quantum Well Structures", Phys. Rev. Lett. 74, 1633, 1995.

[60] R.P. Feynman, "Statistical Mechanics", W.A. Benjamin, INC, 1972.

[61] J.F. Annett, "Superconductivity, Superfluids and Condensates", Oxford University Press, 2010. J.R. Schrieffer, "Theory of Superconductivity", Addison-Wesley Publising Company, (1988).

[62] Mostame S, Claudio Castelnovo, Roderich Moessner, and Shivaji L. Sondhi, "Tunable non-equilibrium dynamics of field quenches in spin ice", PNAS, 111, 241, 2014.

[63] M. Lublinsky, C. Ratti, and E. Shuryak, Phys. Rev. D, 81, 014008 2010. M. Detrixhe et. Al. (ANITA Collaboration), "Relativistic magnetic monopole seach with the ANITA-II balloon-borne radio interferometer", Phys. Rev. D, 83, 023513, 2011.

[64] M. Detrixhe et. Al. (ANITA Collaboration), "Relativistic magnetic monopole seach with the ANITA-II balloon-borne radio interferometer", Phys. Rev. D, 83, 023513, 2011.

[65] F. I. López-Bara and F. López-Aguilar, "Analytic model for low energy excitation states and phase transitions in spin-ice systems", J. of Phys.: Conden. Matter, 29, 155803, 2017.

[66] Magnus O. Borgh, Muneto Nitta, and Janne Ruostekoski, "Stable Core Symmetries and Confined Textures for a Vortex Line in a Spinor Bose-Einstein Condensate", Phys. Rev. Lett. 116, 085301, 2016.

[67] F. I. López-Bara and F. López-Aguilar, "Electrodynamics in cylindrical symmetry in the magnetic plasma state", Journal of Physics D: Applied Physics, J. Phys. D: A ppl. Phys. 51 195004, 2018.

[68] R.K. Pathria and P.D. Beale, "Statistical Mechanics", Elsevier (Third Edition), 2011.

[69] G.D. Mahan, "Many-Particle Physics", Plenun Press, 1999.

[70] F. I. López-Bara and F. López-Aguilar, "Analysis of Electromagnetic Propagation in the Magnetic Plasma State in Spin-ice Systems", Journal of Applied Physics, 121, 175108, 2017.

[71] Cheng-Ju Lin, Chen-Nan Liao, and Chyh-Hong Chern, "Spin structure factor and thermodynamics in the antiferromagnetic transverse-field Ising model on the pyrochlore lattice", Phys. Rev. B 85, 134434, 2012.

[72] V. Kaiser, S. T. Bramwell, P. C.W. Holdsworth and R. Moessner, "Onsager'sWien effect on a lattice", Nat. Mat 12, 1033, 2013

[73] Zhou H.D., S.T. Bramwell, J.G. Cheng, C.R. Wiebe, G. Li, L. Balicas, J.A. Bloxsom, H.J. Silverstein, J.S. Zhou, J.B. Goodenough, and J.S. Gardner, "High pressure route to generate magnetic monopole dimers in spin ice", Nat. Comm. Published, Sep 20th, 2011.

[74] S. Scharffe, O. Breunig, V. Cho, P. Laschitzky, M. Valldor J. F. Welter, and T. Lorenz, "Suppression of Pauling's residual entropy in the dilute spin ice", Phys. Rev. B 92, 180405(R), 2015.

[75] LiDong Pan, N. J. Laurita, Kate A. Ross, Bruce D. Gaulin and N. P. Armitage, "A Measure of Monopole Inertia in the Quantum Spin Ice Yb2Ti2O7", Nature Physics, 12, 361-366, Nat. Phys. 3608, 2015.

[76] W. H. Toews, Songtian S. Zhang, K. A. Ross, H. A. Dabkowska, B. D. Gaulin, and R.W. Hill, "Thermal Conductivity of Ho2Ti2O7 along the [111] Direction", Phys. Rev. Lett., 110, 217209, 2013.

[77] M. W. Ray, E. Ruokokoski, S. Kandel, M. Möttönen & D. S. Hall, K.A. Milton, "Observation of Dirac monopoles in a synthetic magnetic field", Nature, 505, 647, (2014).

[78] Gia-Wei Chern, Charles Reichhardt, and Cristiano Nisoli, Appl. Phys. Lett. 104, 013101, 2014; Y. Perrin, B. Canals and N. Rougemaille, "Topology by Design in Magnetic nano-Materials: Artificial Spin Ice", Nature, 5 4 0, 410, 2016.

[79] R.P. Loreto, L.A. Morais, C.I.L. de Araujo, W.A. Moura-Melo, A.R. Pereira, R.C. Silva, F.S. Nascimento and L.A.S. Mól, "Analysis of electromagnetic propagation in the magnetic plasma state in spin-ice systems", Nanotechnology 26, 295303, 2015.

[80] Gia-Wei Chern, Saurabh Maiti, Rafael M. Fernandes, and Peter Wölfle, "Electronic Transport in the Coulomb Phase of the Pyrochlore Spin Ice", Phys. Rev. Lett. 110, 146602, 2013.

[81] O.P.S. Negi, H. Dehnen, "Gauge Formulation for Two Potential Theory of Dyons", Int. Jour. Theor. Phys. 50, 2446, 2011.

[82] S.S. Serova and S.A. Serov, "Full Action for an Electromagnetic Field with Electrical and Magnetic Charges", Int. Jour. Theor. Phys. 50, 436, 2011.

[83] P.C. Ferreira "Explicit actions for electromagnetism with two-gauge fields with only one electric and one magnetic physical field" Journal of Mathematical Physics, 47, 072902, 2006.

[84] P.C.R. Cardoso de Mello, S. Carneiro and M.C. Nemes, "Action principle for the classical dual electrodynamics", Phis Lett. B, 384, 197, 1996.

[85] Tai Tsun Wu and Chen Ning Yang, "Dirac's monopole without strings: Classical Langrangian theory", Physical Review D, 14, 437, 1976.

[86] Xiao-Tian Zhang and Ryuichi Shindou, "Transport properties of density wave phases in three-dimensional metals and semimetals under high magnetic field", Phys. Rev. B 95, 205108, 2017.

[87] L. J. Bannenberg, A. J. E. Lefering, K. Kakurai, Y. Onose, Y. Endoh, Y. Tokura, andC. Pappas, "Magnetic relaxation phenomena in the chiral magnet Fe1-xCoxSi: An ac susceptibility study", Phys. Rev. B 94, 134433, 2016.